

# SkyTEM survey, Varde

## Data processing and inversion of SkyTEM dataset – Varde

Giulio Vignoli



# **SkyTEM survey, Varde**

## Data processing and inversion of SkyTEM dataset – Varde

Giulio Vignoli

# Contents

<b>1.</b>	<b>Introduction</b>	<b>4</b>
<b>2.</b>	<b>Data Collection</b>	<b>7</b>
2.1	The acquisition system.....	7
2.2	Instrument.....	7
2.3	Calibration of the SkyTEM system.....	15
2.4	SkyTEM repeatability test .....	15
2.5	High altitude test.....	15
2.6	Bias tests during production flight .....	16
<b>3.</b>	<b>Processing of the SkyTEM data</b>	<b>17</b>
3.1	Positioning .....	17
3.2	Tilt data .....	17
3.3	Altitude data .....	18
3.4	Voltage data .....	18
3.5	Processing - Technical specifications .....	20
<b>4.</b>	<b>Inversion of the SkyTEM data</b>	<b>21</b>
4.1	Spatially constrained inversion.....	21
4.2	Depth of Investigation (DOI).....	23
4.3	Inversion - Technical specifications .....	25
<b>5.</b>	<b>Thematic maps and cross sections</b>	<b>26</b>
5.1	Mean resistivity maps.....	26
5.2	Cross sections .....	27
5.3	Location map, QC-maps .....	27
<b>6.</b>	<b>Conclusion</b>	<b>29</b>
<b>7.</b>	<b>References</b>	<b>30</b>
	<b>Appendix I:</b>	<b>Location maps, QC maps (1 - 9)</b>
	<b>Appendix II:</b>	<b>Mean Resistivity maps as depth slices (1 – 51)</b>
	<b>Appendix III:</b>	<b>Cross Sections (1 – 10)</b>
	<b>Appendix IV:</b>	<b>Digital deliveries (1 – 2)</b>

# 1. Introduction

This report details the processing and inversion of the data collected by SkyTEM Surveys A/S for Varde Vandforsyning A/S during the period: 11-12 March 2015. The survey area is in the surrounding of Varde and is shown in Fig. 1.

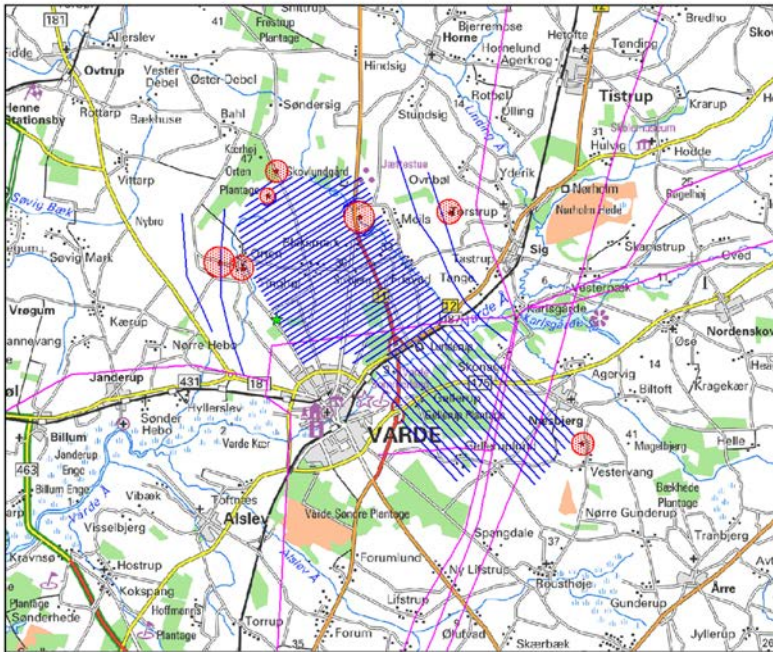


*Figure 1. The Varde survey area with the originally planned flight lines (the blue lines). The red circles are the safety buffer zone around the sensitive areas (e.g. farms). The magenta lines indicate the electrical power lines.*

The goal of the survey was to locate and characterize potential area for future possible groundwater abstraction development.

In this respect, the outcomes of the study highlight the presence of an interesting area, just outside the main body of the present survey (on the North-West side) where two additional lines were planned and flown (Fig. 2).

In pursuing the goal of the survey, an iterative procedure has been implemented and followed. Hence, every step of processing and inversion phases has been performed with the tight involvement of experienced geologists in order to ensure the geological significance of the outcomes. As a side effect, this geophysics-geology close interaction has allowed preserving and effectively using a larger number of the original soundings. However, for sake of compactness, this report is dealing uniquely with the final geophysical results and the associated processing and inversion settings.

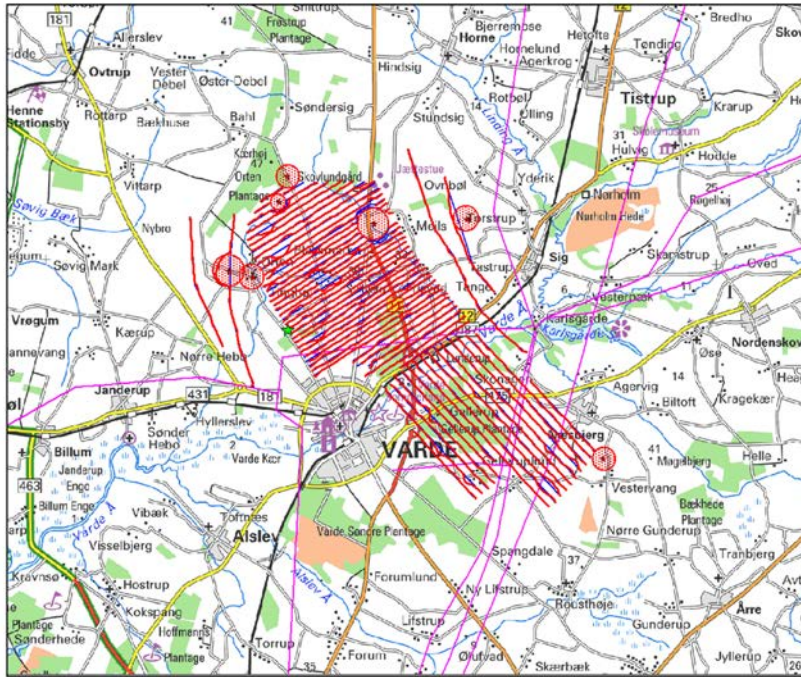


Figure 2. The Varde survey area with the originally planned flight lines (the blue lines) and the actually flown path (the red lines). The red circles are the safety buffer zone around the sensitive areas (e.g. farms). The magenta lines indicate the electrical power lines.

<b>Varde Project 2015</b>	
Client	Varde Vandforsyning A/S Gl. Kærvej 15 DK-6800 Varde
Contact person for the Client	Kenneth Ejsbøl
Locality	Varde, Denmark
Field Period	March 11th to March 12th, 2015
Line km planned	240 km
Line km acquired	240 km
Line separation	~200 m
Flight speed	~25 m/s
Average flight altitude (frame height)	30 m above the ground
Moment	SLM: $(344,28 \text{ m}^2) * (\sim 6 \text{ A}) * (2 \text{ turns})$ = $\sim 4100 \text{ Am}^2$ HM: $(344,28 \text{ m}^2) * (\sim 115\text{A}) * (12 \text{ turns})$ = $\sim 475000 \text{ Am}^2$
Responsible person for the data processing and inversion	Giulio Vignoli (Senior Researcher at GEUS)
Project manager	Flemming Jørgensen (Senior Researcher at GEUS)

*Table 1. Project summary.*

## 2. Data Collection

### 2.1 The acquisition system

The SkyTEM is a time-domain helicopter borne electromagnetic system designed for hydrogeophysical, environmental and mineral investigations. The following contains a general introduction to the SkyTEM system. A more thorough description of the system can be found, for example, in Sørensen and Auken, 2004. A general description of geological applications of the TEM method can be found in Jørgensen et al., 2003a,b and of the method in Nabighian and Macnae, 1991.

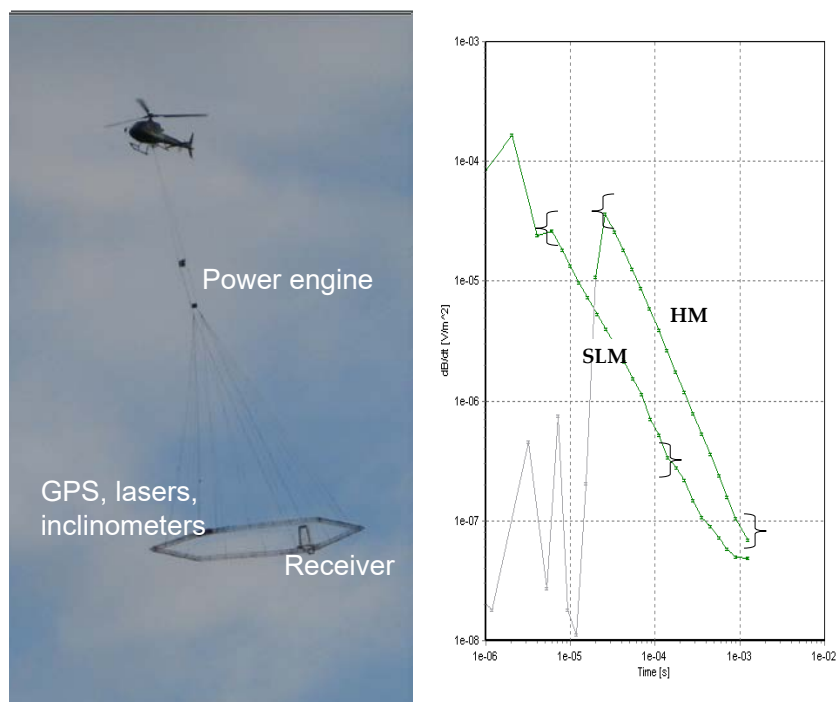


Figure 3. Left: The SkyTEM system in operation. Right: a typical  $dB/dt$  sounding curve from the SkyTEM system with both the Super Low (SLM) and the High (HM) moment curves. Braces indicate the gates that can be reliably used during the inversion in a typical dataset.

### 2.2 Instrument

Figure 3 shows a picture of the SkyTEM system with the hexagonal frame below the helicopter. The lengths of the frame sides are approximately 30 m. The transmitter loop is mounted on the frame in an octagonal polygon configuration. The receiver loop is placed approximately 2 m above the frame in what is roughly a central loop configuration with a vertical offset. Two lasers placed on the frame measure the distance to terrain continuously while

flying, and two inclinometers measure the tilt. Power is supplied by a generator placed between the helicopter and the frame.

### **Measurement procedure**

Generally, the configuration of the system is customized for each survey. Measurements are carried out with one or two transmitter moments, depending on the target geology. The standard configuration uses a low (SLM) and a high (HM) transmitter moment applied sequentially. Each sequence has 60 individual transient measurements for the HM, followed by 180 measurements for the SLM (this corresponds to a full measurement cycle in ~1.6 s).

The flight altitude is depending on flight speed, topography, etc. A typical nominal flight altitude is 30-50 m. Over forested areas, the altitude is increased to maintain a necessary safety distance to the treetops. The operating speed is specific for the survey area and target. The nominal speed for the present SkyTEM system was set between 80 and 100 km/h. The chosen speed guaranteed the required lateral resolution for the geological characterization of the area.

Apart from GPS-, altitude- and TEM data, a number of instrument parameters are monitored and stored digitally in order to be used for quality control when the data are processed.

### **Penetration depth**

The penetration depth for the SkyTEM system depends on the moment, the geological conditions (in particular, the electrical conductivity distribution of the subsurface), the level of the background noise and the speed and altitude of the frame. The influence of the latter is important, and to achieve good quality data, the altitude should normally be smaller than 50 m. A penetration depth of approximately 250-300 m can be achieved for the present SkyTEM system for a medium resistivity of 50  $\Omega$ m. During the inversion a depth of investigation is estimated for each resistivity model (see below in this report the associated thematic maps).

### **SkyTEM – technical specifications**

The SkyTEM system was configured in a standard two-moment setup (super low moment, SLM and high moment, HM) to obtain a full dB/dt decay curve (sounding curve).

The system instrument setup is shown in Figure 4. The positioning of the instruments and the corners of the octagon described by the transmitter coil are found in Table 2. The origin is defined as the center of the transmitter coil.

The parameters for the measured moments are summarized in Table 3. The waveforms in the transmitter loops are described by the piecewise linear function in Table 4 (for the SLM) and Table 5 (for the HM). Figures 5-6 and Figures 7-8 shows the ramps up and ramps down of the current during, the SLM and HM phases respectively.

The receiver coil and the receiver instrument are modeled using first order low-pass filters with the values shown in Table 6.

Gate and receiver specifications are summarized in Tables 7 – 8.

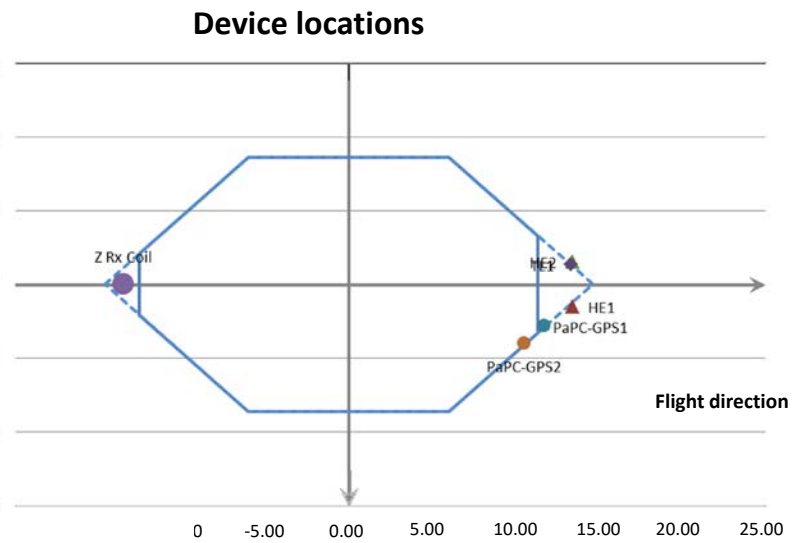


Figure 4. Instrument setup for the SkyTEM system used. The blue polygon represents the transmitter frame; HE1 and HE2 are the altimeters; TL1 and TL2 are the tiltmeters; Z Rx Coil is the Z-component receiver. The axes origin corresponds to the center of the transmitter loop.

Unit	X (m)	Y (m)	Z(m)
GPS1	11.68	2.79	-0.16
GPS2	10.51	3.95	-0.16
HE 1 (Altimeter)	13.44	1.51	-0.14
HE 2 (Altimeter)	13.44	-1.51	-0.14
TL 1 (inclinometer)	-13.31	-1.51	-0.13
TL 2 (inclinometer)	-13.31	1.51	-0.11
Rx (Receiver Coil)	-13.50	0.00	-2.02
Tx (Transmitter Coil)	13.64	-0.16	-0.22
Loop corner 1	-12.64	-2.13	0.00
Loop corner 2	-6.15	-8.59	0.00
Loop corner 3	5.74	-8.59	0.00
Loop corner 4	12.61	-1.72	0.00
Loop corner 5	12.61	1.72	0.00
Loop corner 6	5.74	8.59	0.00
Loop corner 7	-6.15	8.59	0.00
Loop corner 8	-12.64	2.13	0.00

Table 2. Summary of equipment locations and transmitter geometry. The origin is defined as the center of the transmitter coil. Z is negative towards the helicopter (upward).

Parameter	SLM	HM
No. of turns	2	12
Area	344.28 m <sup>2</sup>	344.28 m <sup>2</sup>
Current	~ 6 A	~ 115 A
Tx Moment	~ 4100 Am <sup>2</sup>	~ 475000 Am <sup>2</sup>
Repetition frequency (as in the geometry file)	312.5 Hz	25 Hz
Tx-on-time	8.00E-4 s	5.00E-4 s
Tx-off-time	1.422E-4 s	15E-4 s
Waveform	piece-wise linear	piece-wise linear
Duty cycle	36%	50%

Table 3. Summary of SLM and HM specifications.

Time (s)	Normalized current
-3.0220E-03	0.0000E+00
-2.8502E-03	-2.4971E-001
-2.6570E-03	-4.7453E-001
-2.3142E-03	-8.9044E-001
-2.2241E-03	-1.0000E+000
-2.2219E-03	-1.0000E+000
-2.2213E-03	-9.7325E-001
-2.2199E-03	-7.9865E-001
-2.2182E-03	-5.3172E-001
-2.2163E-03	-2.7653E-001
-2.2148E-03	-1.5062E-001
-2.2135E-03	-7.5073E-002
-2.2119E-03	-3.1423E-002
-2.2100E-03	-7.9197E-003
-2.2089E-03	0.0000E+00
-8.0000E-04	0.0000E+00
-7.6473E-04	6.3431E-002
-6.2818E-04	2.4971E-001
-4.3497E-04	4.7453E-001
-9.2197E-05	8.9044E-001
-2.0929E-06	1.0000E+000
6.6270E-08	1.0000E+000
6.9564E-07	9.7325E-001
2.1480E-06	7.9865E-001
3.7941E-06	5.3172E-001
5.6822E-06	2.7653E-001
7.1829E-06	1.5062E-001
8.5385E-06	7.5073E-002
1.0136E-05	3.1423E-002
1.1976E-05	7.9197E-003
1.3138E-05	0.0000E+00

Table 4. Piecewise linear description of the SLM waveform as it has been used during the processing and inversion.

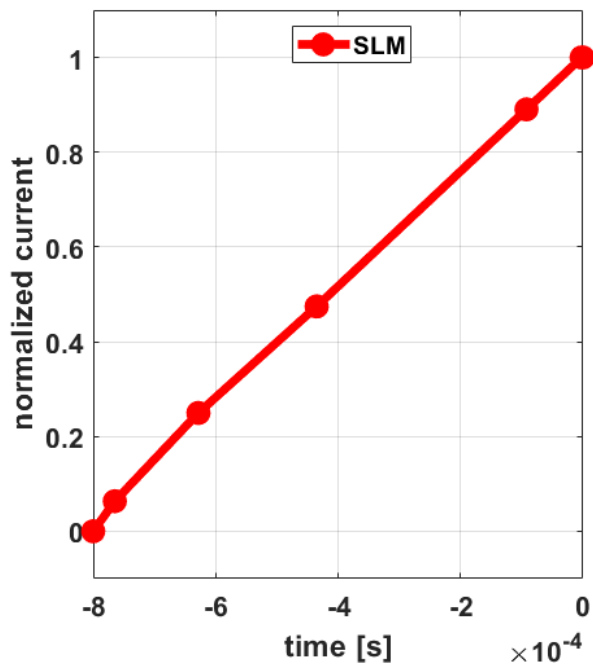


Figure 5. Ramp up of the SLM waveform

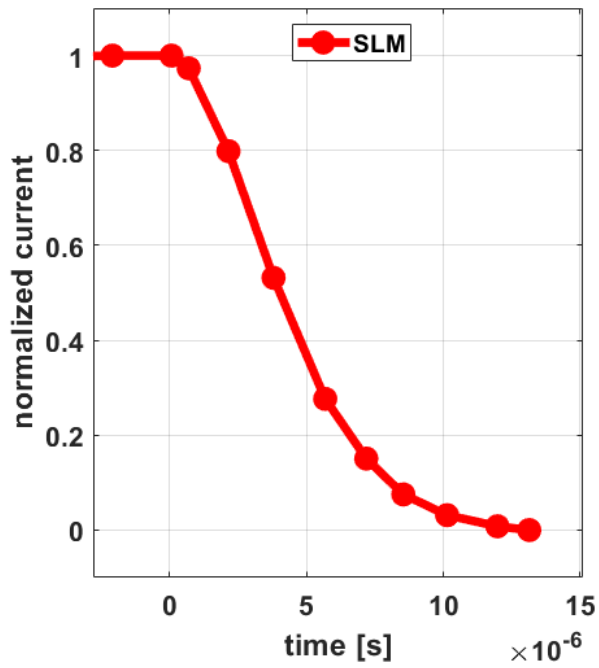


Figure 6. Ramp down of the SLM waveform

Time (s)	Normalized current
-2.5000E-002	0.0000E+00
-2.4868E-002	-4.9380e-001
-2.4708E-002	-9.2737e-001
-2.4690E-002	-9.5949e-001
-2.0000E-002	-1.0000e+000
-1.9993E-002	-9.7920e-001
-1.9900E-002	-6.9067e-001
-1.9713E-002	-6.5734e-002
-1.9698E-002	-1.5661e-002
-1.9695E-002	-7.0146e-003
-1.9693E-002	-2.8248e-003
-1.9688E-002	0.0000E+00
-5.0000E-003	0.0000E+00
-4.8681E-003	4.9380e-001
-4.7076E-003	9.2737e-001
-4.6904E-003	9.5949e-001
0.0000E+00	1.0000E+00
7.2018E-006	9.7920e-001
9.9971E-005	6.9067e-001
2.8748E-004	6.5734e-002
3.0229E-004	1.5661e-002
3.0504E-004	7.0146e-003
3.0705E-004	2.8248e-003
3.1197E-004	0.0000E+00

Table 5. Piecewise linear description of the HM waveform as it has been used during the processing and inversion.

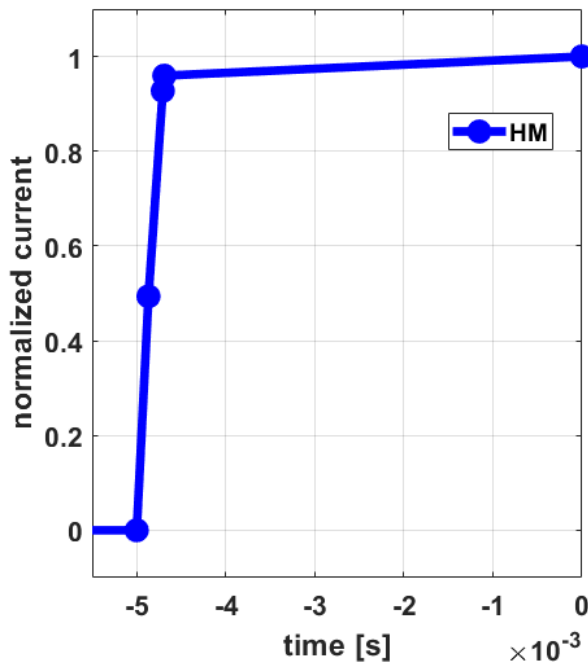


Figure 7. Ramp Up of the HM waveform

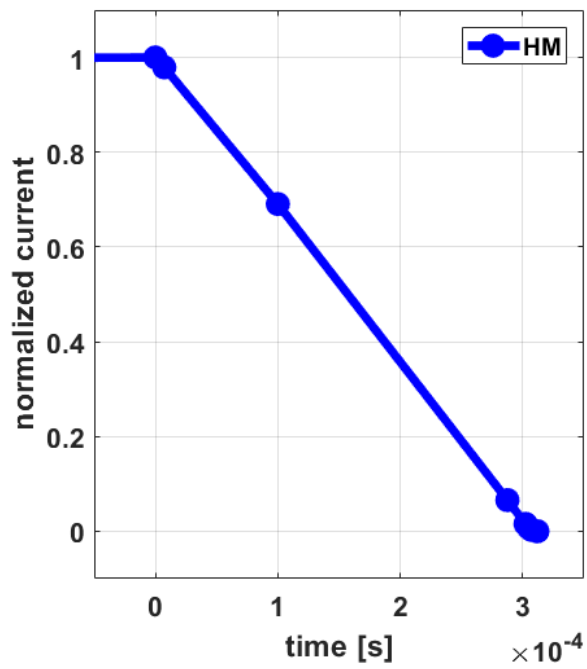


Figure 8. Ramp Down of the HM waveform

Filters	Frequency (kHz)
Receiver Coil	210
Receiver Instrument	300

Table 6. Low-pass filters for the entire survey.

Gate No.	Gate center time [s]	Gate start time [s]	Gate width [s]	SLM	HM
1	0.715E-6	0.43E-6	0.57E-6		
2	2.215E-6	1.43E-6	1.57E-6		
3	4.215E-6	3.43E-6	1.57E-6		
4	6.215E-6	5.43E-6	1.57E-6		
5	8.215E-6	7.43E-6	1.57E-6		
6	10.215E-6	9.43E-6	1.57E-6		
7	12.215E-6	11.43E-6	1.57E-6		
8	14.715E-6	13.43E-6	2.57E-6	█	
9	18.215E-6	16.43E-6	3.57E-6		
10	22.715E-6	20.43E-6	4.57E-6		
11	28.215E-6	25.43E-6	5.57E-6		
12	35.215E-6	31.43E-6	7.57E-6		
13	44.215E-6	39.43E-6	9.57E-6		
14	55.715E-6	49.43E-6	12.57E-6		
15	70.215E-6	62.43E-6	15.57E-6		
16	88.215E-6	78.43E-6	19.57E-6		
17	110.715E-6	98.43E-6	24.57E-6		
18	138.715E-6	123.43E-6	30.57E-6		█
19	174.215E-6	154.43E-6	39.57E-6		
20	219.715E-6	194.43E-6	50.57E-6		
21	276.715E-6	245.43E-6	62.57E-6		
22	348.715E-6	308.43E-6	80.57E-6		
23	439.715E-6	389.43E-6	100.57E-6		
24	553.715E-6	490.43E-6	126.57E-6		
25	697.715E-6	617.43E-6	160.57E-6		
26	879.215E-6	778.43E-6	201.57E-6		
27	1107.715E-6	980.43E-6	254.57E-6		
28	1396.215E-6	1235.43E-6	321.57E-6		
29	1760.215E-6	1557.43E-6	405.57E-6		
30	2218.715E-6	1963.43E-6	510.57E-6		
31	2796.715E-6	2474.43E-6	644.57E-6		
32	3525.715E-6	3119.43E-6	812.57E-6		
33	4444.715E-6	3932.43E-6	1024.6E-6		
34	5603.215E-6	4957.43E-6	1291.6E-6		
35	7063.215E-6	6249.43E-6	1627.6E-6		
36	8904.215E-6	7877.43E-6	2053.6E-6		
37	1044.215E-6	9931.43E-6	2225.6E-6		
38	3312.215E-6	12157.43E-6	2309.6E-6		

Table 7. Gate specifications. Center times for both SLM and HM are shifted according to calibration time shift in Table 9. Grey bars indicate the gates that are actually considered during the data processing. Note that the earliest and latest gates actually used in the inversion highly depend on the local resistivity values and noise conditions.

Parameter	SLM	HM
Front gate time	0.0E-6 s	370.7E-6 s
Number of shoots per cycle	180	60
Gates measured	1-27	1-38
Gates considered	8-27	12-38

Table 8. Receiver specifications.

## 2.3 Calibration of the SkyTEM system

Prior to the survey, the SkyTEM equipment was calibrated by SkyTEM Surveys ApS on the Danish national TEM test site near Aarhus, Denmark. The calibration is performed to establish the absolute time shift and data level in order to facilitate precise data modeling. No additional leveling, or drift corrections are applied subsequently.

In order to perform the calibration, all system parameters (transmitter waveform, low pass filters, etc.) must be known to allow modeling of the used SkyTEM configuration.

The calibration constants are determined by comparing a recorded SkyTEM response on the test site with the reference response. The reference response is calculated from the test site reference model for the used SkyTEM configuration. This procedure is repeated for a number of different attitudes.

Documentation of the calibration can be found in the SkyTEM Surveys ApS data acquisition report SkyTEM, 2015. Final calibration constants are summarized in Table 9.

Moment	Time Shift	Scale Factor
SLM	-1.8 $\mu$ s	0.94
HM	-1.8 $\mu$ s	0.94

Table 9. Calibration constants with regards to the Danish national TEM test site reference model.

## 2.4 SkyTEM repeatability test

To monitor that there are no changes to the system during the mapping, repeated measurements are performed by hovering on a specific spot as described in the data acquisition report (SkyTEM, 2015).

## 2.5 High altitude test

A high-altitude test was conducted near the test area to identify the system response. The test is performed by measuring at an altitude where the ground response is negligible. The

documentation for the high-altitude tests can be found in the SkyTEM Surveys ApS data acquisition report (SkyTEM, 2015).

## **2.6 Bias tests during production flight**

Each production flight includes bias tests performed on the way to and from the production lines. Where cloudiness permitted, they were performed at altitudes of 400 m or more. The bias tests are similar to the high-altitude test and serve to identify changes in the system response between flights and to assess the Primary Filed Correction (PFC) and be able to apply the proper adjustments to the first SLM gates. During the present survey, the PFC was applied to gates 1-12.

### 3. Processing of the SkyTEM data

The software package Aarhus Workbench was used for the processing of the collected data. The aim of processing is to prepare data for the geophysical inversion. The primary processing includes filtering and averaging of data as well as cutting and discarding of distorted or noisy data. The data are stored in a database. The settings for the different processing steps are also stored.

The processing workflow can be divided into the following steps:

1. Import of raw data into a database structure. The raw data appear in the form of .dat, .sps and .geo files. Dat files contain the actual transient data from the receiver; sps files deal with GPS positions, tilts, altitudes, transmitter currents etc.; and the .geo file concerns the system geometry, low-pass filters, calibration parameters, turn-on and turn-off ramps, calibration parameters, etc. For a description of the SkyTEM file formats see HydroGeophysics Group 2011. These files were provided by SkyTEM.
2. Automatic processing: First, an automatic processing of the four data types is used. These are GPS-, altitude-, tilt- and TEM data. This automatic processing is based on a number of criteria adjusted to the survey concerned.
3. Manual processing: inspection and correction of the results of the automatic processing for the data types in question.
4. Adjustment of the data processing based on preliminary inversion results.

All data is recorded with a common time stamp. This time stamp is used as a reference to handle different data types collected in different instants by several devices. The time stamp is given as the GMT time.

In the following a short description of the processing of the different data types is shown. A more thorough description of the SkyTEM processing module of the Aarhus Workbench can be found in HydroGeophysics Group, 2011.

#### 3.1 Positioning

The position of the frame is measured with two independent GPS receivers, which record data continuously with an uncertainty of ~3 m.

#### 3.2 Tilt data

The roll and the pitch of the frame are measured and used to correct the altitude and voltage data. It is presumed that the frame is rigid so that the tilts of the transmitter and receiver are identical. During the processing, a running mean is calculated for the roll and the pitch.

### 3.3 Altitude data

The distance between the transmitter coil and the ground is measured with two independent lasers. Figure 9 shows an example of a typical altitude dataset over open land and a small portion covered by high vegetation.

The aim of the altitude data processing is to remove reflections that do not come from the ground - typically reflections from treetops. The processing is based on the fact that reflections from tree tops etc. result in an apparently lower altitude. Altitude processing is done using an algorithm that filters out data by repeatedly making a polynomial fit to the data while removing data that are some meters below this polynomial. Thereby reflections from treetops are removed. The automatic filtering is followed by a manual inspection and correction. In the end the individual soundings are assigned the correct elevation by using a dense Digital Elevation Model (DEM, here with a grid spacing of 5 m).

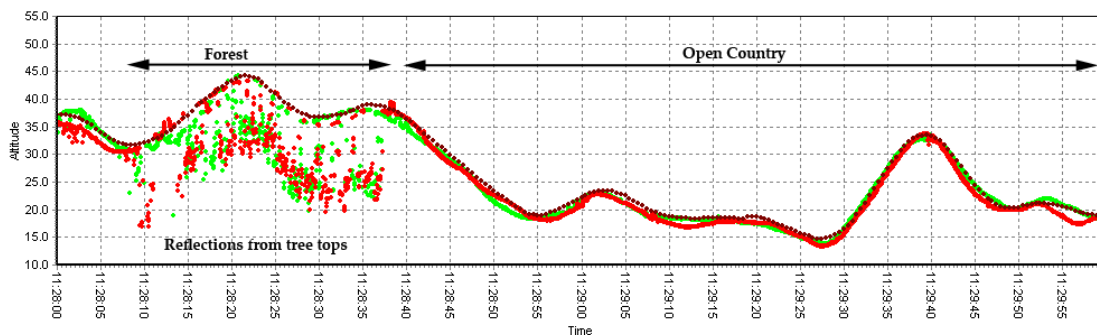


Figure 9. Green and red dots are raw data from the two laser altimeters. Brown dots are the resulting altitude after filtering the data. The time window holds approximate 2 km of data.

### 3.4 Voltage data

The Voltage data are gathered continuously along the flight lines and alternately with a low and a high moment. The processing of voltage data is done in a two-step system approach with alternating an automatic and a manual part. In the former, data are corrected for the transmitter/receiver tilt, and a number of filters designed to cull coupled or noise influenced data are deployed. Further-more, data are averaged to increase the signal-to-noise ratio using a trapezoidal averaging core, where the averaging width of late-time data is larger than that of early-time data, as seen in Figure 10. The data uncertainty is calculated from the data stack. Furthermore, a small uniform data uncertainty of 3% is assigned to all data. Soundings are typically taken out for every 20-30 m depending on flight speed, SkyTEM-setup and target. In the present survey the raw soundings are spaced by about 20 m. The average soundings have the same spacing, but the final lateral resolution of the top 30 m is more likely about 30-50 m depending on the ground resistivity due to the lateral integration of the transmitter loop and to the diffu-sivity of the EM field.

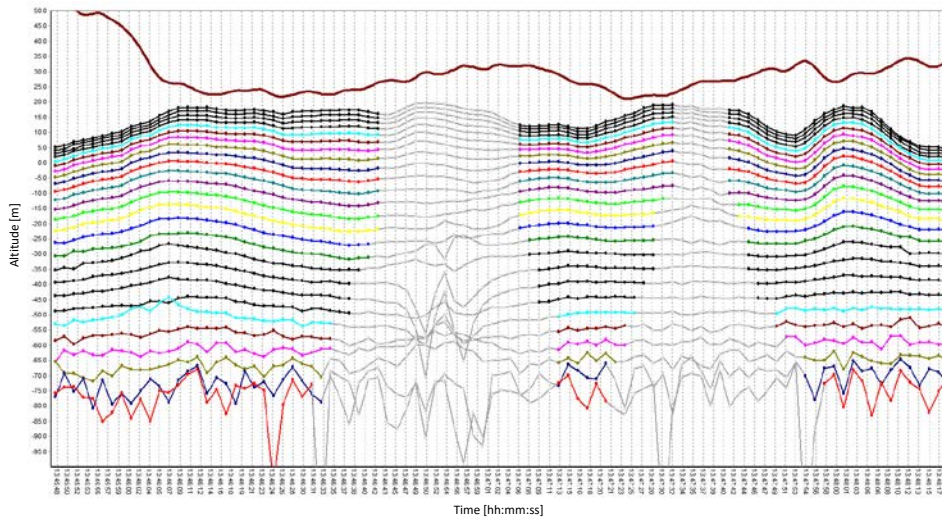


Figure 10. The section displays 3 minutes (~3.5 km) of data. The upper solid brown curve shows the flight altitude (the altitude axis is on the left of the panel). Each of the lower dot curves shows raw HM data for a given gate time. So, the black dot line represents gate 13 of the HM, the orange one the gate 38. The grey lines represent data that have been removed due to couplings. Two couplings can clearly be spotted at ~13:46:54 and 13:47:39. Comparing these locations with a map, it is seen that both couplings have been associated with installations along roads. The couplings particularly affect the late-time signal (the lower curves).

After the automatic processing, soundings were inspected visually using several different data plots. At this stage it is assessed whether data points should be ascribed a higher uncertainty or removed entirely. The evaluation is done by looking at the decay curves, the distance to potential noise sources and the noise measurements. The survey area is significantly urbanized and, so, it is crossed by a number of power lines, roads and characterized by infrastructures. Data collected nearby these installations are often coupled. Hence, it is necessary to inspect all data and remove coupled data when found, in order to produce geophysical maps without artefacts generated by the effects of manmade installations rather than actual geology. In some cases it is not possible to identify the source of the coupling even though data clearly show that there must be a source. Figure 10 shows an example of strongly coupled data near two roads. Once the couplings have been removed, the data are stacked into soundings. The stacked data are then inspected to exclude the part of the late-time data where the background random noise level reaches the level of the earth response. For a description of noise contamination in electromagnetic data, see Munkholm and Auken, 1996.

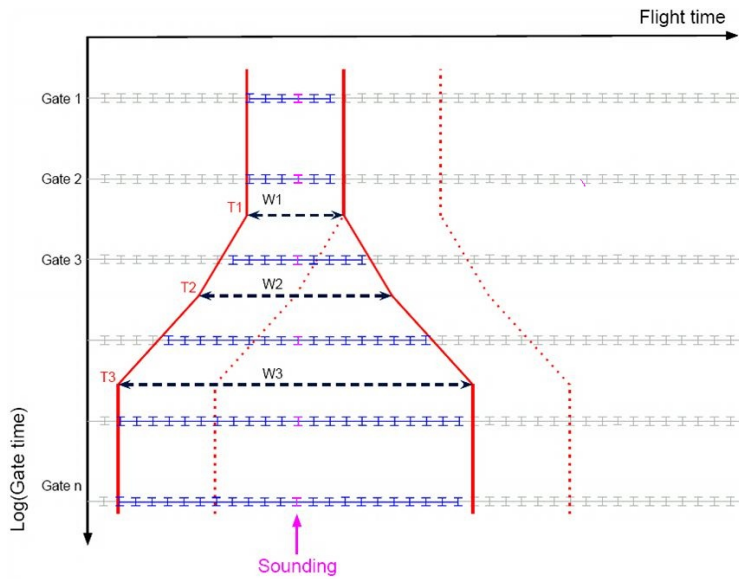


Figure 11. Trapezoid averaging of TEM-data. The raw data series within the red lines (blue points/error bars) are averaged yielding the sounding marked by violet points/error bars. The averaging trapezoid is subsequently moved (red dashed line), and a new sounding is created. The times T1-3 and widths W1-3 define the trapezoid.

### 3.5 Processing - Technical specifications

Table 10 shows the processing settings used in the Aarhus Workbench.

Item		Value
Software	Aarhus Workbench Version	4.2.13
Noise Processing	Data uncertainty: Uniform data STD	Estimated from data stack 3%
Trapezoid filter for flight altitudes	Sounding distance SLM, times: T1, T2, T3 [s] SLM, width: W1, W2, W3 [s] HM, times: T1, T2, T3 [s] HM, width: W1, W2, W3 [s]	0.5s (~20 m) 1e-5, 1e-4, 1e-3 2.5, 4, 12 1e-4, 1e-3, 1e-2 5, 8, 24

Table 10. Processing settings (See Figure 11 for Trapezoid filter description).

## 4. Inversion of the SkyTEM data

Inversion and evaluation of the inversion result were done using the Aarhus Workbench software package. The underlying inversion code is developed over the years by many present and past members of the HydroGeophysics Group, Aarhus University, Denmark (see, for example, Auken et al., 2014).

### 4.1 Spatially constrained inversion

The spatially constrained inversion (SCI) uses constraints between the 1D-models, both along and across the flight lines, as shown in Figure 12. The inversion is a 1D full non-linear damped least-squares solution in which the transfer function of the instrumentation is modeled. The transfer function includes turn-on and turn-off ramps, front gate, low-pass filters, and transmitter and receiver positions. The flight altitude contributes to the inversion scheme as a model parameter with the laser altimeter readings as a constrained prior value.

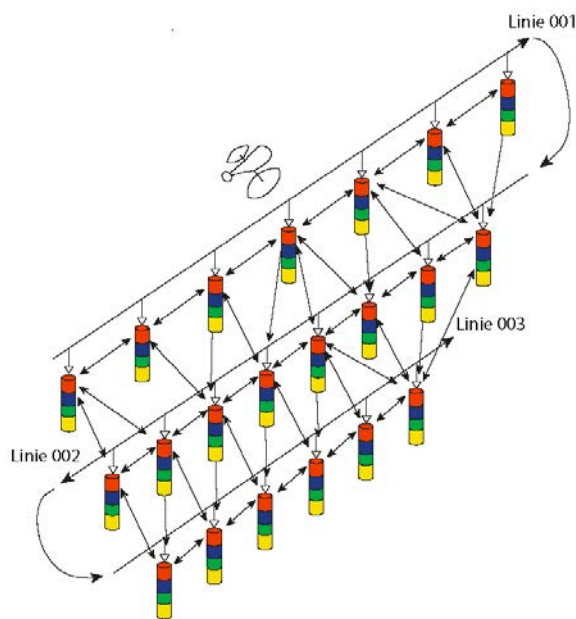
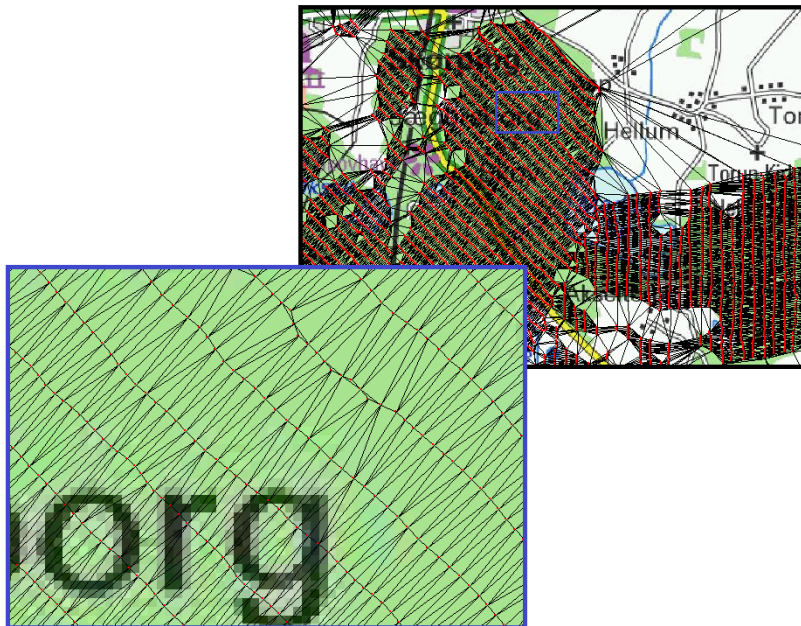


Figure 12. Schematic presentation of the SCI concept. Constraints connect, not only soundings located along the flight line, but also those across them.

In the SCI scheme, the model parameters are tied together with a spatially dependent covariance scaled according to the distance between soundings. The constraints between the soundings are designed using Delaunay triangles (see Figure 13). In this way each sounding is linked to its "best companions". For Airborne EM surveys, Delaunay triangulation always

connects a sounding to its two nearest soundings along the flight line and one or more soundings on each of the adjacent flight lines, which is the preliminary condition for breaking down the line orientation in the data.



*Figure 13. Example of setup of SCI-constraints. The red points are the sounding positions. The black lines show the constraints created with the Delaunay triangles. The line distance in this example is 160 m and the zoomed area is approximately 1.2 x 0.85 km large*

In addition to constraints on model parameters (resistivities, layer interfaces), there are also lateral constraints on the altitude, however, only along the flight line.

Constraining the parameters enhances the resolution of resistivities and layer interfaces which are not well resolved in an independent inversion of the soundings.

The SCI inversion scheme uses a domain parameterization consisting of many layers. In this specific project, 29 layers have been used in order to minimize the effects of discretization on the regularization (and, in turn, to the final solution). Each layer has a fixed thickness, but its (homogeneous) resistivity value is free to vary during the inversion. Vertical constraints are applied to the smooth models to stabilize the inversion. Further details about the SCI-inversion scheme can be found in Viezzoli et al., 2008; Vignoli et al., 2014 and Vignoli et al. 2017.

The SCI-setup parameters for this survey are listed further below in this report.

## 4.2 Depth of Investigation (DOI)

A concept of estimating the depth of investigation (DOI) (Christiansen and Auken, 2010) for the individual models has been applied to this survey. The DOI calculation takes into account the SkyTEM system transfer function, the number of data points, and the data uncertainty.

EM fields are diffusive, and there is no specific depth below which there is no information on the resistivity structure. Therefore, two numbers are presented for the DOI – an upper and a lower number. As a guideline, the sensitivity of the data to the resistivity of the layers above DOI upper is significant. Between DOI upper and DOI lower, the model parameters do not have a strong impact on the data, and below DOI lower the data are weakly affected by the resistivity values. So, interpreting the model parts below the DOIs should be done with utmost caution.

### **DOI – technical description**

Depth of investigation (DOI) is a useful tool for evaluation of inversion results and holds useful information when a geological interpretation is made. However, for diffusive methods, such as ground based or airborne EM, there is no specific depth below which there is no information on the resistivity structure. The question is to which depth the model is most reliable.

The DOI-method used by Aarhus Workbench is based on the actual inverted model, and it includes the full system transfer function and system geometry, using all measured data and their uncertainties. The methodology is based on a calculated sensitivity (Jacobian) matrix of the final model. A priori information, model constraints or other information added to the system are not considered. Thus, the DOI is purely data driven.

To demonstrate the methodology, an example with a SkyTEM setup with the last gate at 3 ms is used. Assuming a simple 3-layer model, the sensitivity function can be plotted versus depth (left image in Figure 14). As expected, the sensitivity to the second layer is low, whereas there are high sensitivities to the first and the third layers.

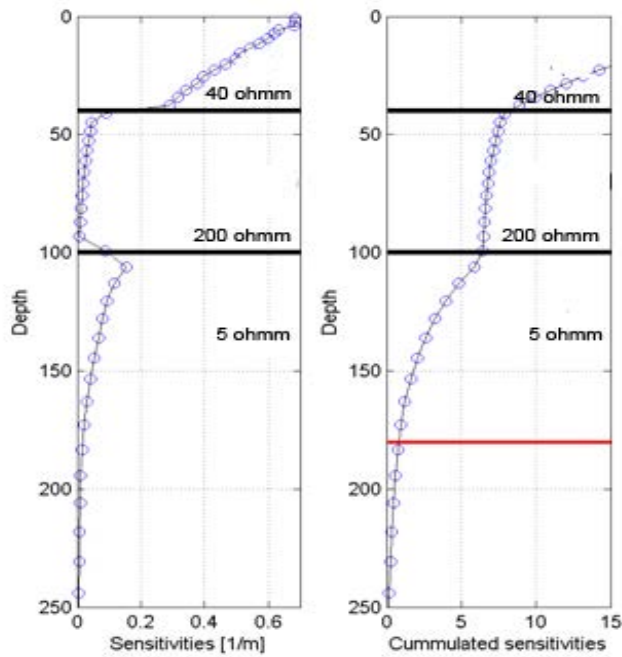


Figure 14. Sensitivities calculated for a (re)discretized version of the model indicated by the black lines; resistivities of layers are written on the plot. The left plot is the sensitivity function itself. The right panel shows the cumulated sensitivities. The red line indicates the DOI given by the global threshold value.

If the sensitivities are summed up from deep to shallow, the right-side image in Figure 4 emerges. This plot shows the total sensitivity in a given depth and downwards. Next, a thresh-older value that indicates the minimum amount of sensitivity needed for indicative information is set. In the example in Figure 4, a threshold value of 0.8 was settled upon, giving a DOI of approximately 180 m.

Setting the threshold value is pretty much a question of tuning based on experience and comparing different models with different methods. The threshold value used here has been tested on many different models and with different systems and produces trustworthy results in the majority of the cases.

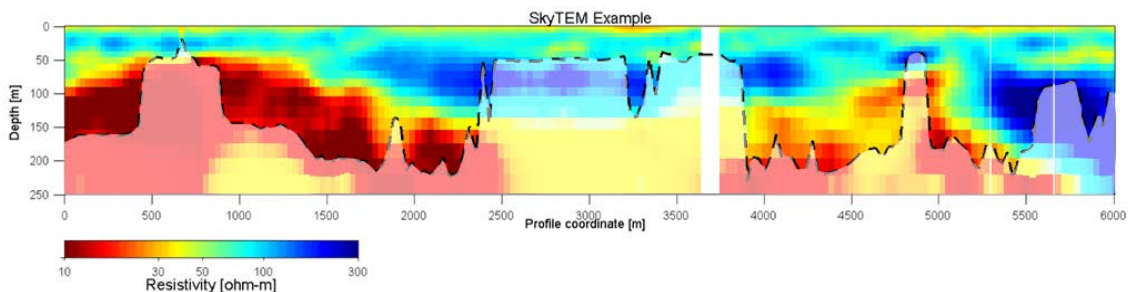


Figure 15. SkyTEM resistivity section example with DOI shown as a black dashed line. In the area at 600 m, the DOI indicates that there is no information on the less

conductive structure. In the area at 3000 m the high-moment data are missing, which results in a shallower DOI.

Given this definition of DOI, it can happen that it is well above the deepest layers. Figure 15 shows an inversion example of airborne data collected in Denmark: the black dashed line indicates the DOI. In the area at 600 m, the DOI indicates that data have no information on the less conductive structure (hence its presence in the reconstructed resistivity distribution is most likely due merely to the resistivity starting model rather than the sensitivity of the data to the geology at that depth). The area at 3000 m indicates an area where the high-moment data are missing, which means a shallower DOI.

### 4.3 Inversion - Technical specifications

The inversion settings used for the smooth inversion in the Aarhus Workbench are listed below.

Item		Value
Software	Aarhus Workbench Version	4.2.13
SCI models	Number of inverted soundings	5830
Starting model	Number of layers	29
	Starting resistivities [ $\Omega\text{m}$ ]	varying*
	Thickness of first layer [m]	4.0
	Depth to last layer [m]	450.0
	Thickness distribution of layers	Log increasing with depth
SCI constraint/ Prior constraint	Horizontal constraints on resistivities [factor]	2.0**
	Reference distance [m]	30
	Power law scaling dependency	2
	Vertical constraints on resistivities [factor]	4.0
	Prior, thickness	Fixed
	Prior, resistivities	None
	Prior on flight altitude [m]	+/- 1
	Lateral constraints on flight altitude [factor]	1.3
	Minimum number of gates per moment	7

Table 11. Inversion settings, 29-layer SCI setup. \*The starting model has been automatically selected based on the sounding curve values. \*\*This is the value used for the lateral constraints as defined in Aarhus Workbench (it corresponds to 1.0 accordingly to the definition in Aarhusinv). This is a quite loose constrain with respect to those generally used in Denmark; the reason is that the Varde's area presents a particularly complex geology with significant lateral variations.

# 5. Thematic maps and cross sections

To visualize the resistivity structures in the mapping area, a number of geophysical maps and cross sections have been created from the smooth inversion results by using the Aarhus Workbench. Furthermore, a location map and a number of maps made for quality control (QC-maps) are found in the appendices to this report. The Aarhus Workbench Workspace that holds the inversion results including mean resistivity maps, cross sections, etc. is enclosed to the pre-sent report as well.

## 5.1 Mean resistivity maps

The inversion result consists of a large number of 1D-models described by depth intervals (i.e. layers) and resistivities within each model. These are then normally used to calculate mean resistivities to obtain a visualization of the resistivity distribution in the mapping area. Figure 16 shows how the resistivities of the layers in a model influence the calculation of the mean resistivity in a depth interval [A, B].  $d_0$  is the surface,  $d_1$ ,  $d_2$  and  $d_3$  are the depths to the layer boundaries in the model.  $\rho_1, \rho_2, \rho_3$  and  $\rho$  are the resistivities of the layers.

The model is subdivided into sub-thicknesses  $\Delta t_{1-3}$ . The mean resistivity ( $\rho_{vertical}$ ) is calculated as:

$$\rho_{vertical} = \frac{\rho_1 \cdot \Delta t_1 + \rho_2 \cdot \Delta t_2 + \rho_3 \cdot \Delta t_3}{\Delta t_1 + \Delta t_2 + \Delta t_3}$$

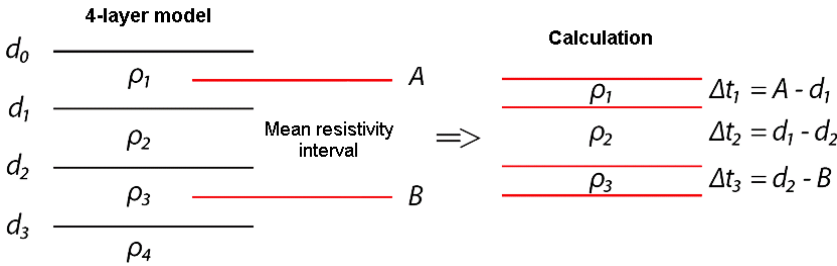


Figure 16. The figure illustrates how the resistivities of the layers influence the mean resistivities in a depth interval [A,B]

Hence, in general, the mean resistivity in a depth interval is calculated using the equation below:

$$\bar{\rho} = \frac{\sum_{i=1}^n \rho_i \cdot \Delta t_i}{\sum_{i=1}^n \Delta t_i}$$

where  $i$  runs through the interval from 1 to the number of sub-thicknesses. The mean resistivity calculated by the above ( $\rho_{vertical}$ ) is named the vertical mean resistivity - equal to the total resistance if current flows vertically through the interval.

When the TEM method is used, the current flows only horizontally in the ground. Therefore, the mean resistivity is calculated as if the current runs horizontally in the depth interval. This resistance is described as the horizontal mean resistance ( $\rho_{horizontal}$ ) and is the reciprocal of the mean conductivity ( $\sigma_{mean}$ ). The horizontal mean resistivity is calculated in the following way:

$$\rho_{horizontal} = \frac{1}{\sigma_{mean}} = \left[ \frac{\sum_{i=1}^n \left( \frac{1}{\rho_i} \right) \cdot \Delta t_i}{\sum_{i=1}^n \Delta t_i} \right]^{-1}$$

Normally, there is no major difference in the maps of mean resistivities calculated in the two different ways. The horizontal mean resistivity weights the low resistivities more than the vertical mean resistivities in exactly the same way as the TEM-method does.

For this report, elevation horizontal mean resistivity themes have been generated from the 29-layer model inversion. The elevation slices are all 5 m thickness (note that the vertical resolution of TEM results is still decaying with depth). The DOI has been used to blind resistivities of models below the DOI lower. The generated themes, consisting of mean resistivity values at each sounding position, are then gridded using the Kriging (Pebesma and Weseling, 1998), with a node spacing of 20 m and a search radius of 300 m. Elevation slices can be found in Appendix II.

## 5.2 Cross sections

Several cross sections covering the two survey areas in a regular grid is plotted in Appendix III. Each cross section shows a slice through an interpolated resistivity grid overlaid by the actual 1D models retrieved by the inversion procedure. The individual 1D resistivity models are shaded by using the corresponding DOI lower value for that specific model.

## 5.3 Location map, QC-maps

The maps listed below are included in Appendix I:

### Model locations and flight lines

This map shows the flight line positions overlaid by the model positions. Where no models are present, data has been discarded due to coupling. Line turns and some non-production intervals are also marked as discarded data. The couplings are mainly associated with major roads and power lines.

**Moment indications**

This map shows the moments (low/high) present in each model. Both moments are in general present for the whole survey. Due to the moment sampling, models with a single moment can often be observed after intervals where data has been discarded. In some cases, coupling have only affected one of the moments and it has been possible to keep the other moment.

**Flight altitude**

This map shows the processed flight altitudes (heights) from the laser altimeters. The flight altitude reflects the necessary safety distance to the treetops, the ground and any man-made structures. In addition to a few forested areas there are some man-made structures that have caused the pilot to go to higher altitudes. The nominal flight altitude without particular obstacle is about 30 m.

**Data residual**

This map shows the data residual (the data fit) for the individual models of the smooth model inversion. The data residual is normalized with the data standard deviation, so a data residual below one corresponds to a data misfit within the data standard deviation. In general, the data residual is low (below one).

**Depth of investigation (DOI) as depth**

This map shows the DOI lower (as depth) based on the model inversion (see the section above in this report for a description of the DOI-calculation). The DOI lower varies considerably over the survey area mainly due to hydrology, geology and number of data points.

**Depth of investigation (DOI) as elevation**

The same as before, but now the DOIs are displayed in elevation instead of depth.

## 6. Conclusion

The discussed field campaign was performed in the surrounding of Varde. In that occasion, dual-moment, time-domain electromagnetic data were acquired by SkyTEM. The collected data were afterwards carefully processed to remove couplings and noise in preparation to the inversion. The inversion was done with a multi-layer model using the spatially constrained inversion (SCI) approach.

Differently from what is usually done, the processing and inversion of the Varde dataset have not been performed in a unique phase. In fact, the resistivity distribution has not been simply delivered to the geological interpreter (without any following attempt of incorporating geological feedbacks into the geophysical inversion). Instead, GEUS has implemented an iterative workflow where all the processing and inversion steps (and their effects on the final result) have been carefully discussed with the geologists. The idea is, that in any case, the geophysical data processing is the first step of the geological interpretation. This is actually the real rationale behind the regularized inversion: the goal is not to merely provide a smooth solution to the interpreter, but rather to include any possible piece of prior geological information into the inversion process in order to select, among all the possible solutions compatible with the geophysical data, the one, that at the same time, better matches the geological expectations.

This approach has guaranteed: the reconstruction of quite complex geological features (highly non-1D, hence, otherwise, difficult to infer in a 1D scheme as the one implemented in Aarhus Workbench); the detection of areas that follow-up field surveys have confirmed to be a buried valley, that, in turn, could be potential reservoirs of good quality water; and, the minimization of the number of soundings (and data points) that needed to be removed compared to a standard (conservative) processing. In this respect, for example, we could safely use earlier gates with respect to those originally suggested by SkyTEM.

## 7. References

- Christiansen, A. V. and Auken, E., 2010, A Global Measure for Depth of Investigation, Proceedings of the EAGE-NS, Zurich.
- HydroGeophysics Group, 2011, Guideline and standards for skytem measurements, processing and inversion, [www.hgg.au.dk](http://www.hgg.au.dk)
- Jørgensen, F., Lykke-Andersen, H., Sandersen, P., Auken, E. and Nørmark, E., 2003a, Geophysical investigations of buried Quaternary valleys in Denmark: An integrated application of transient electromagnetic soundings, reflection seismic surveys and exploratory drillings: *Journal of Applied Geophysics*, 53, 215-228.
- Jørgensen, F., Sandersen, P. and Auken, E., 2003b, Imaging buried Quaternary valleys using the transient electromagnetic method: *Journal of Applied Geophysics*, 53, 199-213.
- Munkholm, M.S. and Auken, E., 1996, Electromagnetic noise contamination on transient electromagnetic soundings in culturally disturbed environments. *Journal of Environmental & Engineering Geophysics*, Vol. 1, Issue 2, 119-127.
- Nabighian, M. N. and Macnae, J. C., Time Domain Electromagnetic Prospecting Methods. In Nabighian, M. N. (editor), 1991, *Electromagnetic Methods in Applied Geophysics*, Vol. 2, Application, Part A, SEG.
- Pebesma, E. J. and Wesseling, C. G., 1998, Gstat: A Program for geostatistical Modelling, Prediction and Simulation: *Computers & Geosciences*, 24, 17-31.
- SkyTEM ApS, 2015, SkyTEM kortlægning af: Varde Afrapportering af rådata.
- Sørensen, K. and Auken, E., 2004, SkyTEM - a new high-resolution helicopter transient electromagnetic system: *Exploration Geophysics*, 35, 191-199.
- Viezzoli, A., Christiansen, A. V., Auken, E., and Sørensen, K. I., 2008, Quasi-3D-modeling of airborne TEM data by Spatially Constrained Inversion: *Geophysics*, 73, F105-F113.
- Vignoli, G., Fiandaca, G., Christiansen, A. V., Kirkegaard, C., and Auken, E., 2014, Sharp spatially constrained inversion with applications to transient electromagnetic data: *Geophysical Prospecting* doi: 10.1111/1365-2478.12185
- Vignoli, G., Sapia, V., Menghini, A., and Viezzoli, A., 2017, Examples of Improved Inversion of Different Airborne Electromagnetic Datasets Via Sharp Regularization: *Journal of Environmental & Engineering Geophysics* 22(1):51-61 doi: 10.2113/JEEG22.1.51

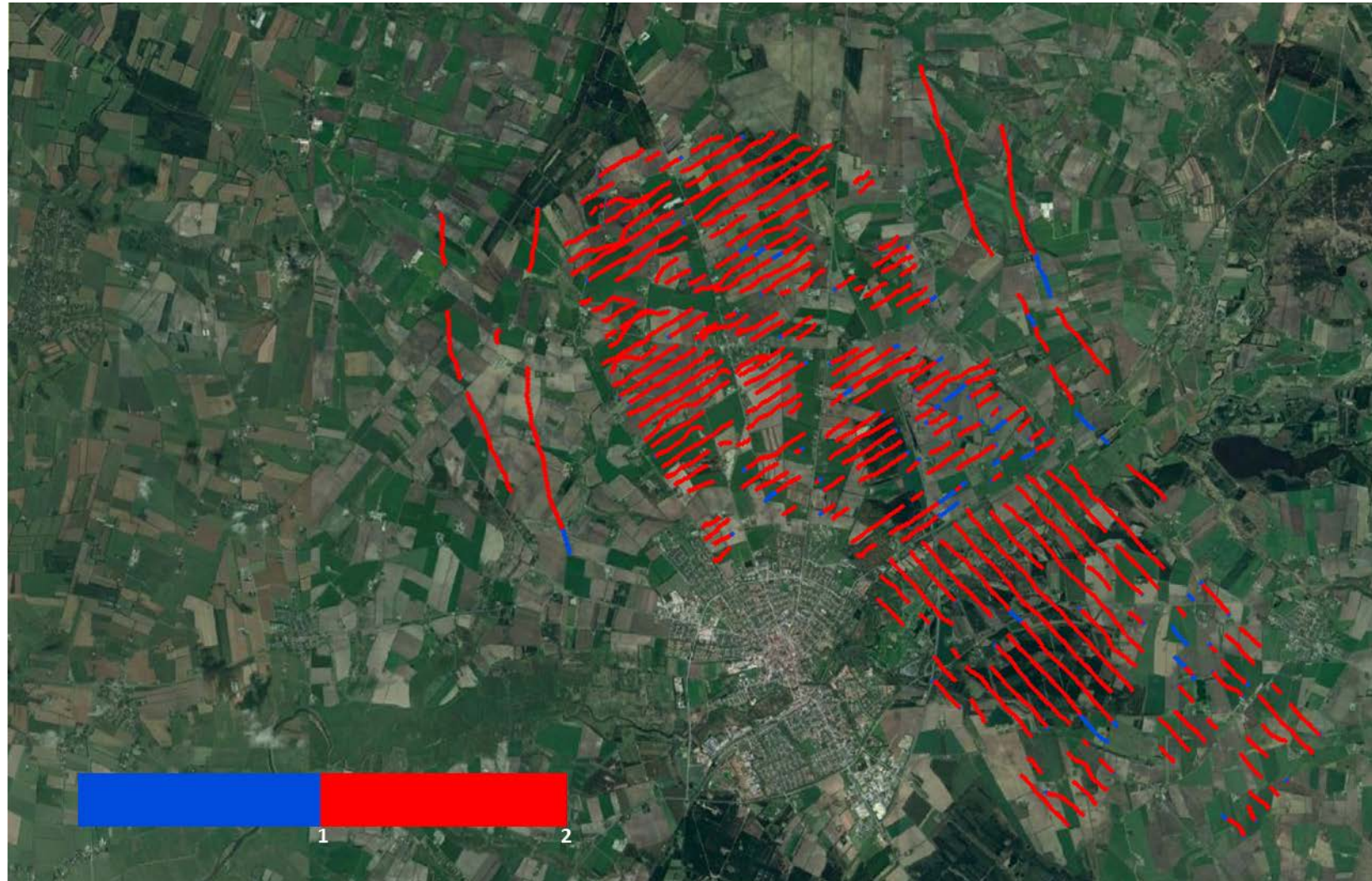
# **Appendix I: Loction maps, QC maps**



## Model locations and flight lines

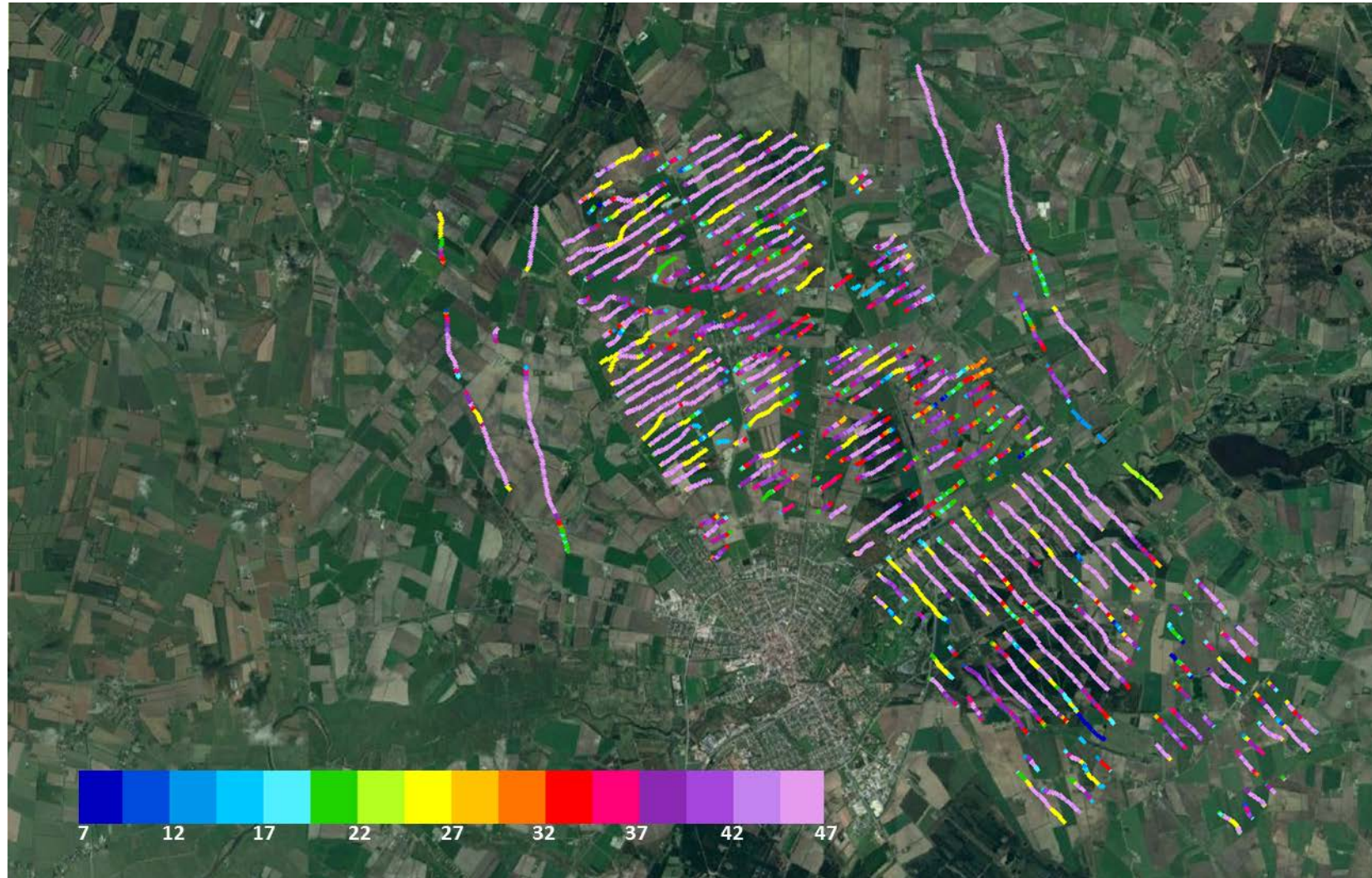
The two parts of the Varde survey's area:

- i) The purple dots represent the location of the soundings collected during the first day of acquisition.
- ii) The turquoise dots show the locations of the data collected during the second day.
- iii) The yellow dots are the location of the soundings actually inverted (those remaining after the manual data processing).



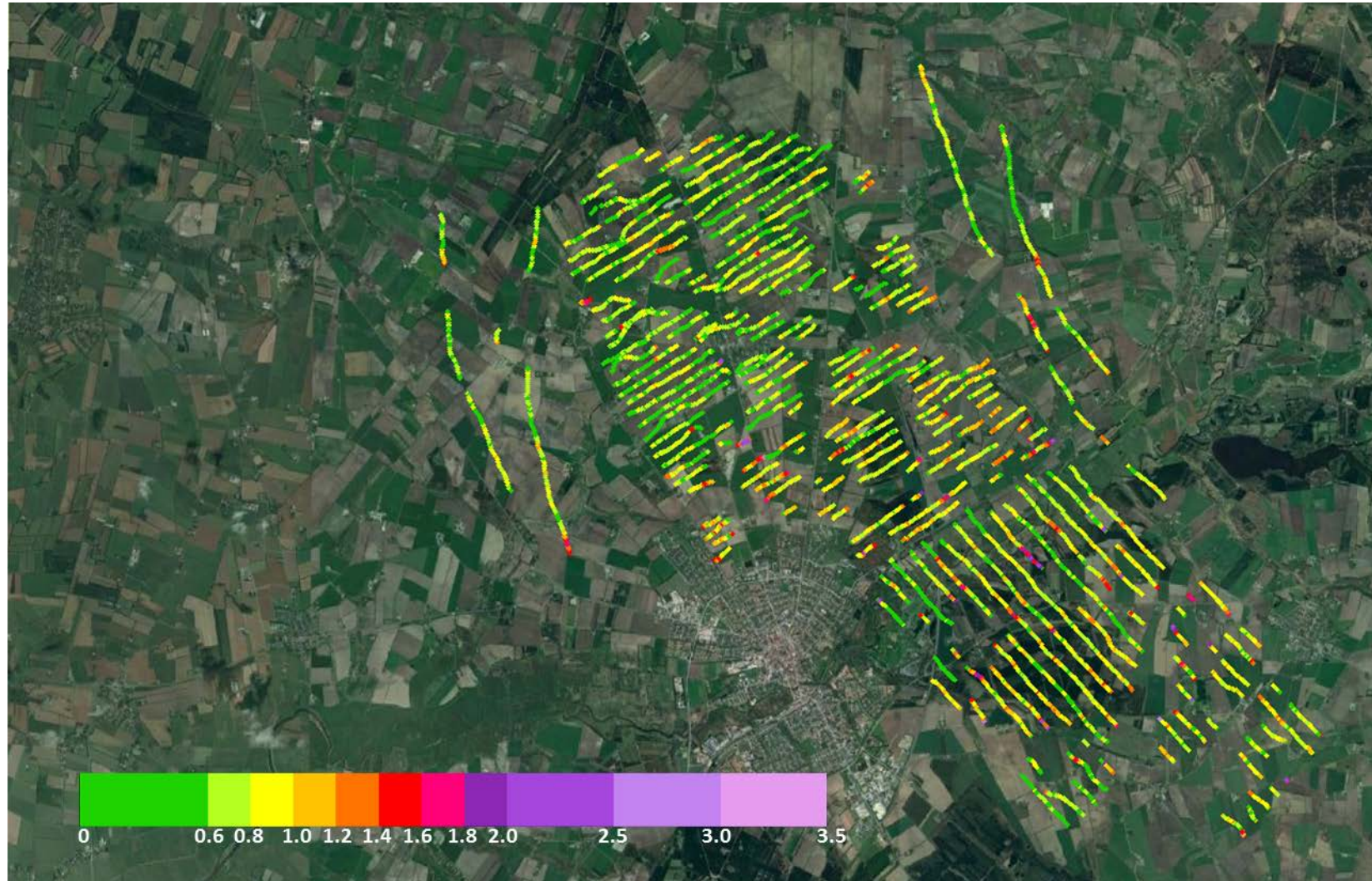
## Moment indications

The large majority of the inverted soundings is characterized by the presence of data from both the SLM and HM.



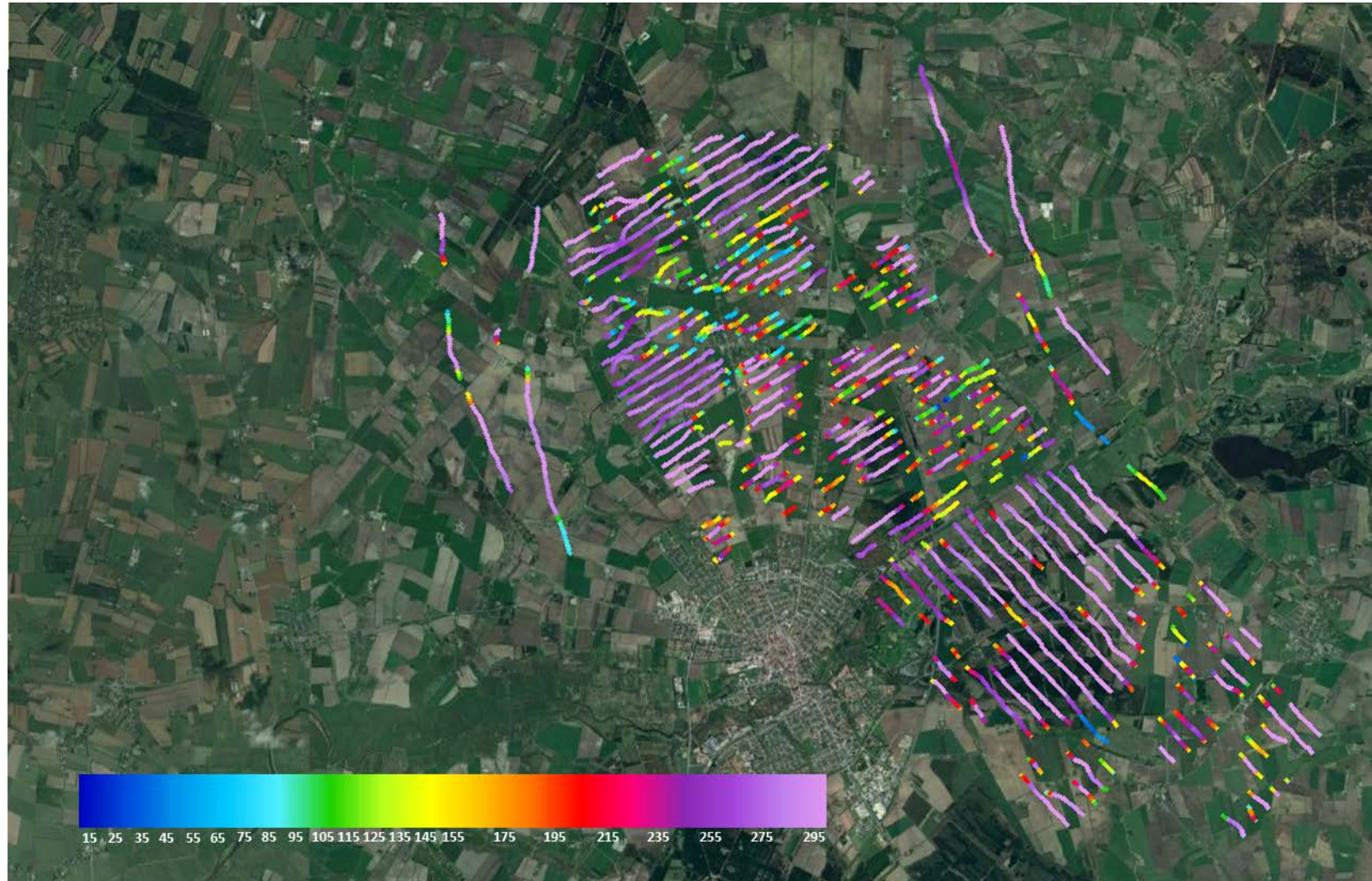
### Data points per sounding

The number of the actually inverted data points per sounding.



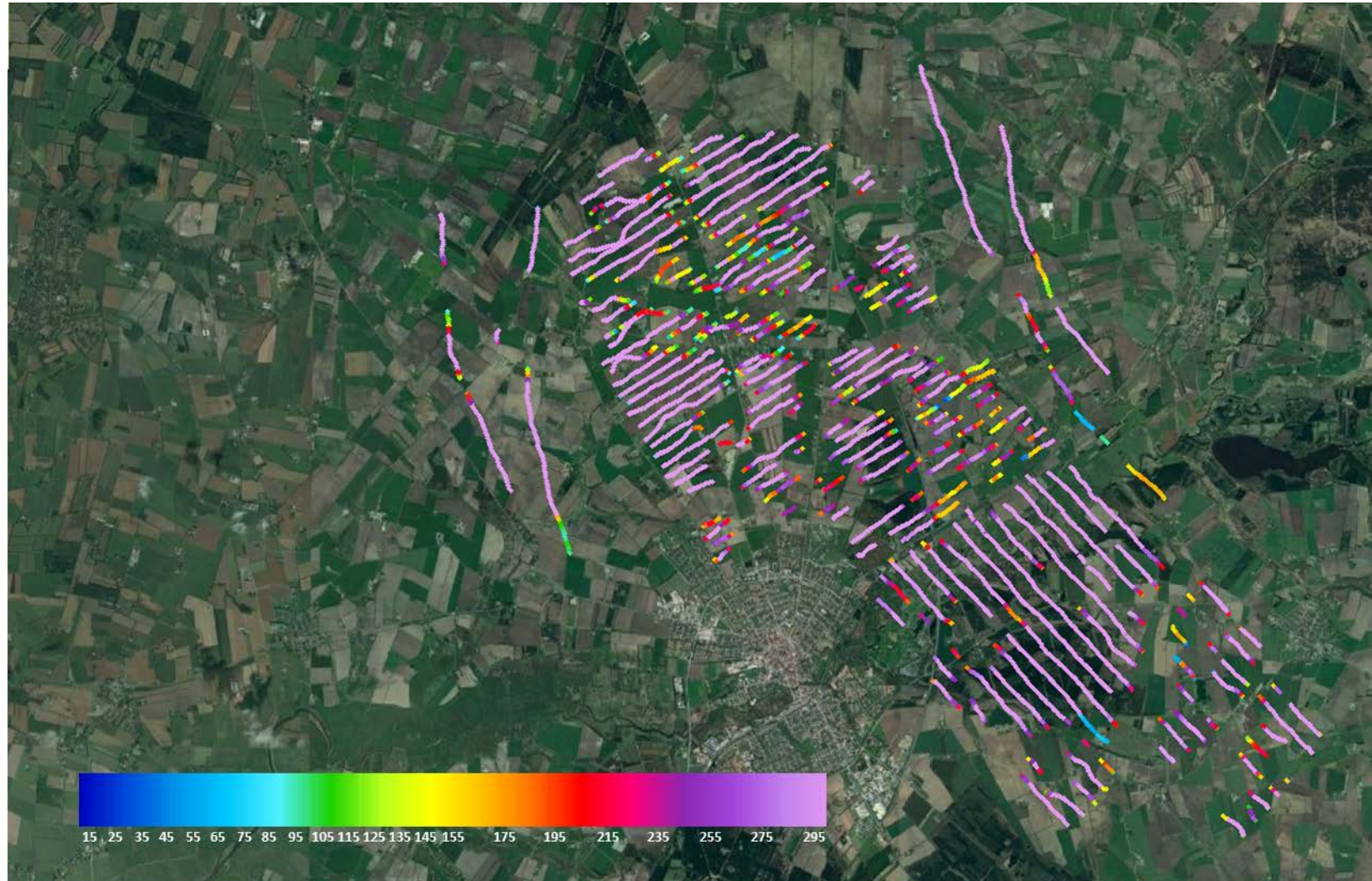
## Data residual

The large majority of the inverted sounding is characterized by a very good agreement with the observed data (misfit smaller than 1.0). In all cases the data residual is acceptable ( $<2.5$ ).



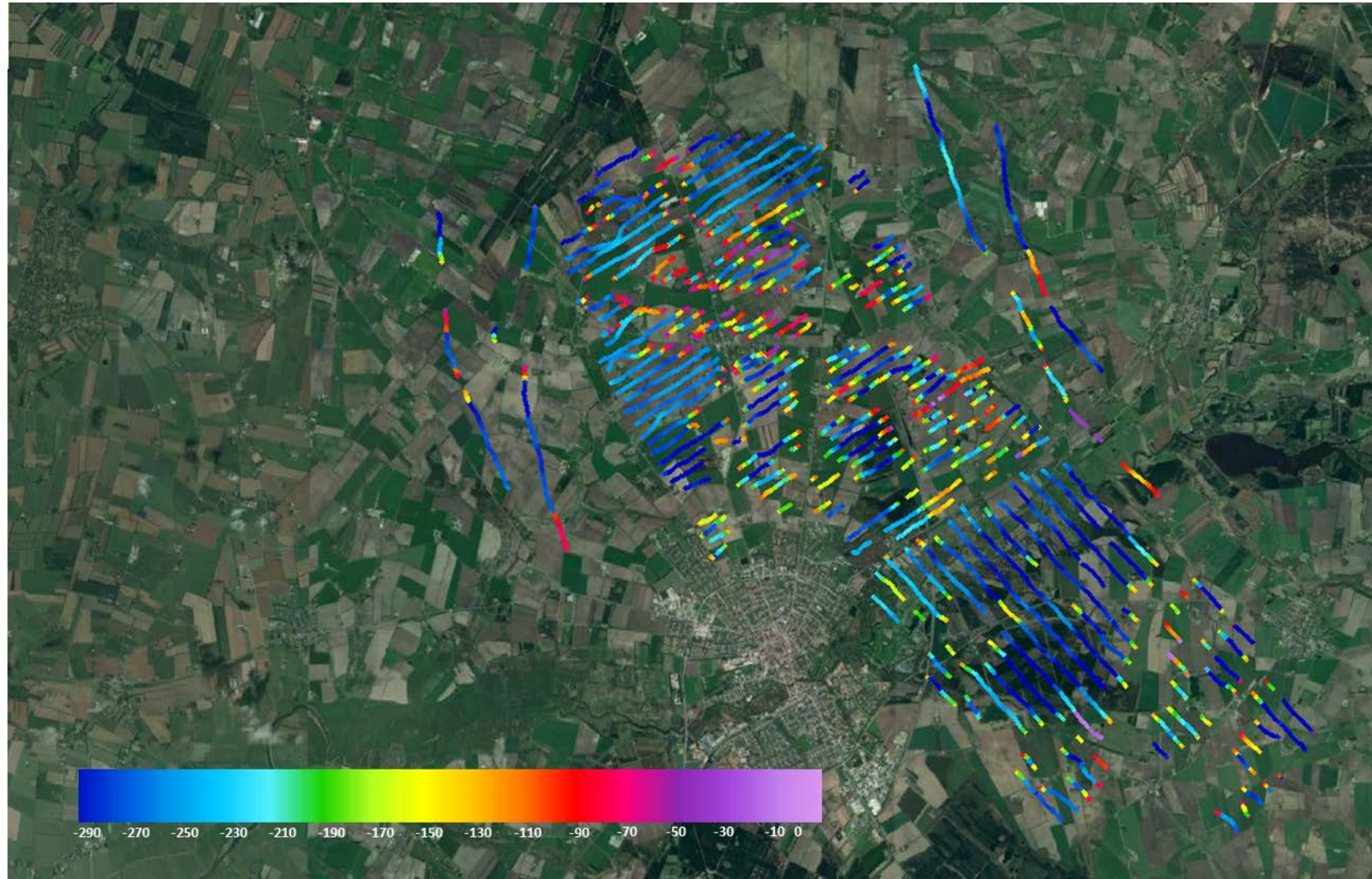
**DOI upper  
(depth)  
[meters]**

The (more conservative) Depth of Investigation is generally as deep as ~300 m. In this survey, the parameters that is actually affecting the variations of DOI is not the soil electrical conductivity, but the number of data points available per sounding.

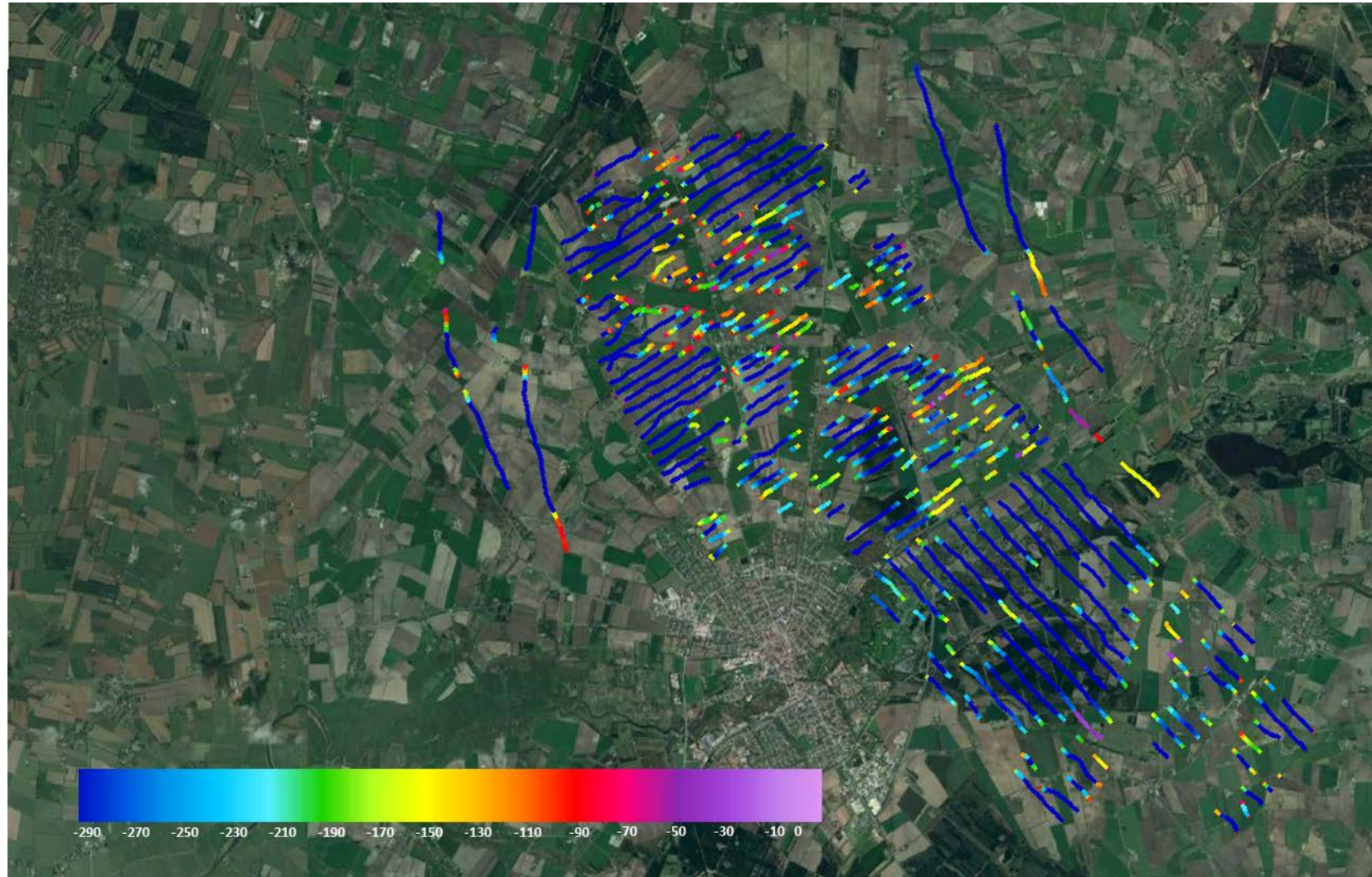


**DOI lower  
(depth)  
[meters]**

The less conservative estimation of the Depth of Investigation is clearly consistent with what shown in the previous thematic maps (concerning the DOI upper).



DOI upper  
(elevation)  
[meters]

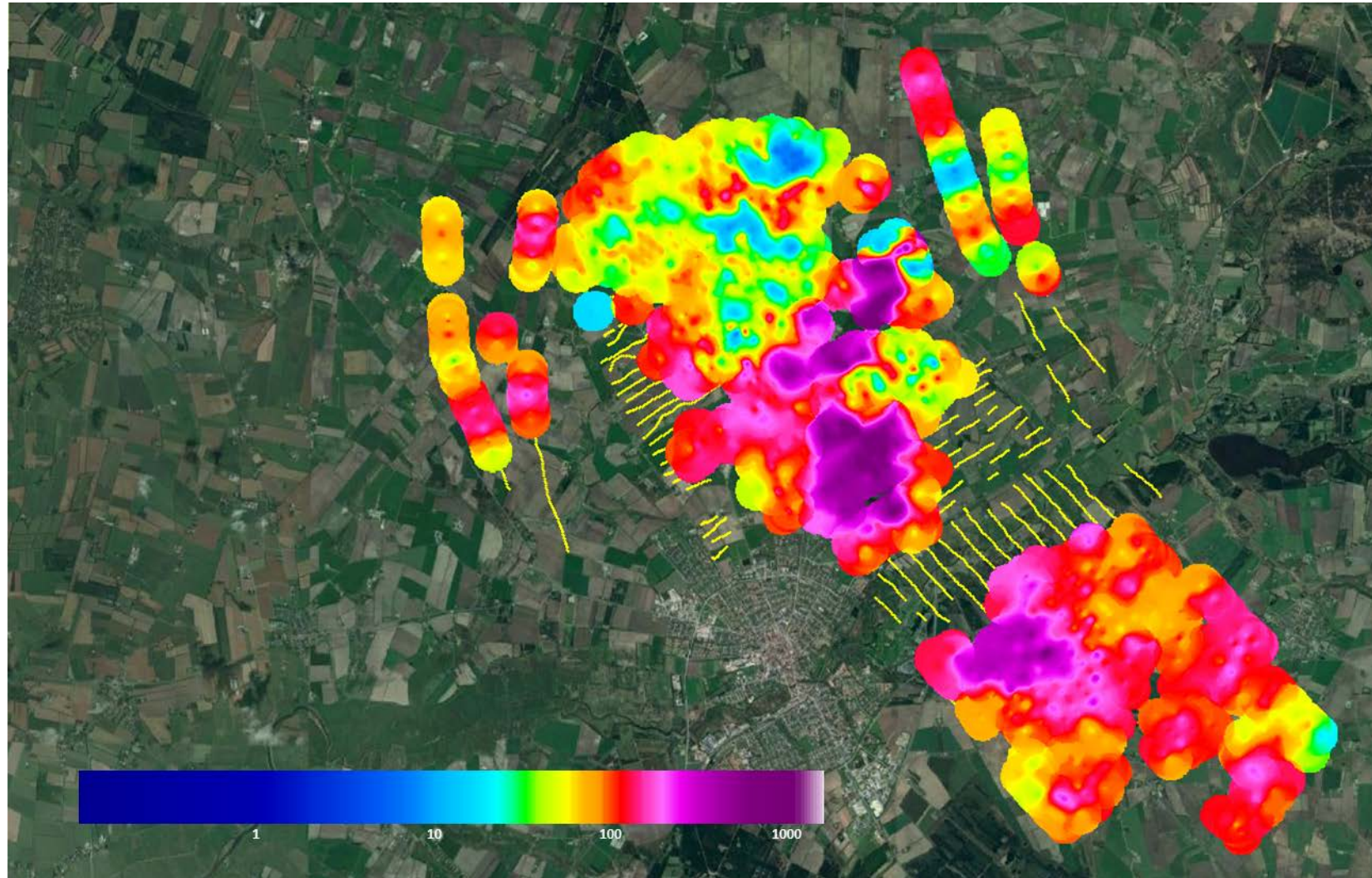


DOI lower  
(elevation)  
[meters]

## **Appendix II: Mean Resistivity maps as depth slices**

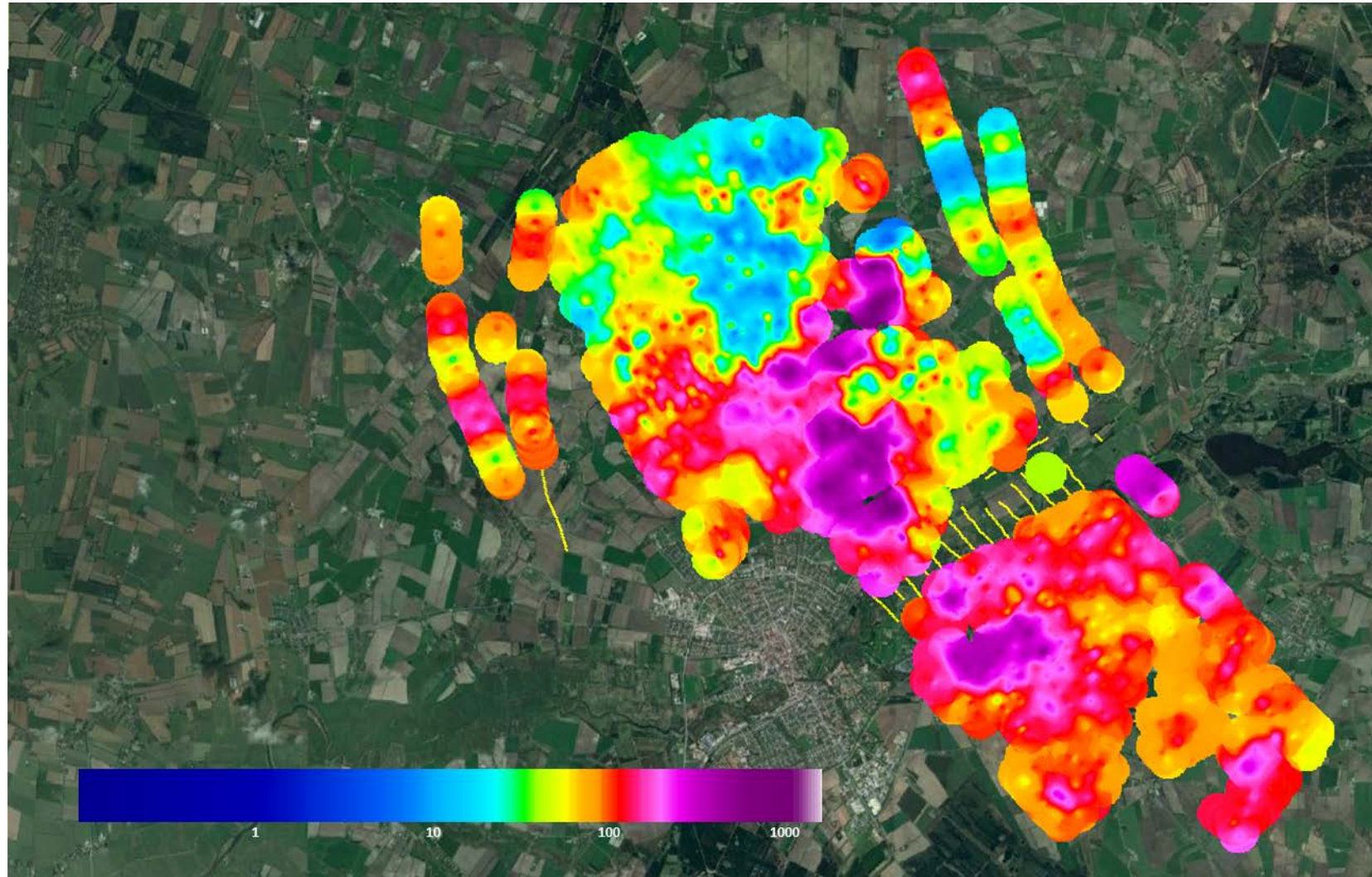
This This appendix shows mean resistivity maps generated from the inversion results. The maps correspond to depth slices of 5 m from the surface to a depth of 160 m. Below this, the depth slices average the resistivity within a 10 m range.

Models below the DOI lower have been blinded. The gridding is done using the Kriging method, with a node spacing of 20 m and a search radius of 300 m.



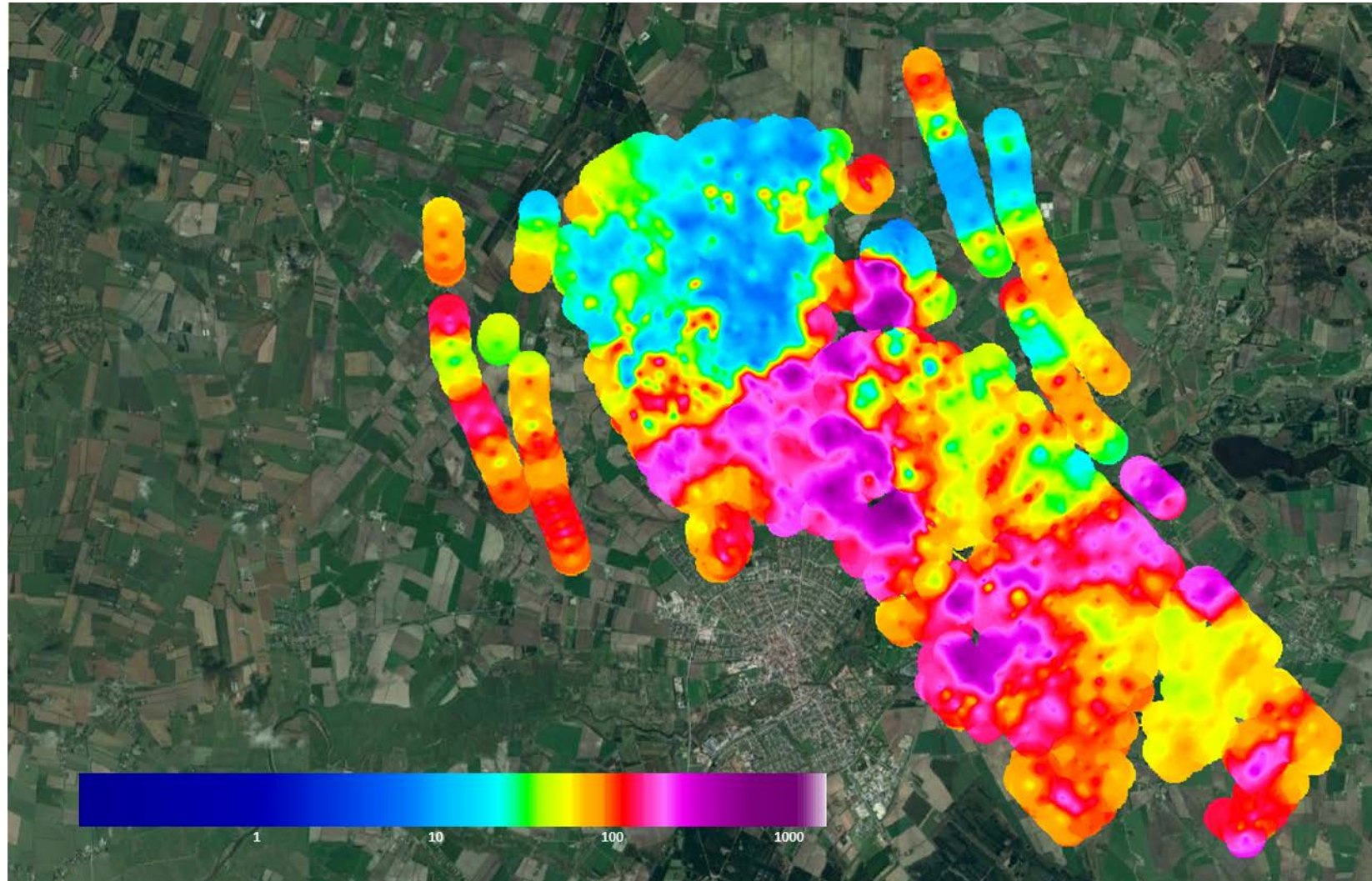
**Mean Resistivity Map [Ohmm].**

Elevation:  
15m to 20m



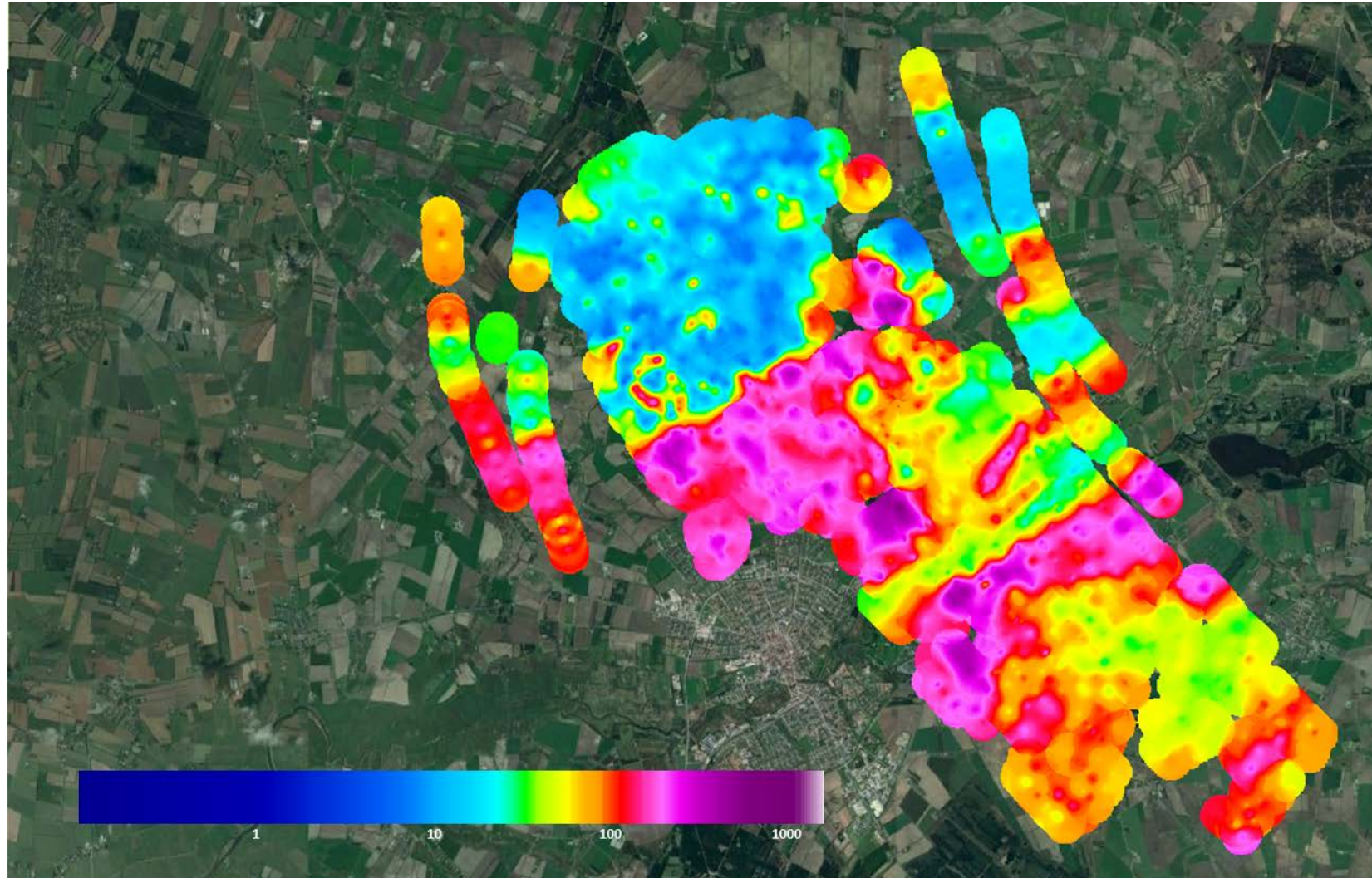
**Mean Resistivity  
Map [Ohmm].**

Elevation:  
10m to 15m



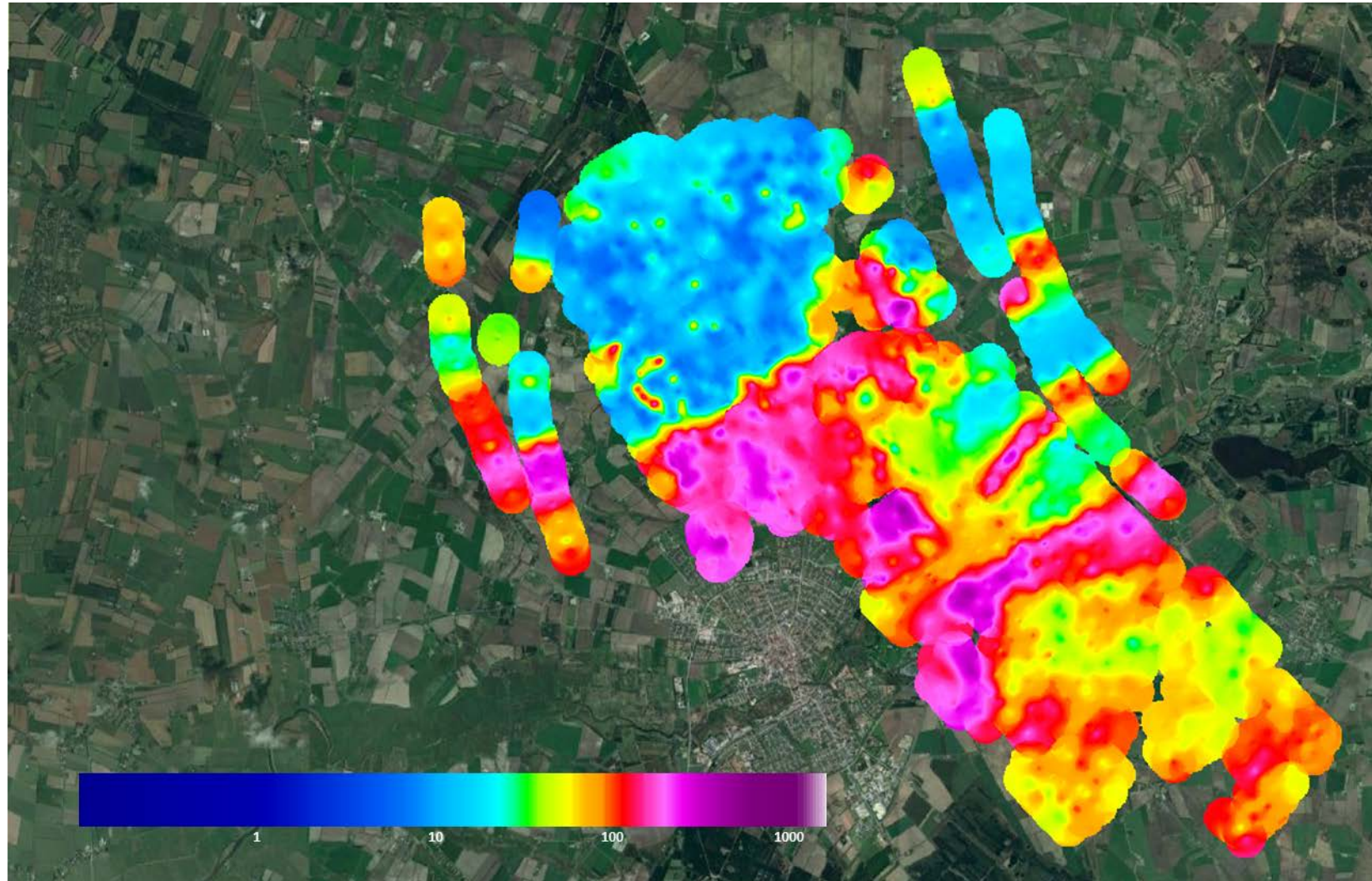
**Mean Resistivity Map [Ohmm].**

Elevation:  
5m to 10m



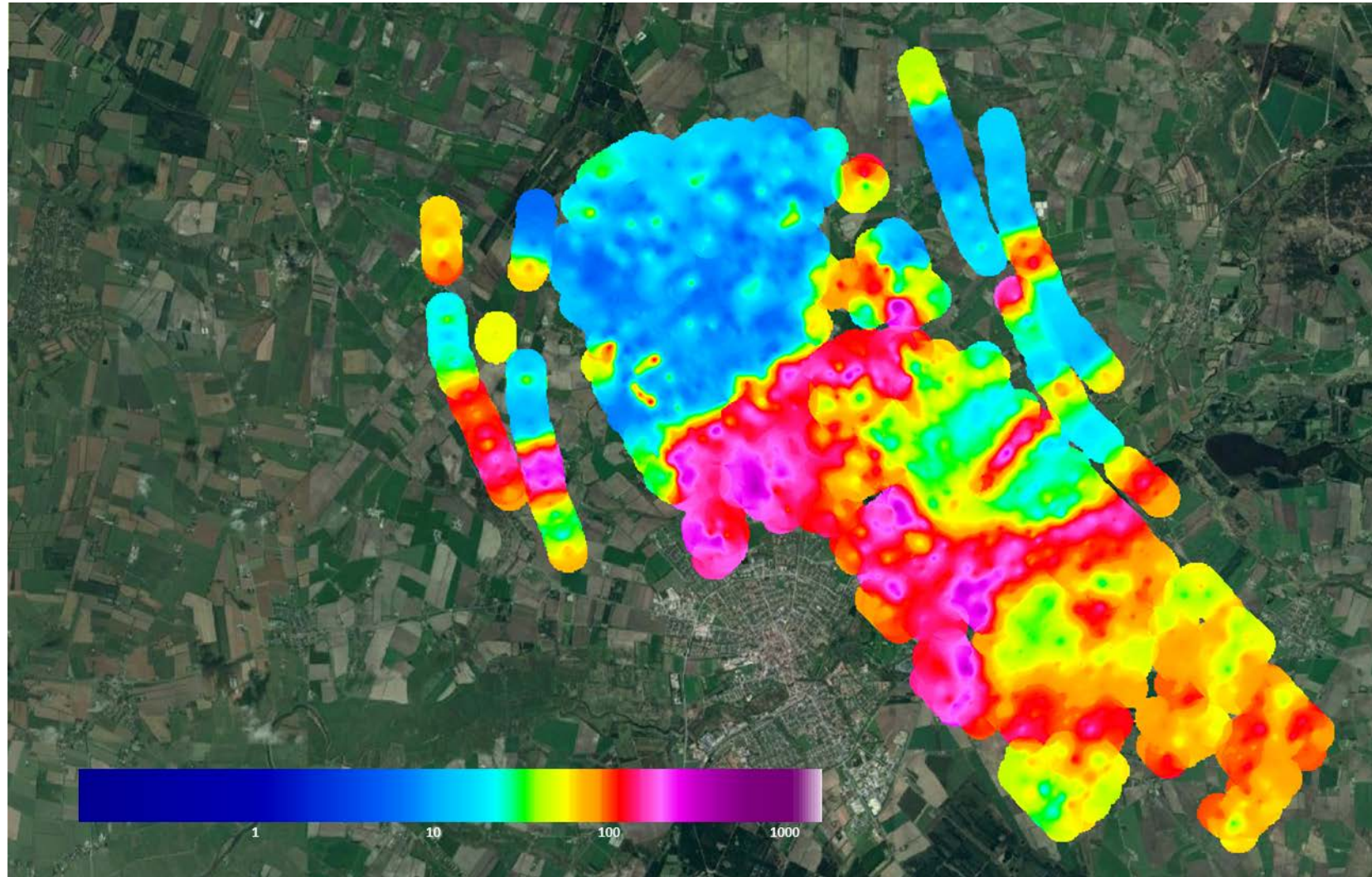
**Mean Resistivity Map [Ohmm].**

Elevation:  
0m to 5m



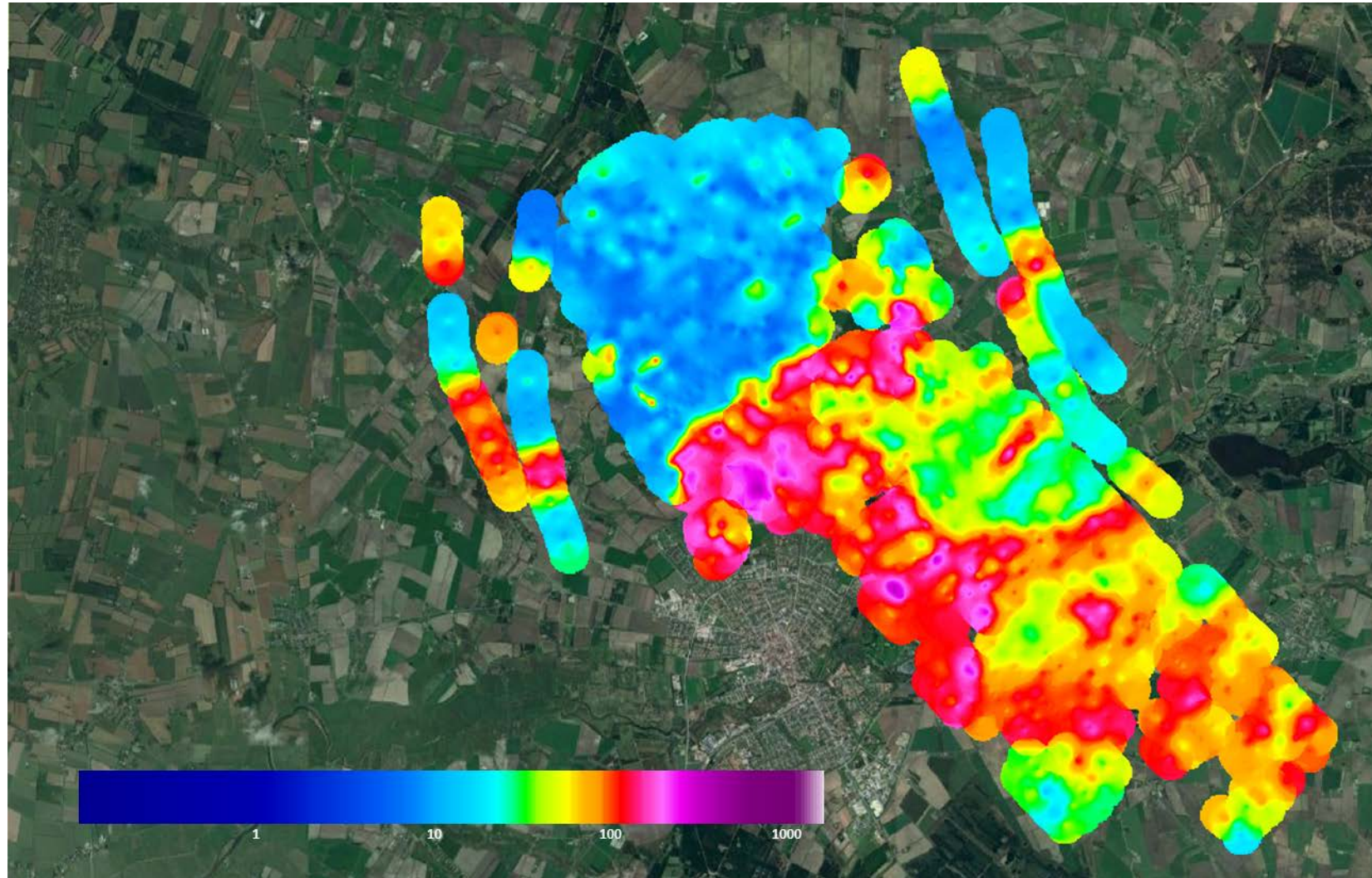
**Mean Resistivity Map [Ohmm].**

Elevation:  
-5m to 0m



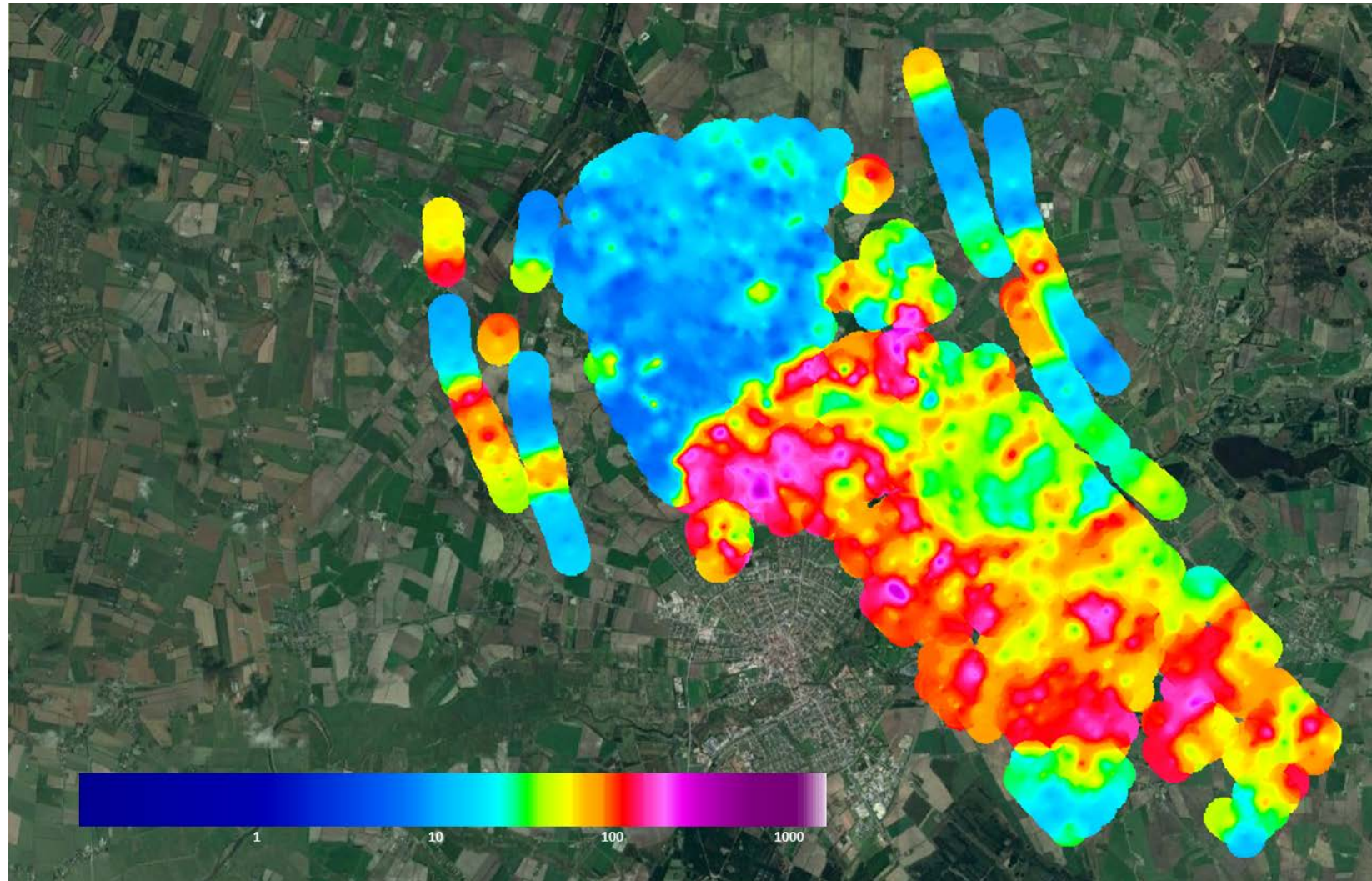
**Mean Resistivity Map [Ohmm].**

Elevation:  
-10m to -5m



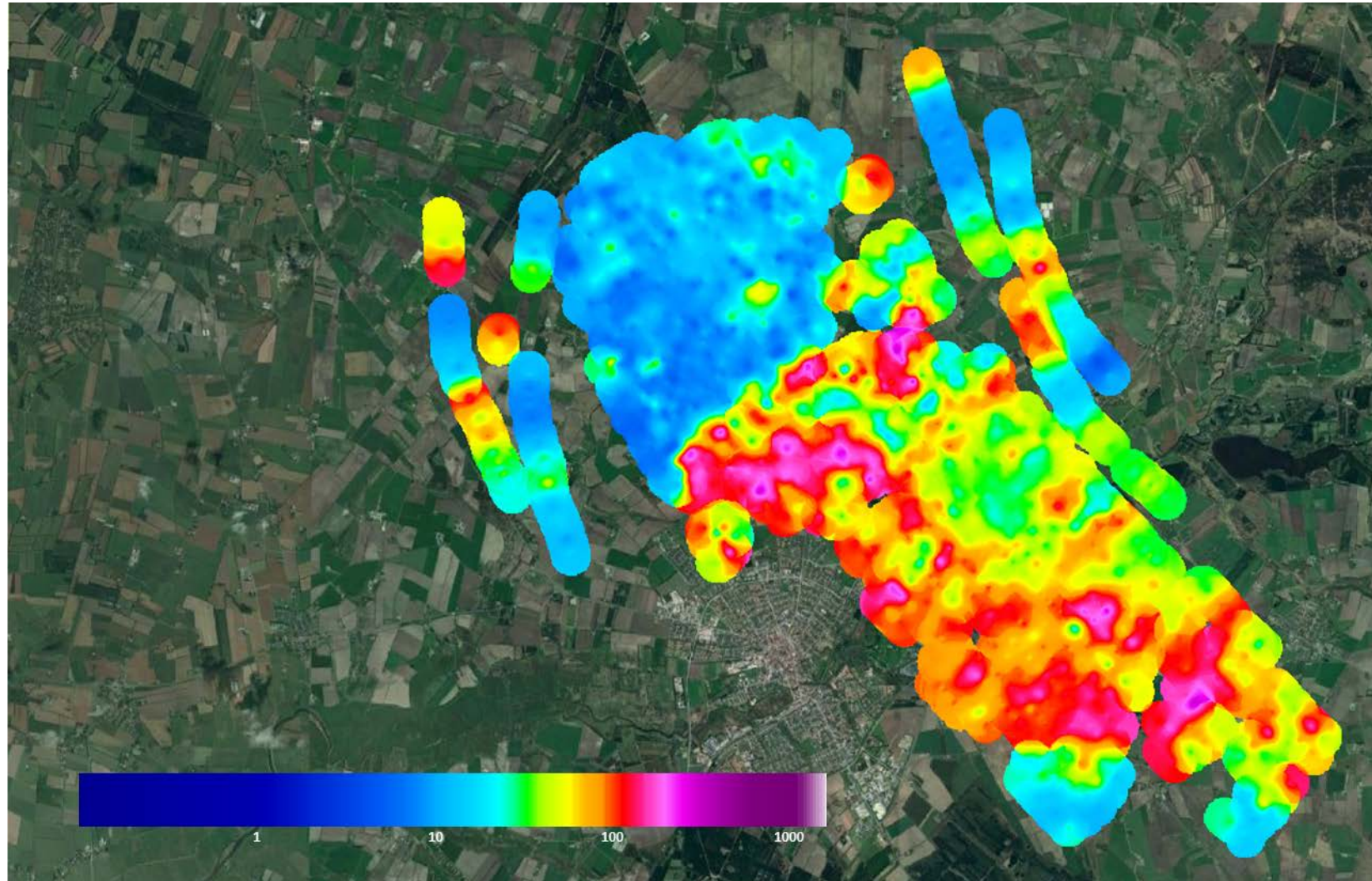
**Mean Resistivity Map [Ohmm].**

Elevation:  
-15m to -10m



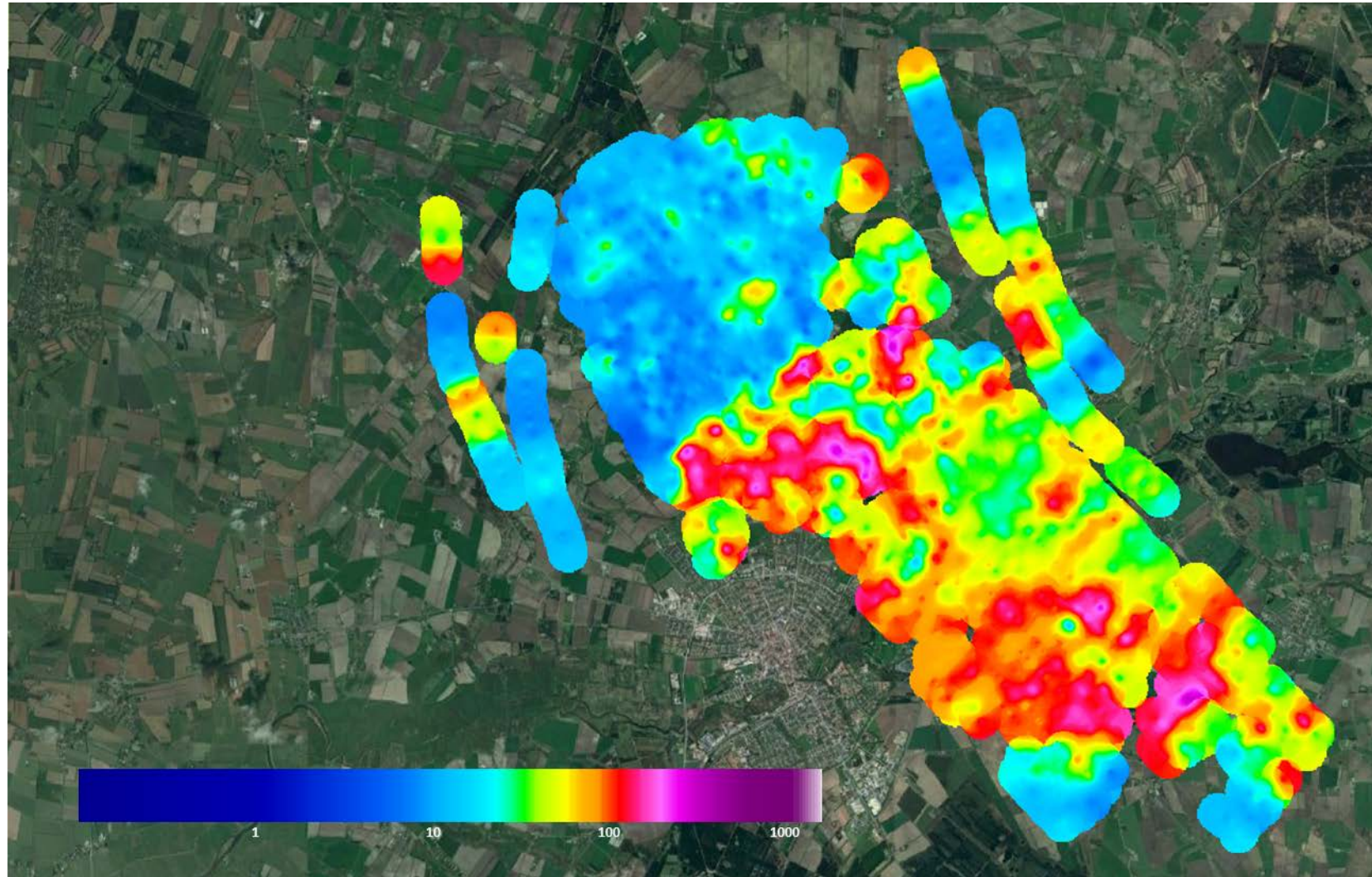
**Mean Resistivity Map [Ohmm].**

Elevation:  
-20m to -15m



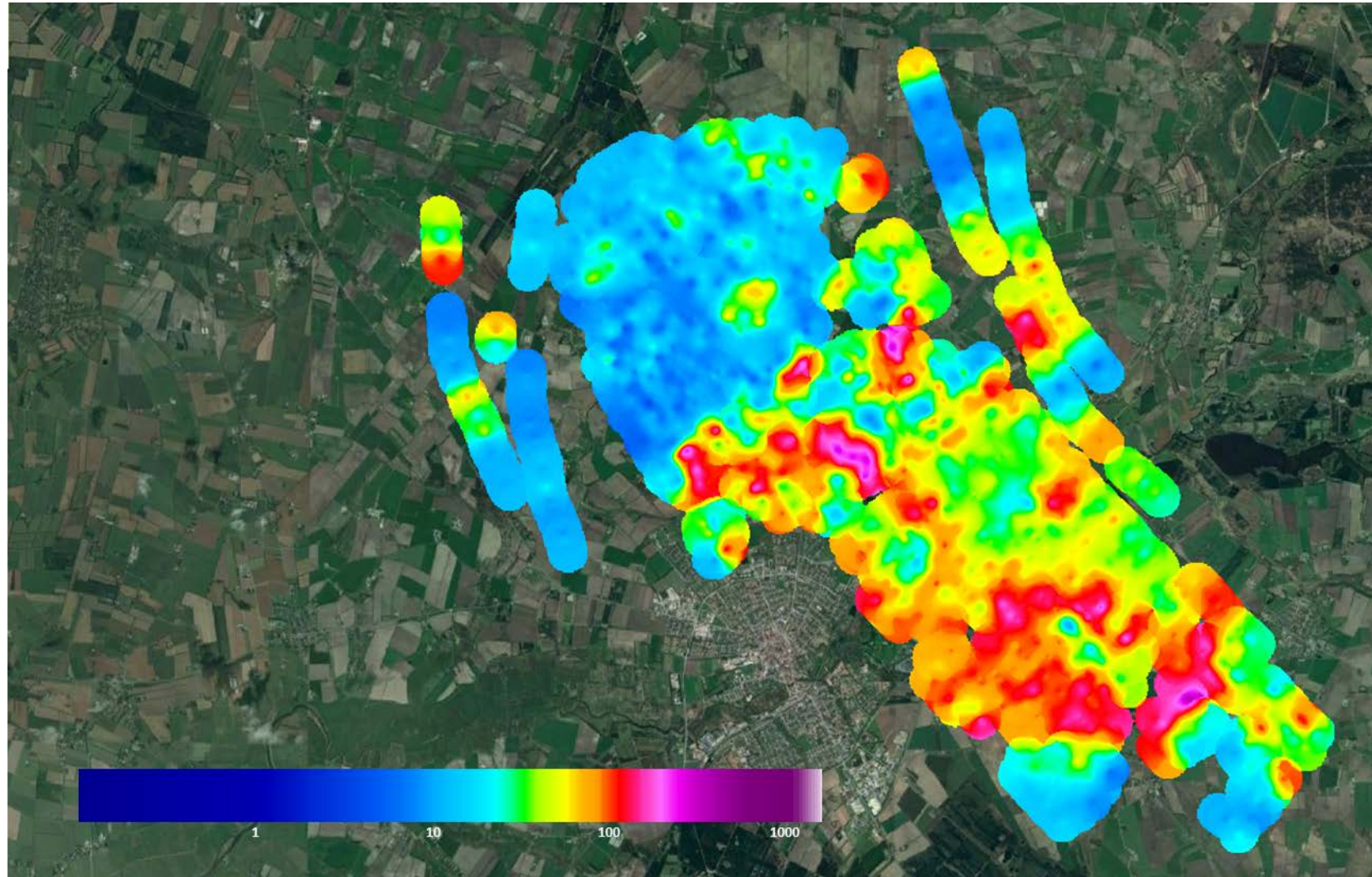
**Mean Resistivity  
Map [Ohmm].**

Elevation:  
-25m to -20m



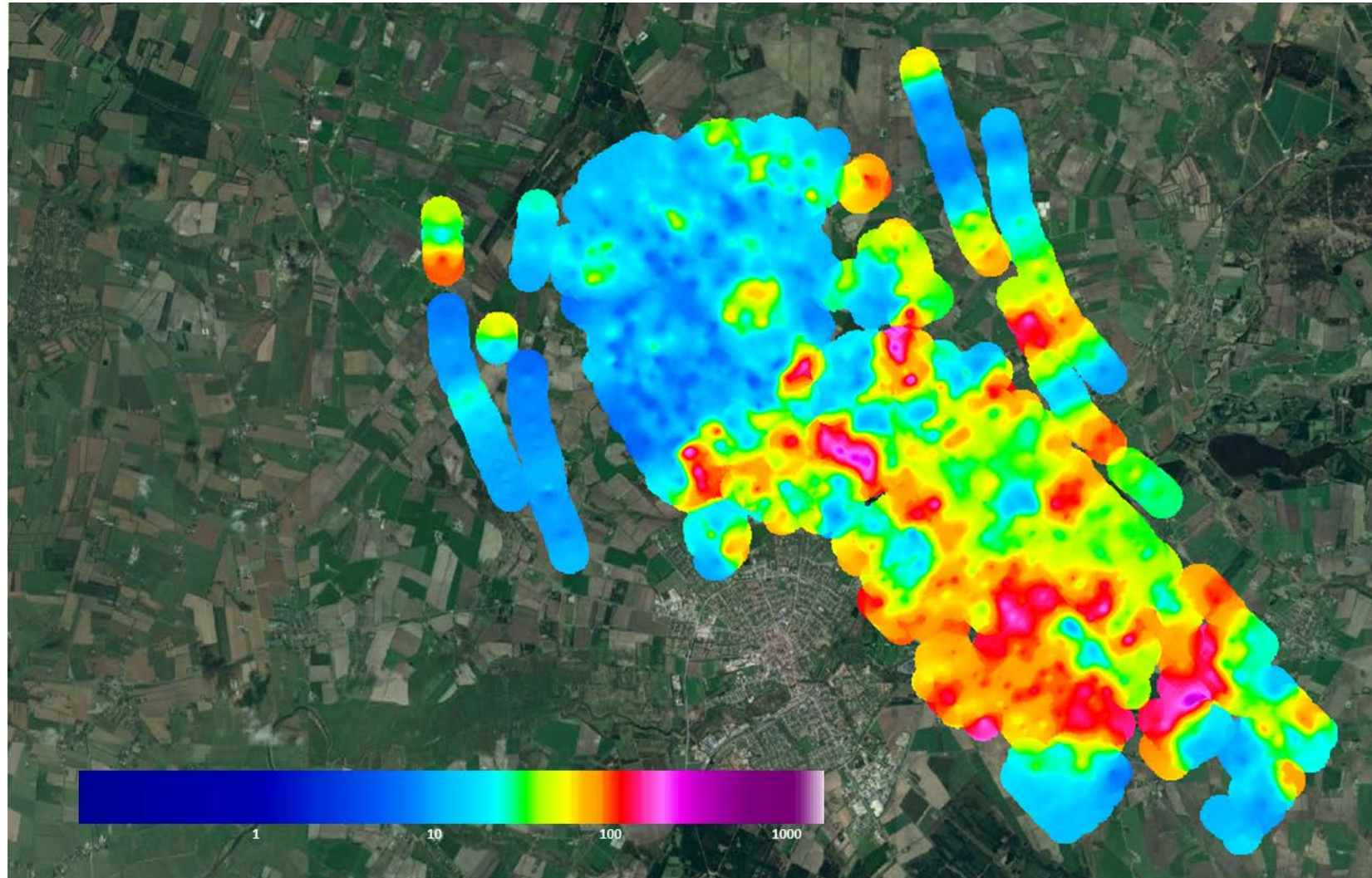
**Mean Resistivity  
Map [Ohmm].**

Elevation:  
-30m to -25m



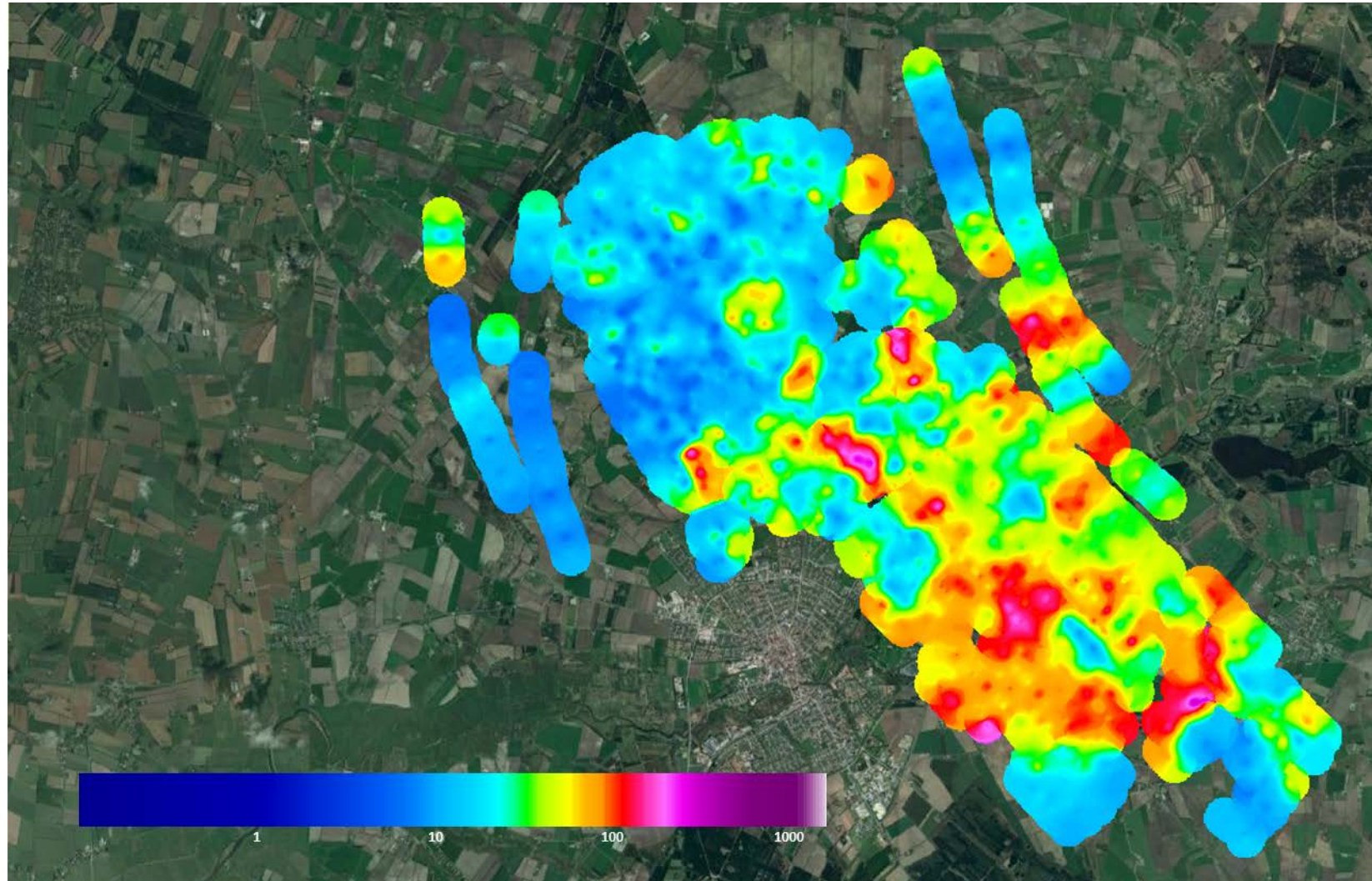
**Mean Resistivity Map [Ohmm].**

Elevation:  
-35m to -30m



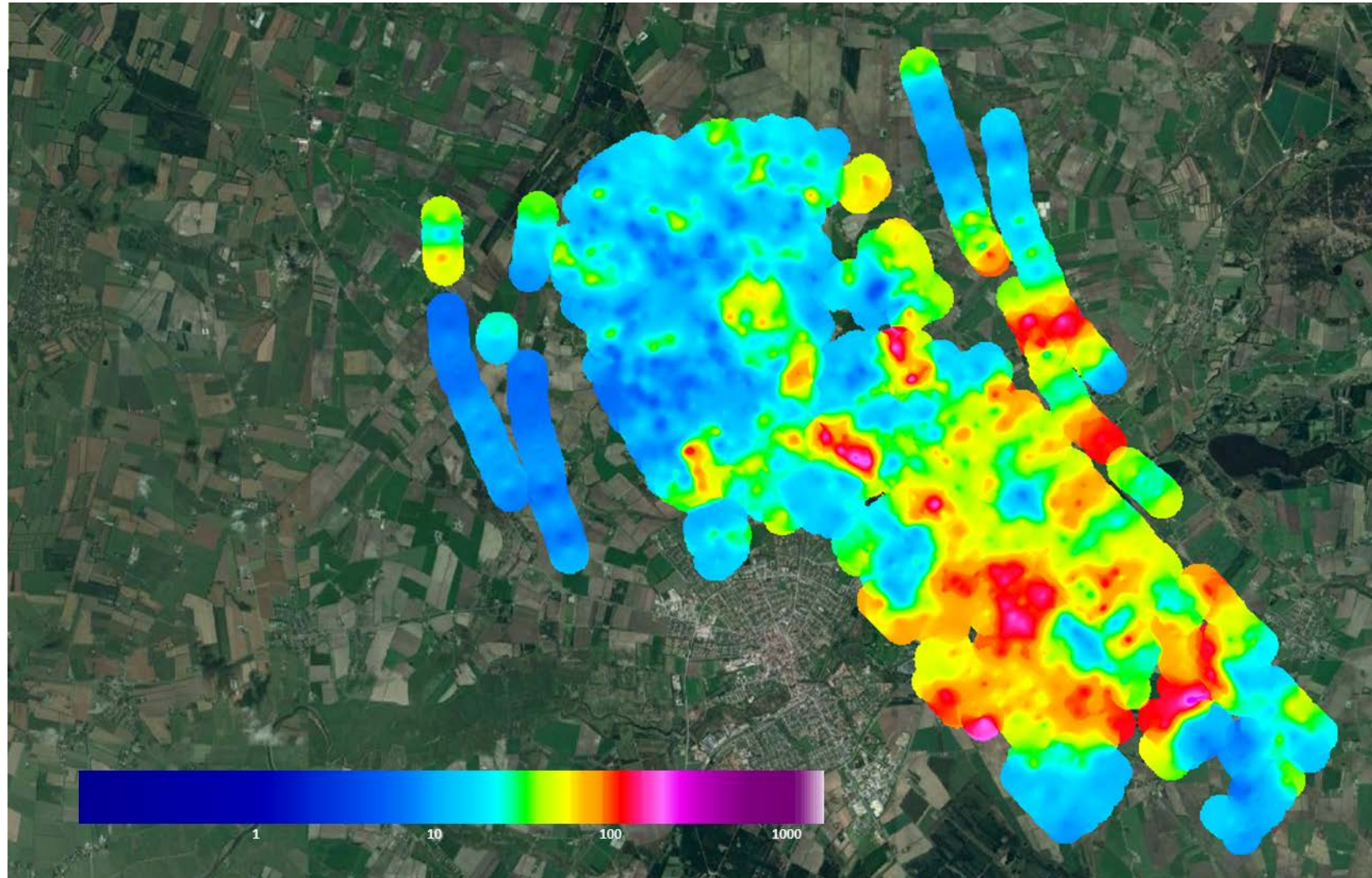
**Mean Resistivity Map [Ohmm].**

Elevation:  
-40m to -35m



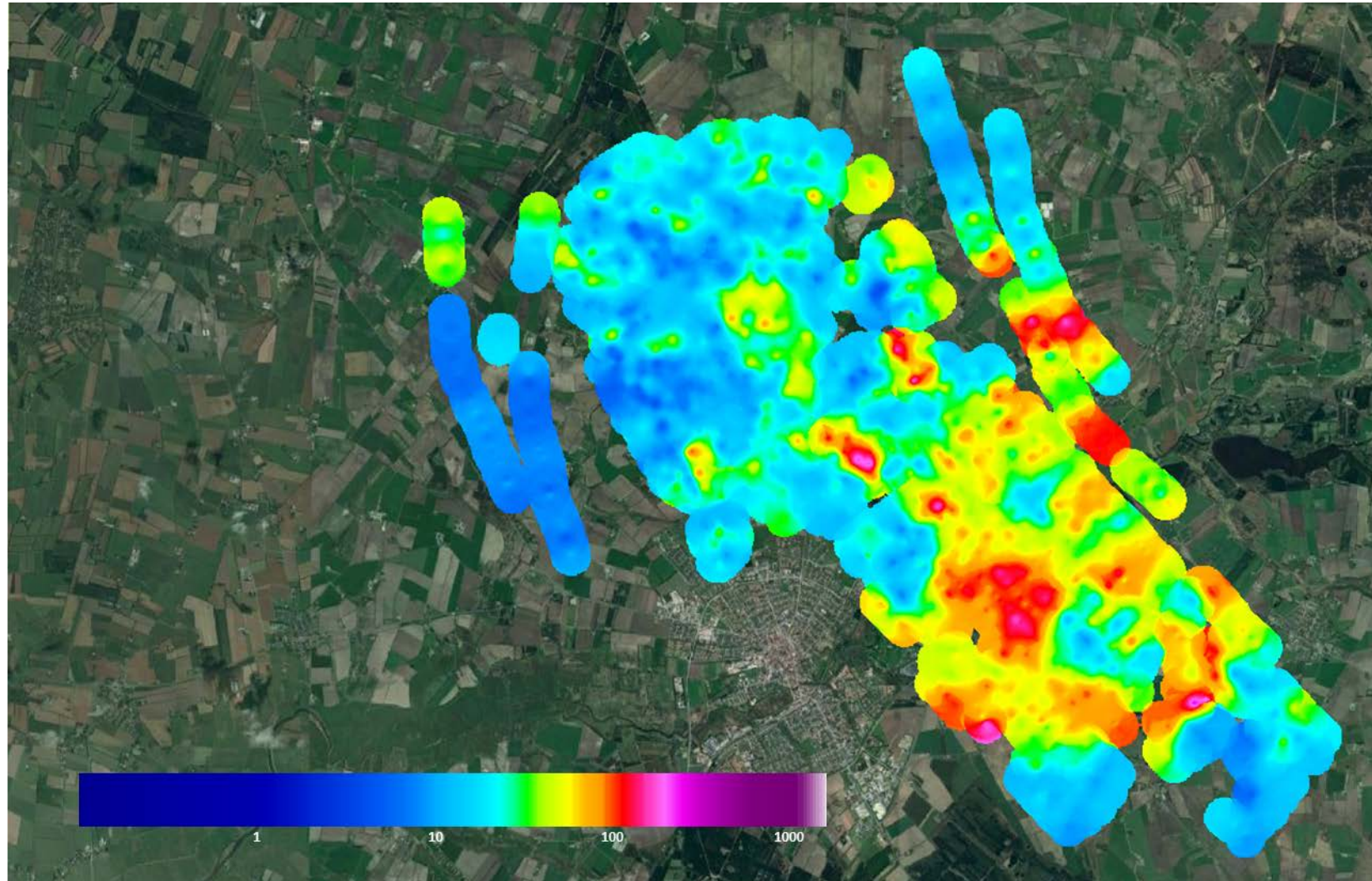
**Mean Resistivity Map [Ohmm].**

Elevation:  
-45m to -40m



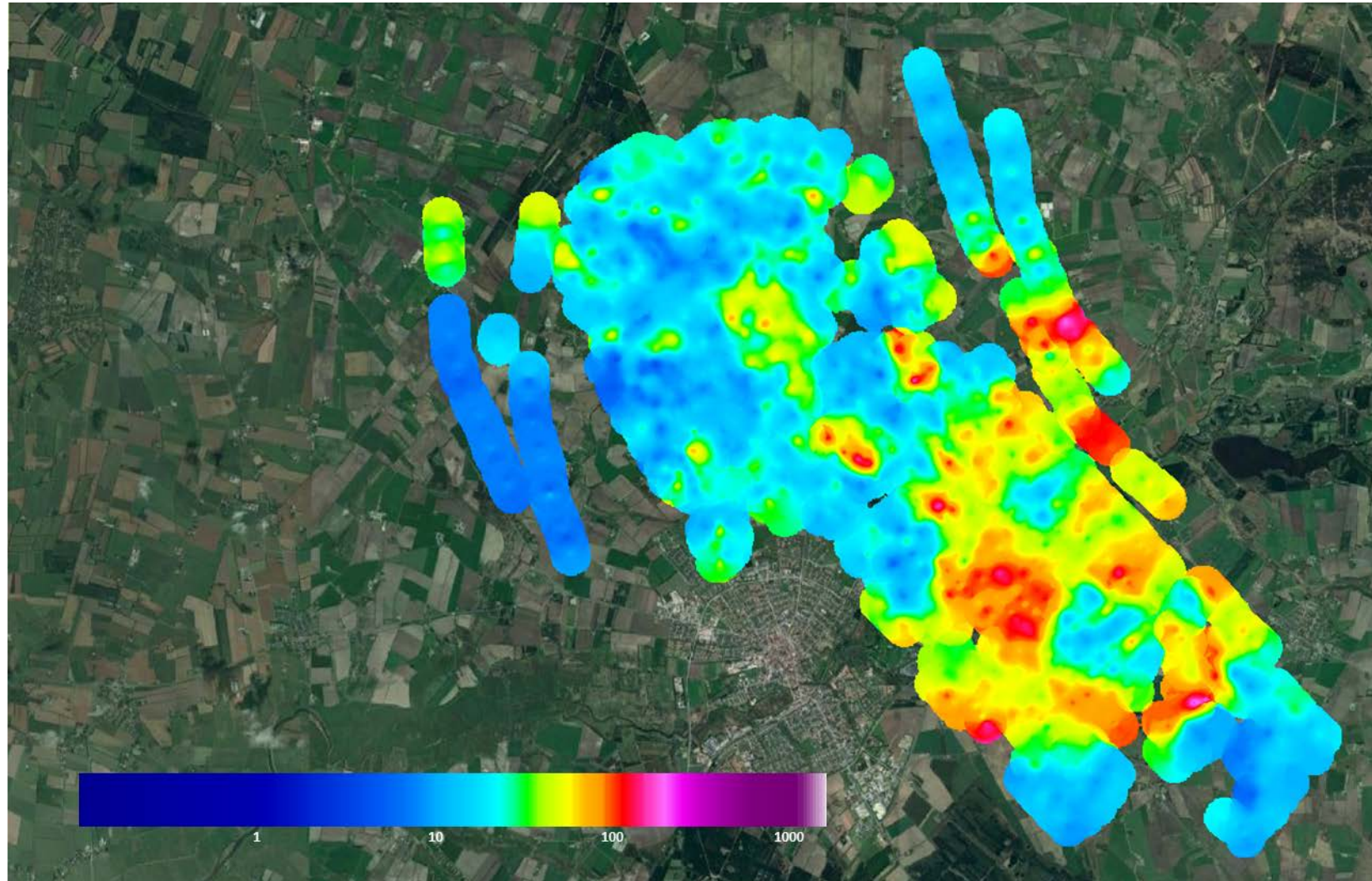
**Mean Resistivity Map [Ohmm].**

Elevation:  
-50m to -45m



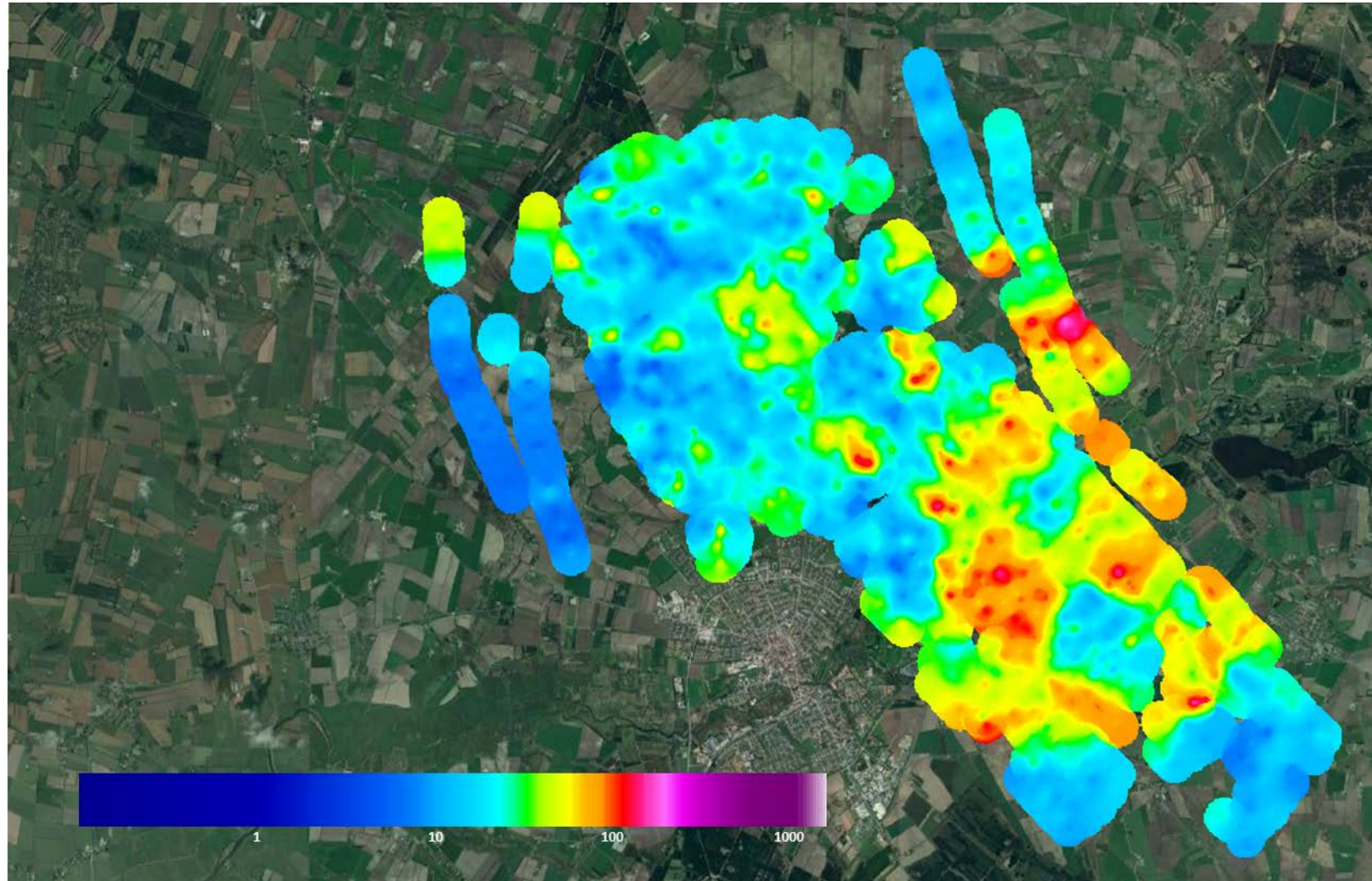
**Mean Resistivity Map [Ohmm].**

Elevation:  
-55m to -50m



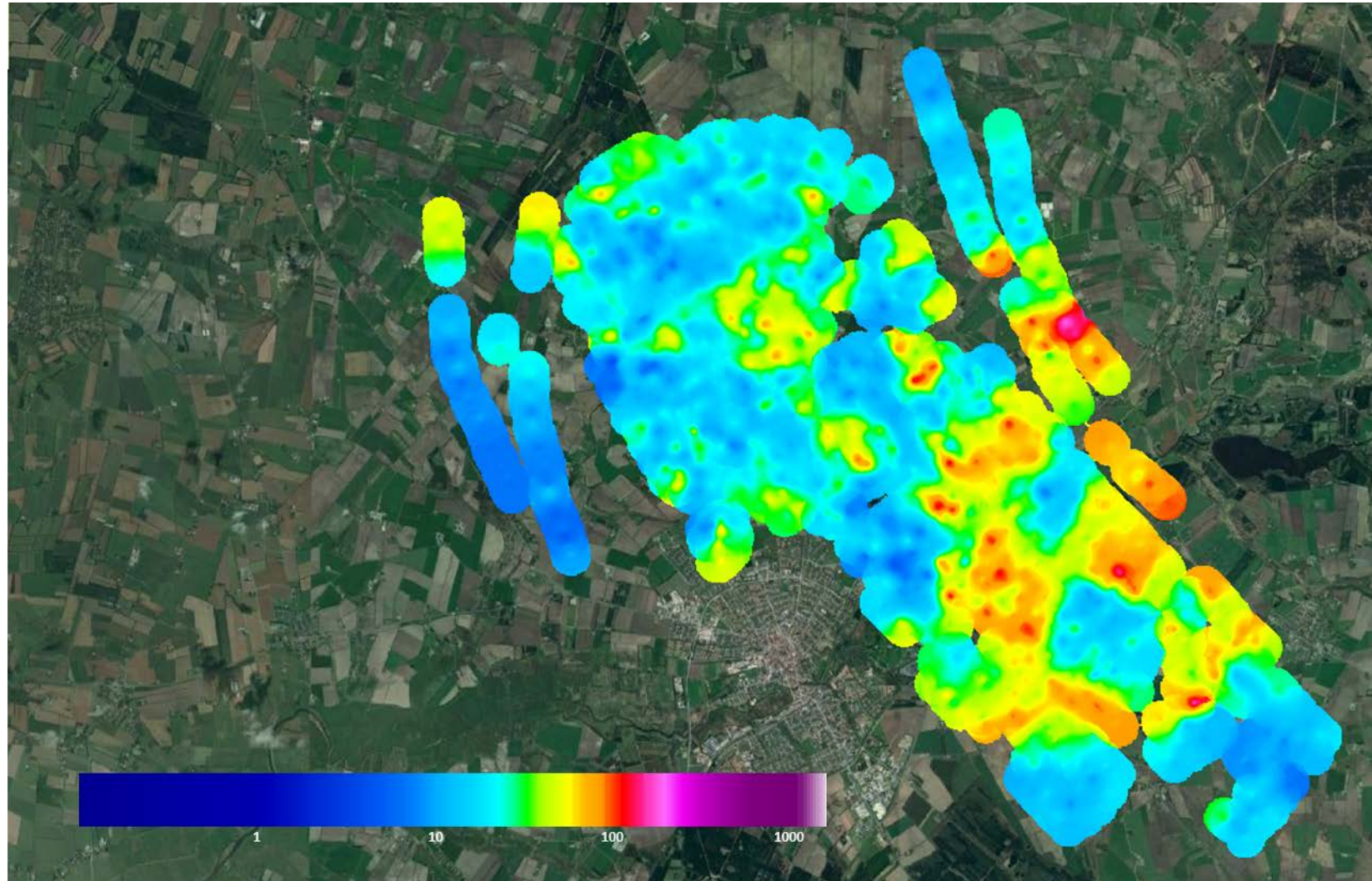
**Mean Resistivity Map [Ohmm].**

Elevation:  
-60m to -55m



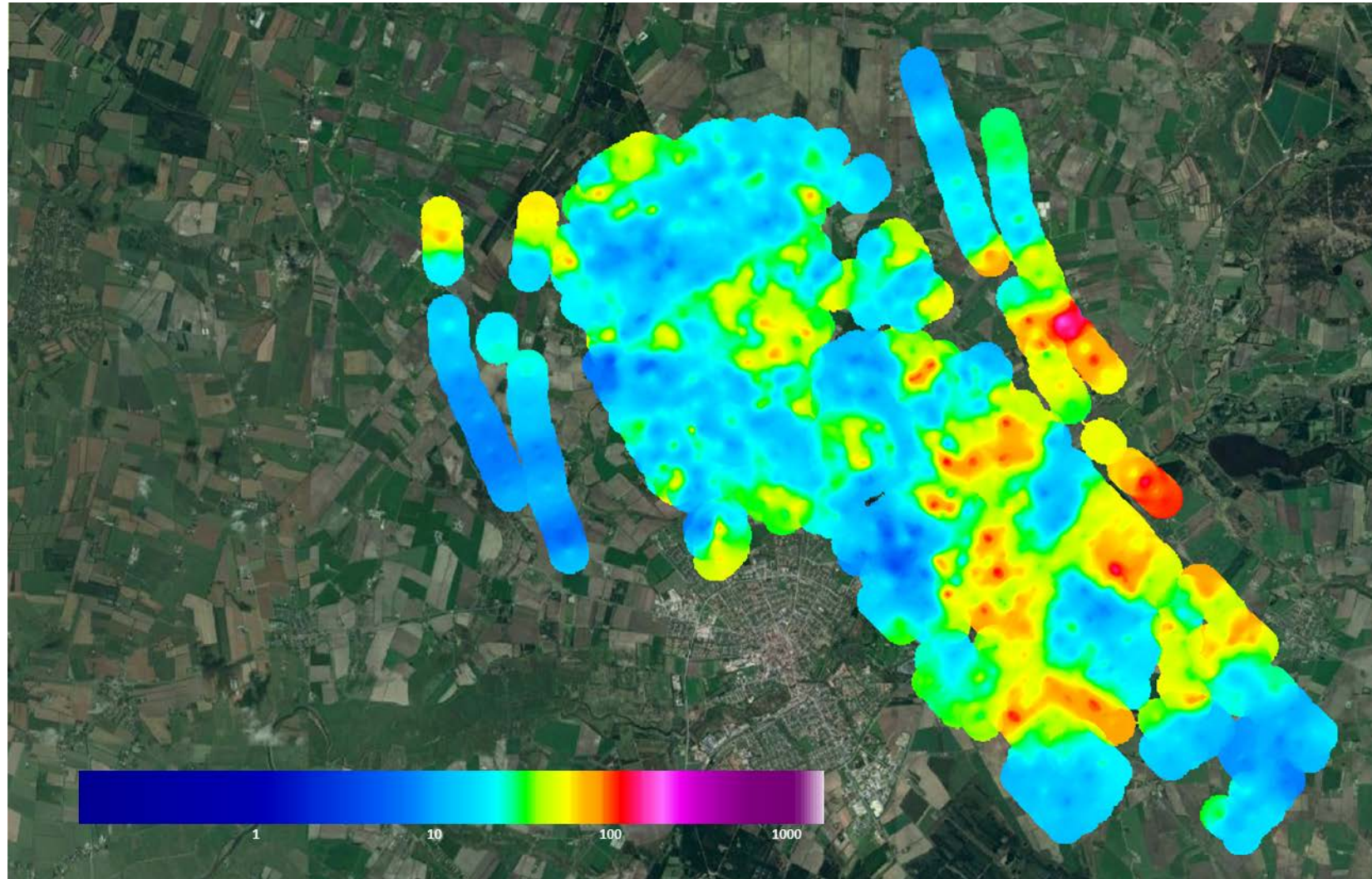
**Mean Resistivity Map [Ohmm].**

Elevation:  
-65m to -60m



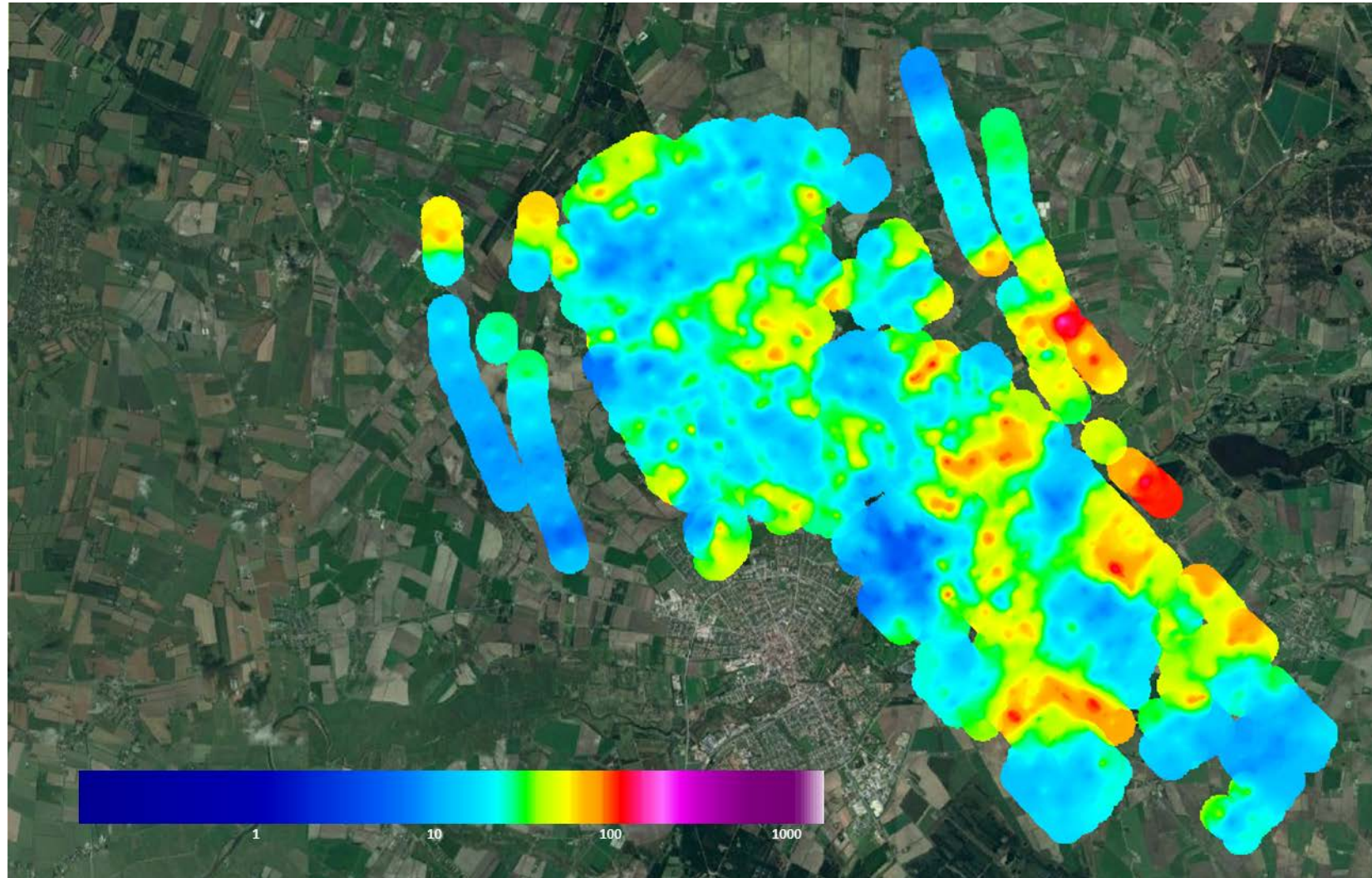
**Mean Resistivity  
Map [Ohm].**

Elevation:  
-70m to -65m



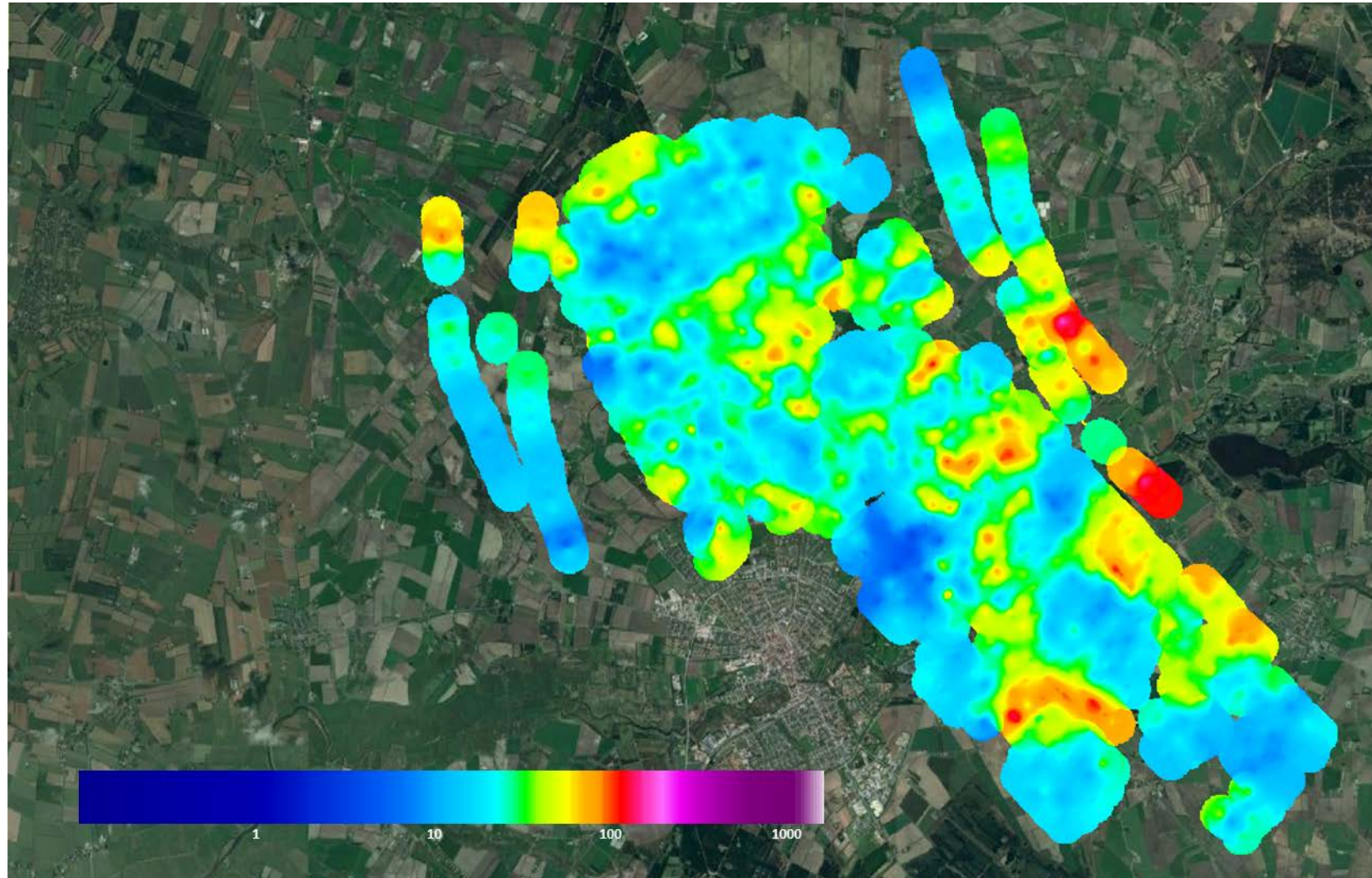
**Mean Resistivity Map [Ohmm].**

Elevation:  
-75m to -70m



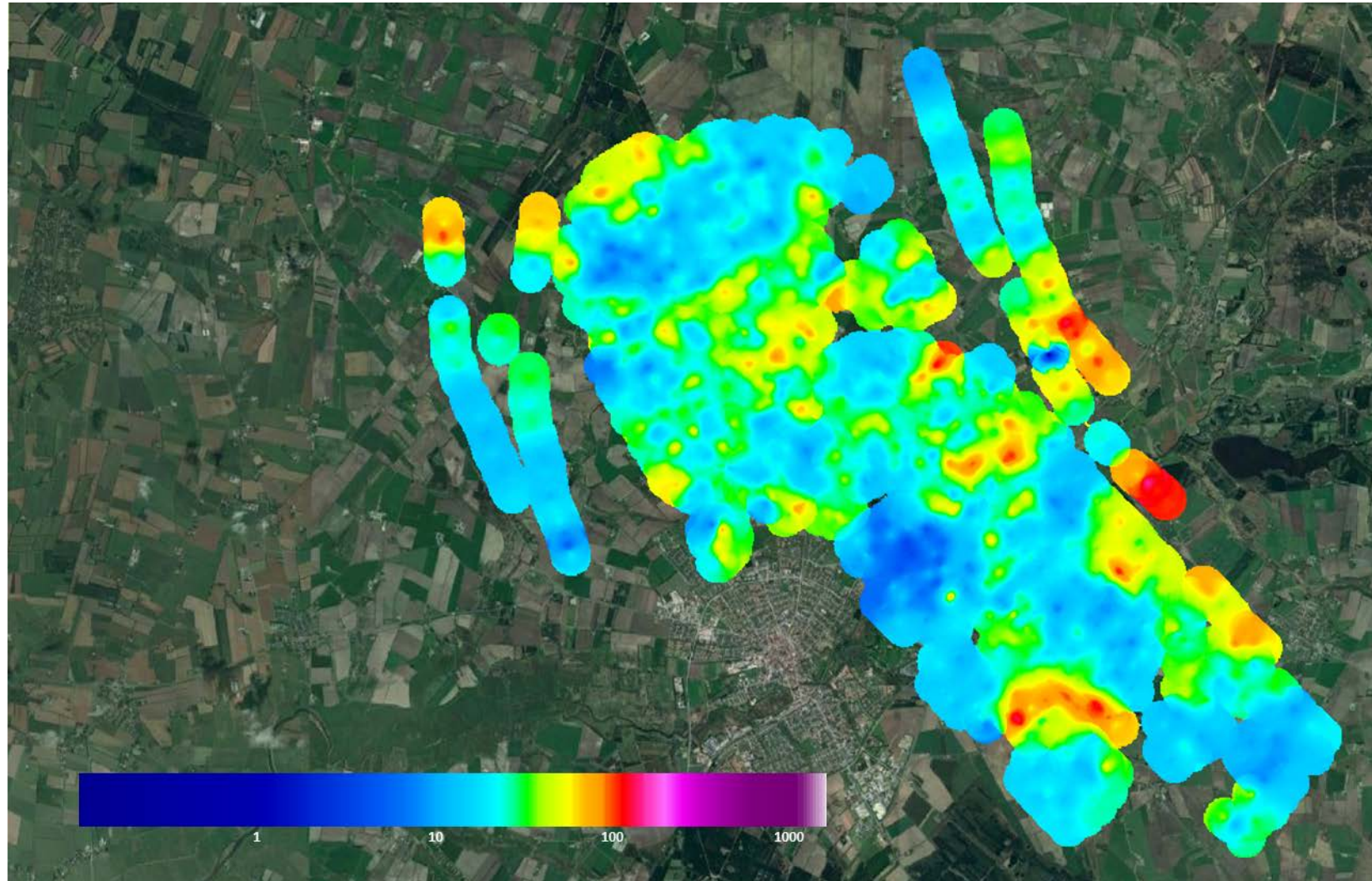
**Mean Resistivity Map [Ohmm].**

Elevation:  
-80m to -75m



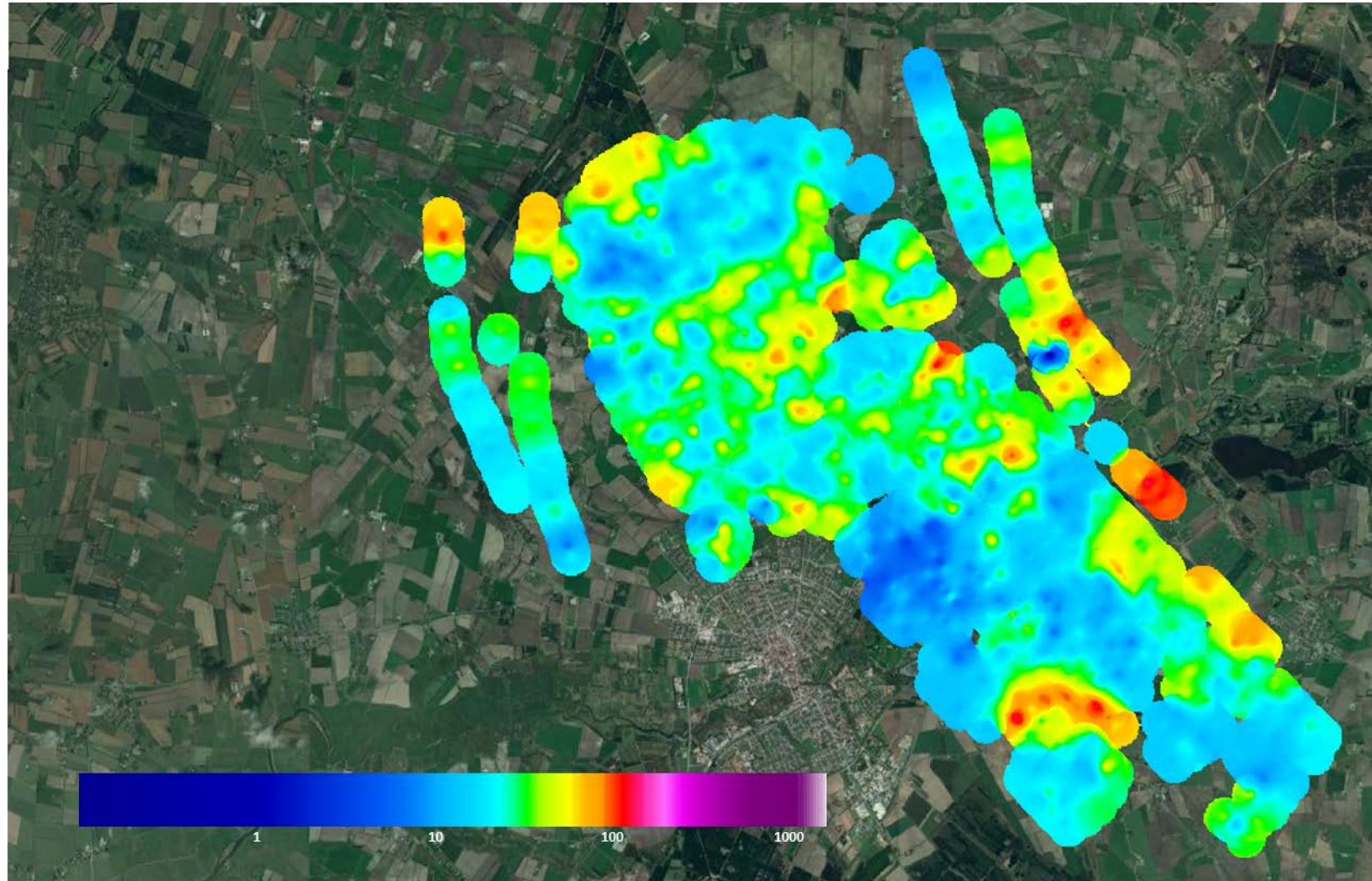
**Mean Resistivity  
Map [Ohmm].**

Elevation:  
-85m to -80m



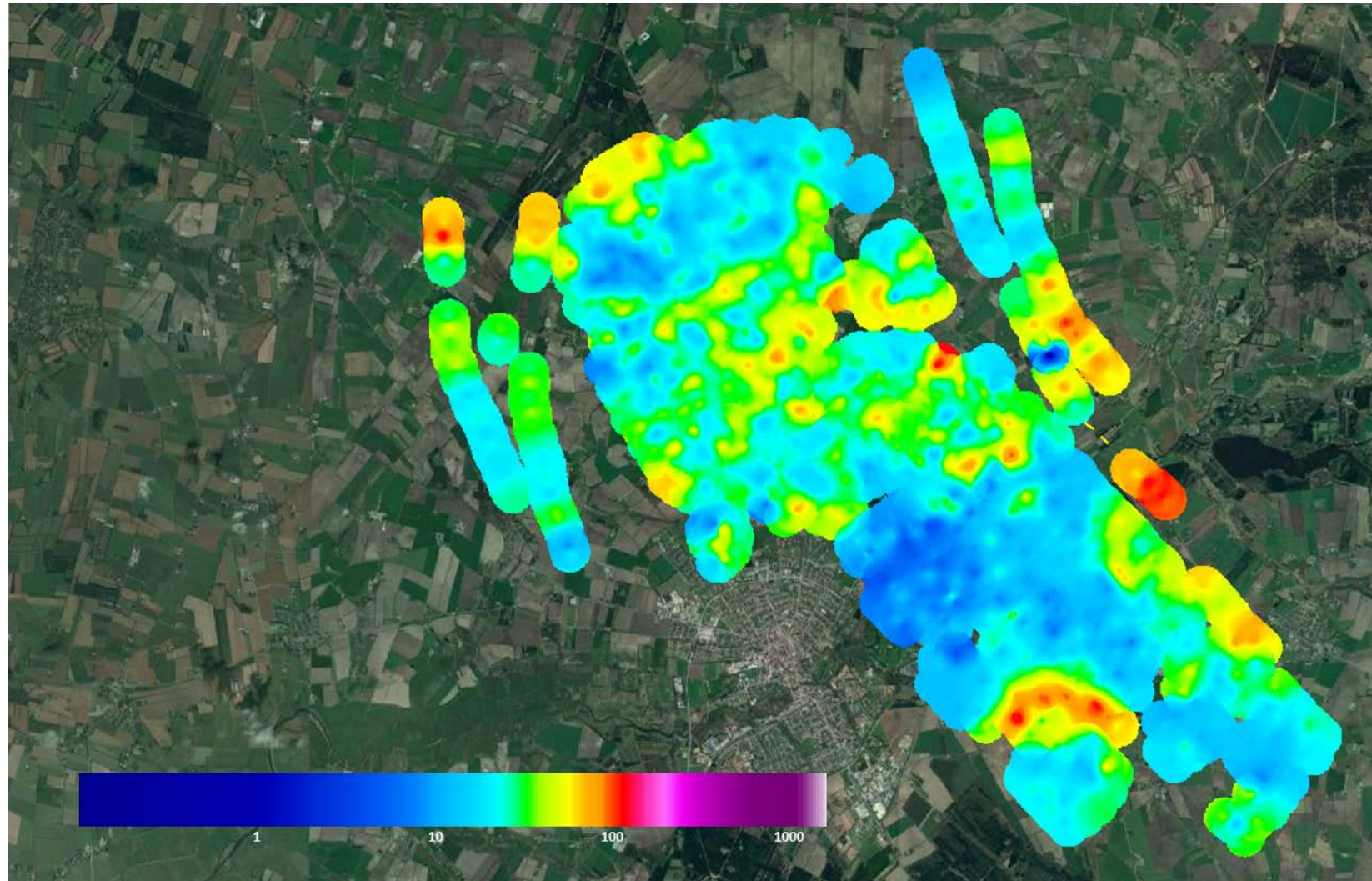
**Mean Resistivity Map [Ohmm].**

Elevation:  
-90m to -85m



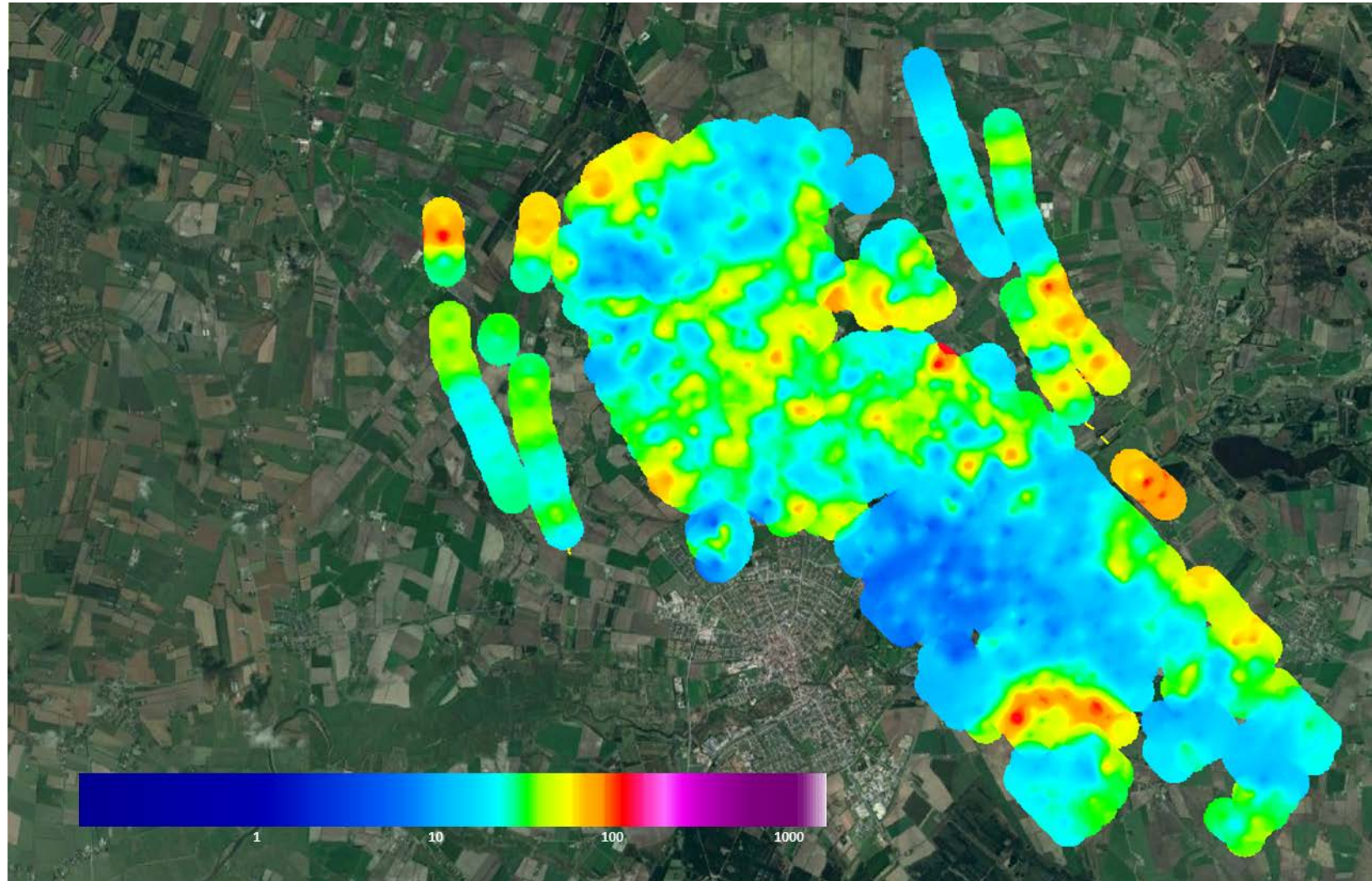
**Mean Resistivity Map [Ohmm].**

Elevation:  
-95m to -90m



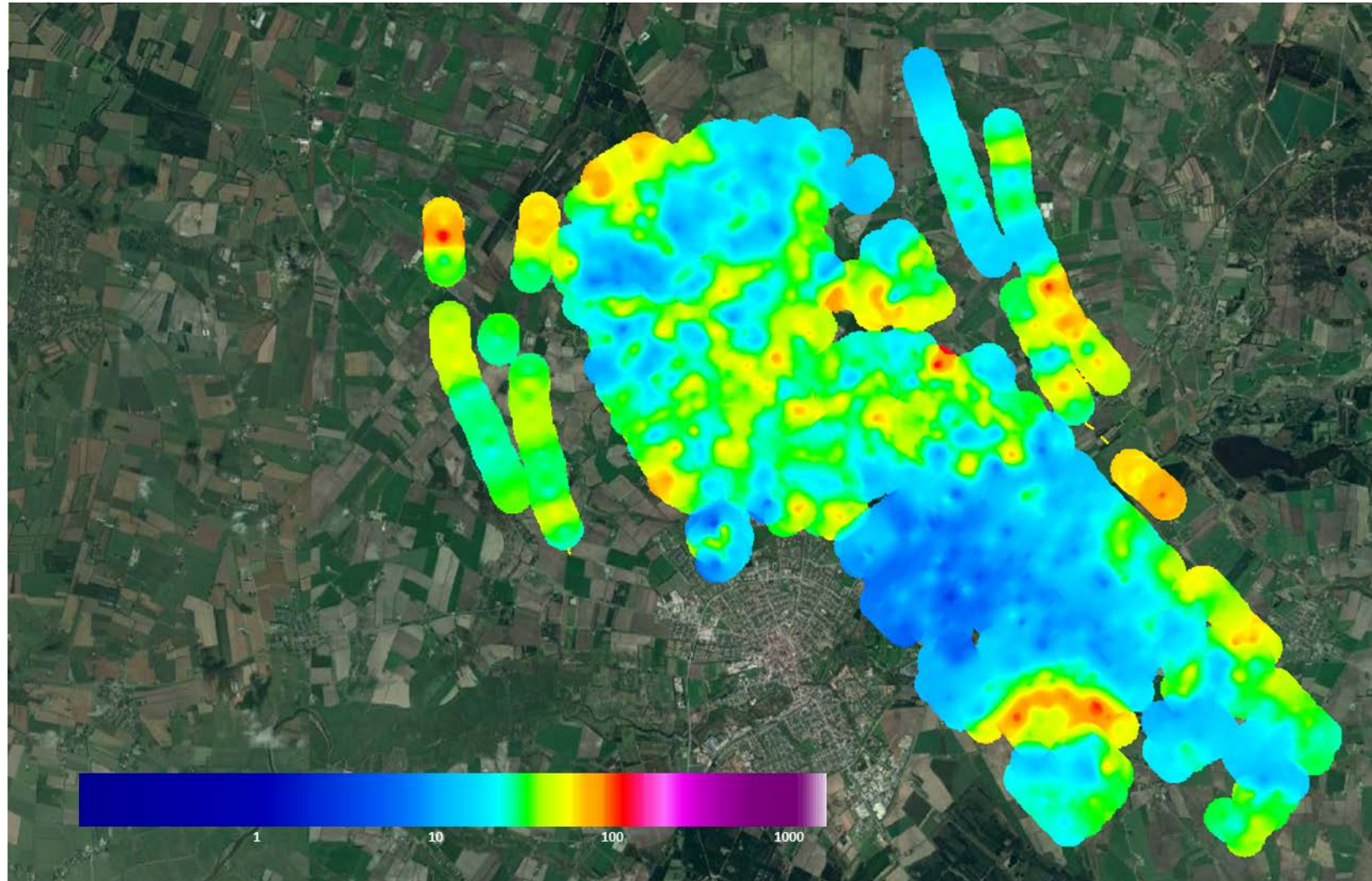
**Mean Resistivity Map [Ohm].**

Elevation:  
-100m to -95m



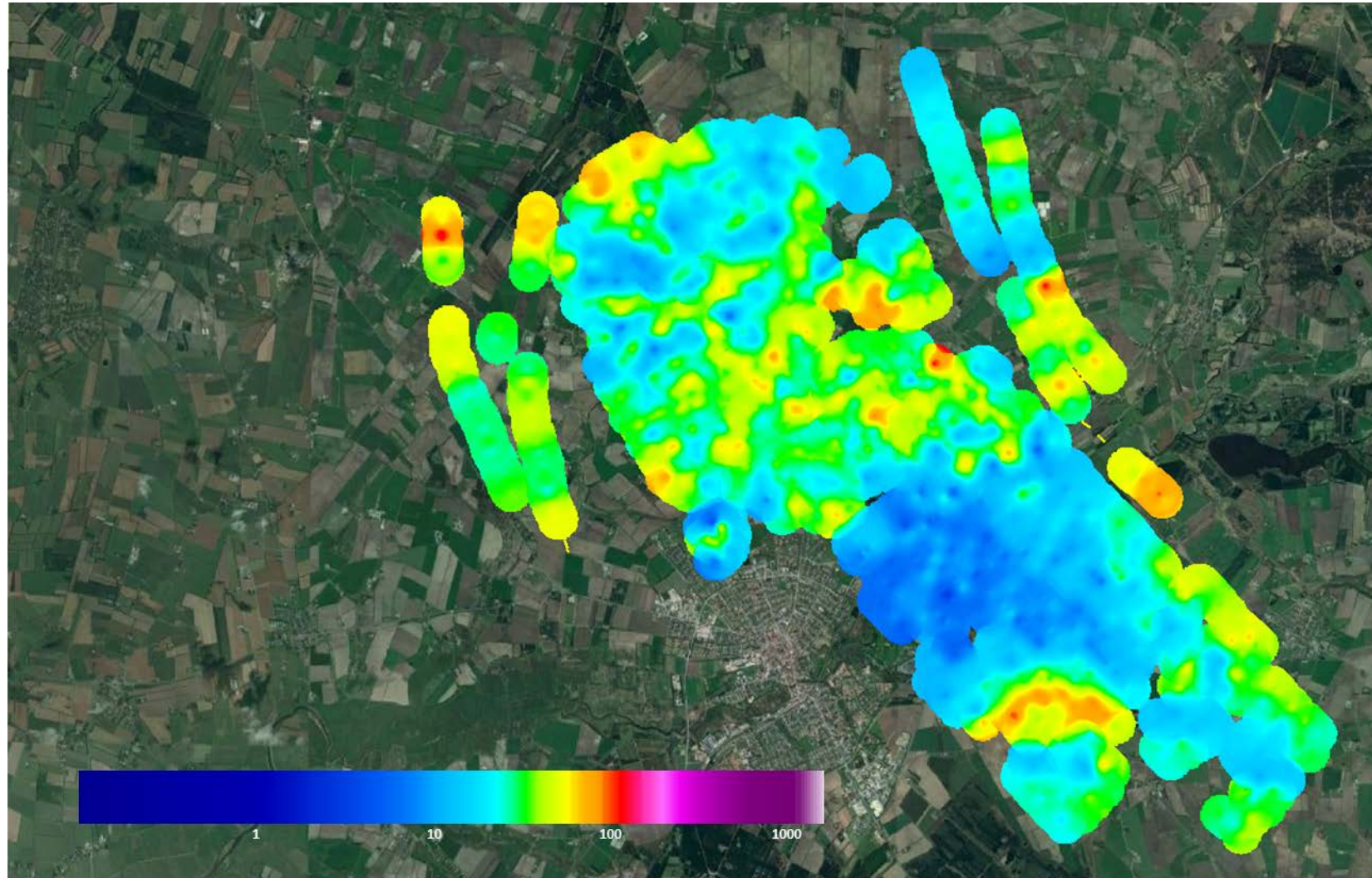
**Mean Resistivity Map [Ohmm].**

Elevation:  
-105m to -100m



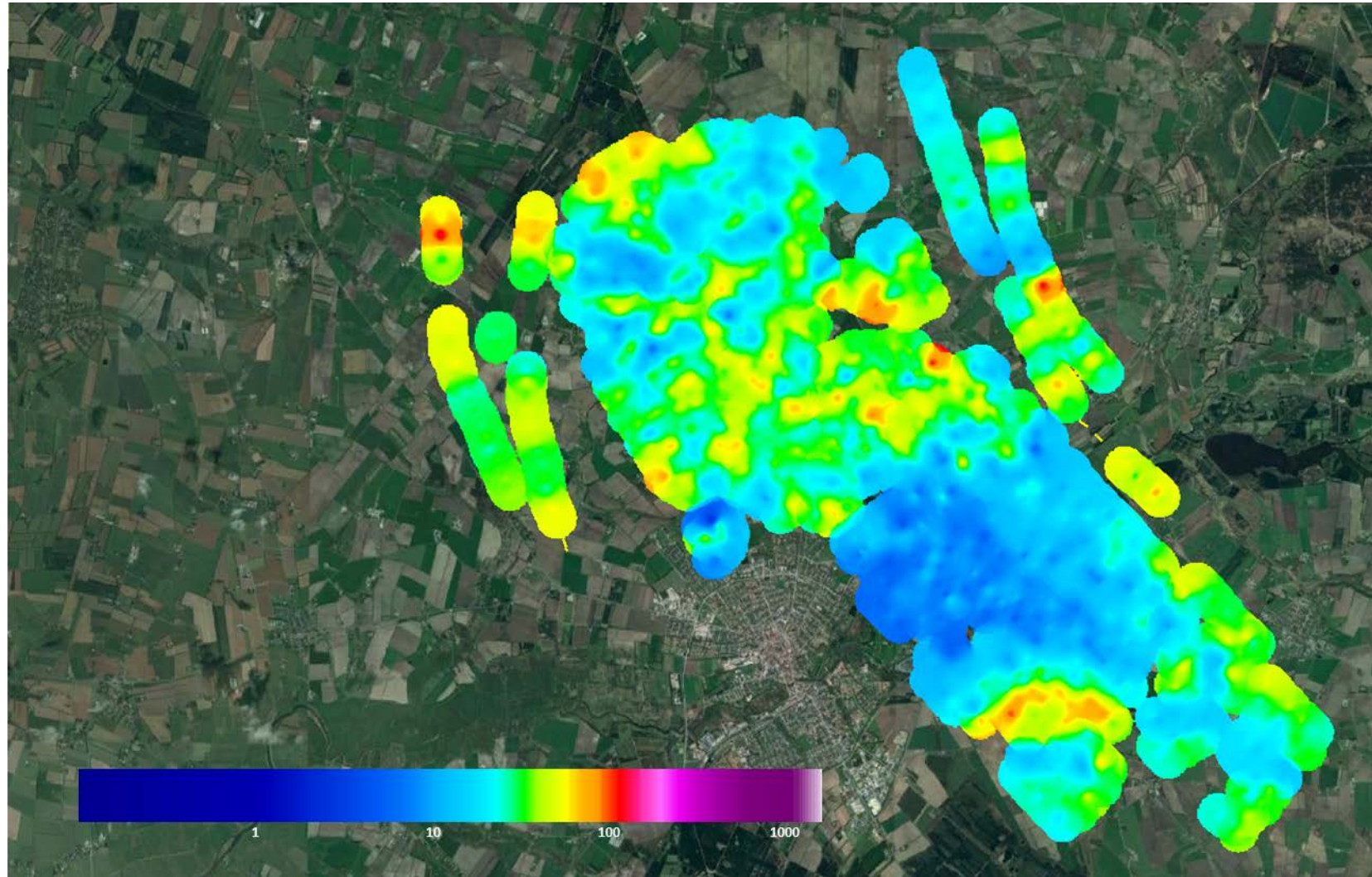
**Mean Resistivity Map [Ohmm].**

Elevation:  
-110m to -105m



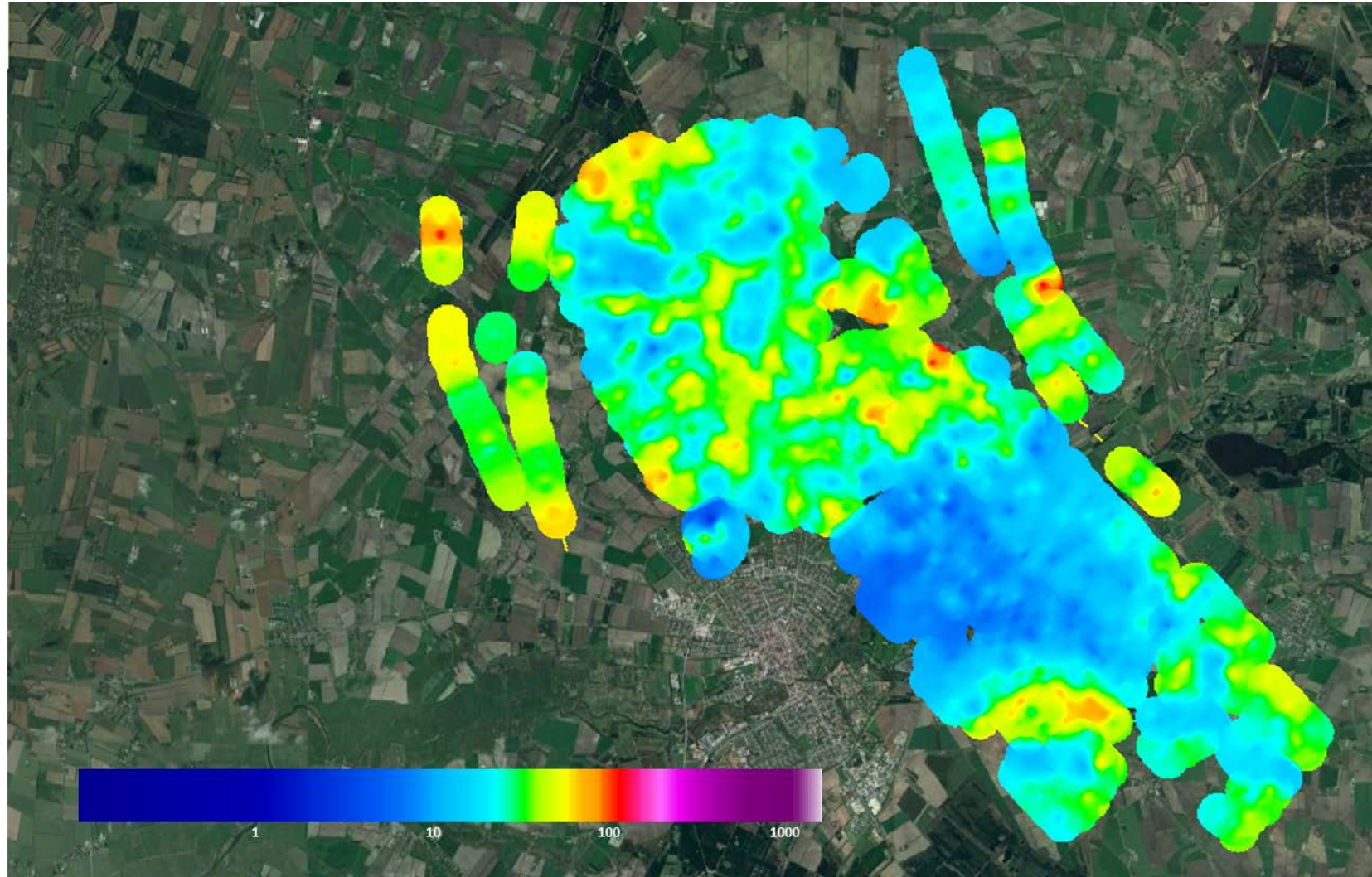
**Mean Resistivity Map [Ohmm].**

Elevation:  
-115m to -110m



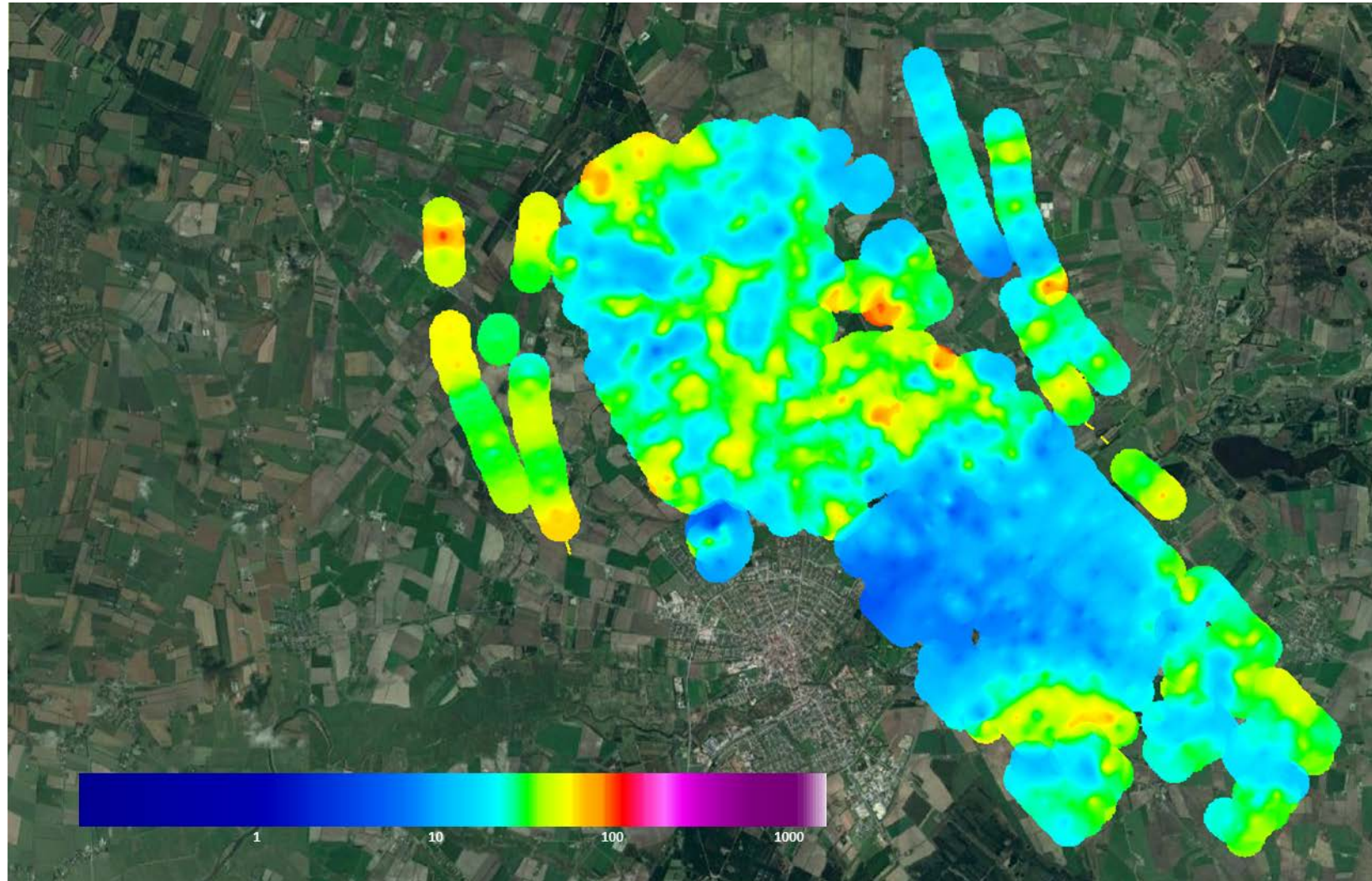
**Mean Resistivity Map [Ohmm].**

Elevation:  
-120m to -115m



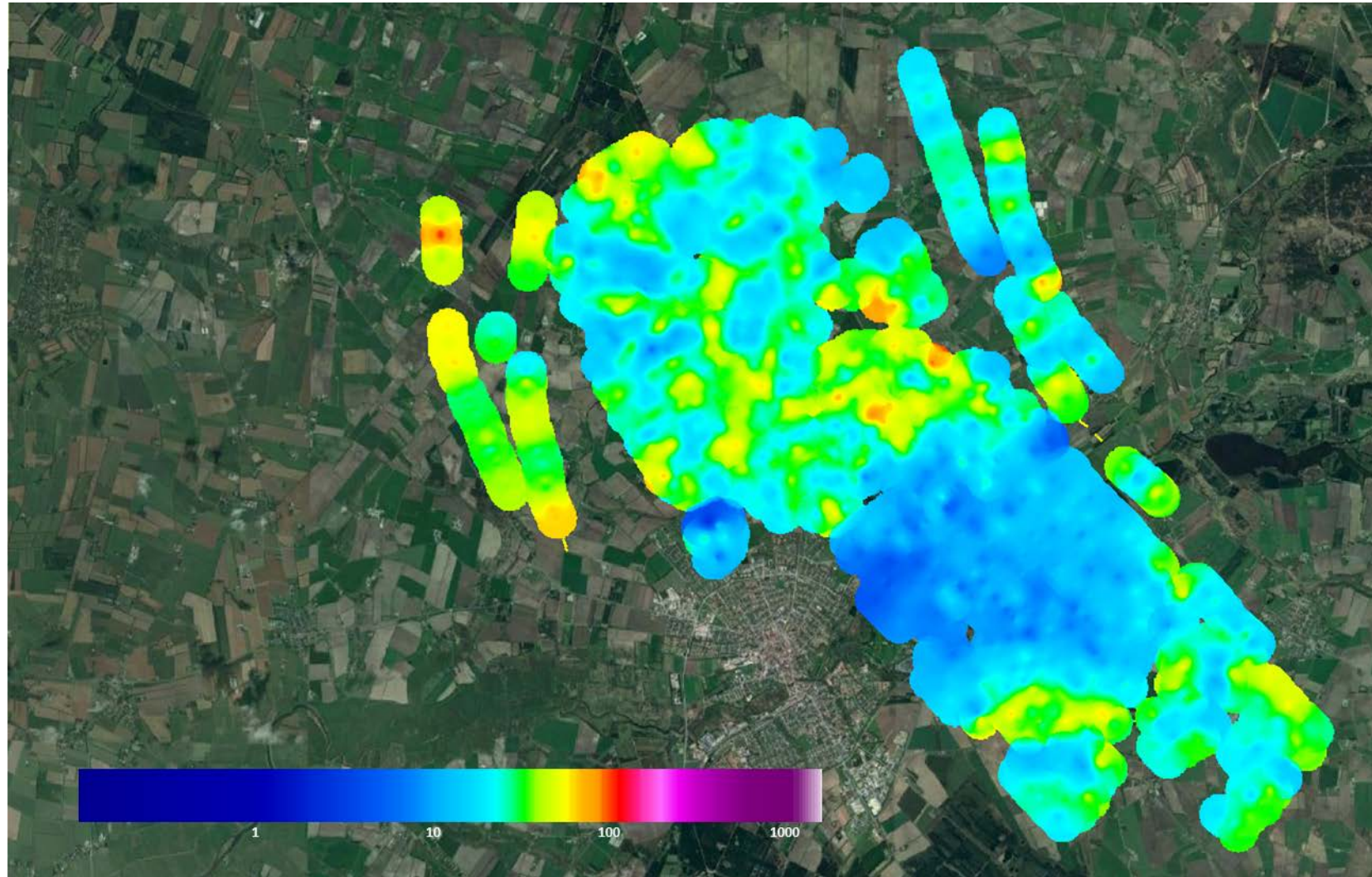
**Mean Resistivity Map [Ohmm].**

Elevation:  
-125m to -120m



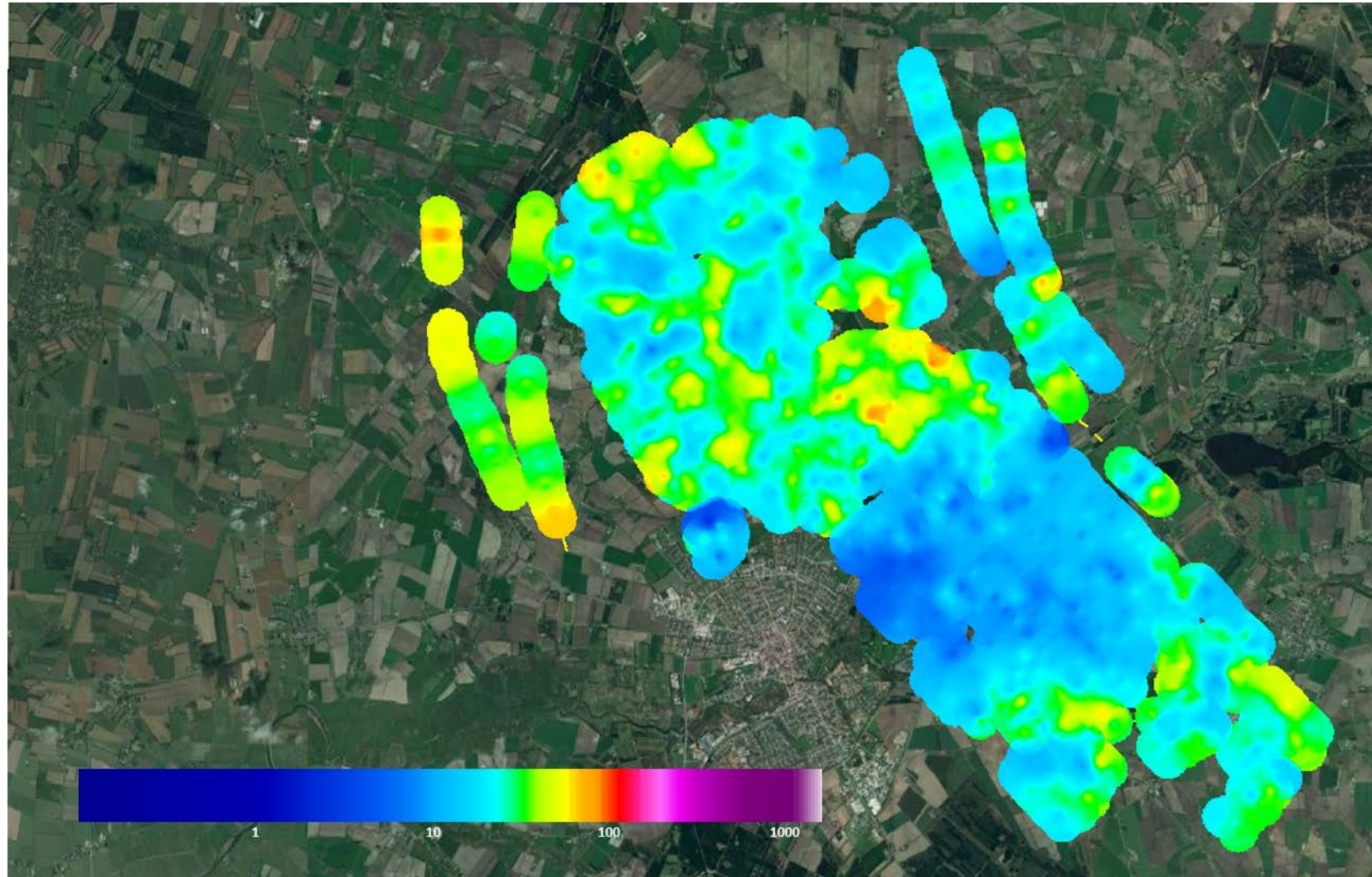
**Mean Resistivity Map [Ohmm].**

Elevation:  
-130m to -125m



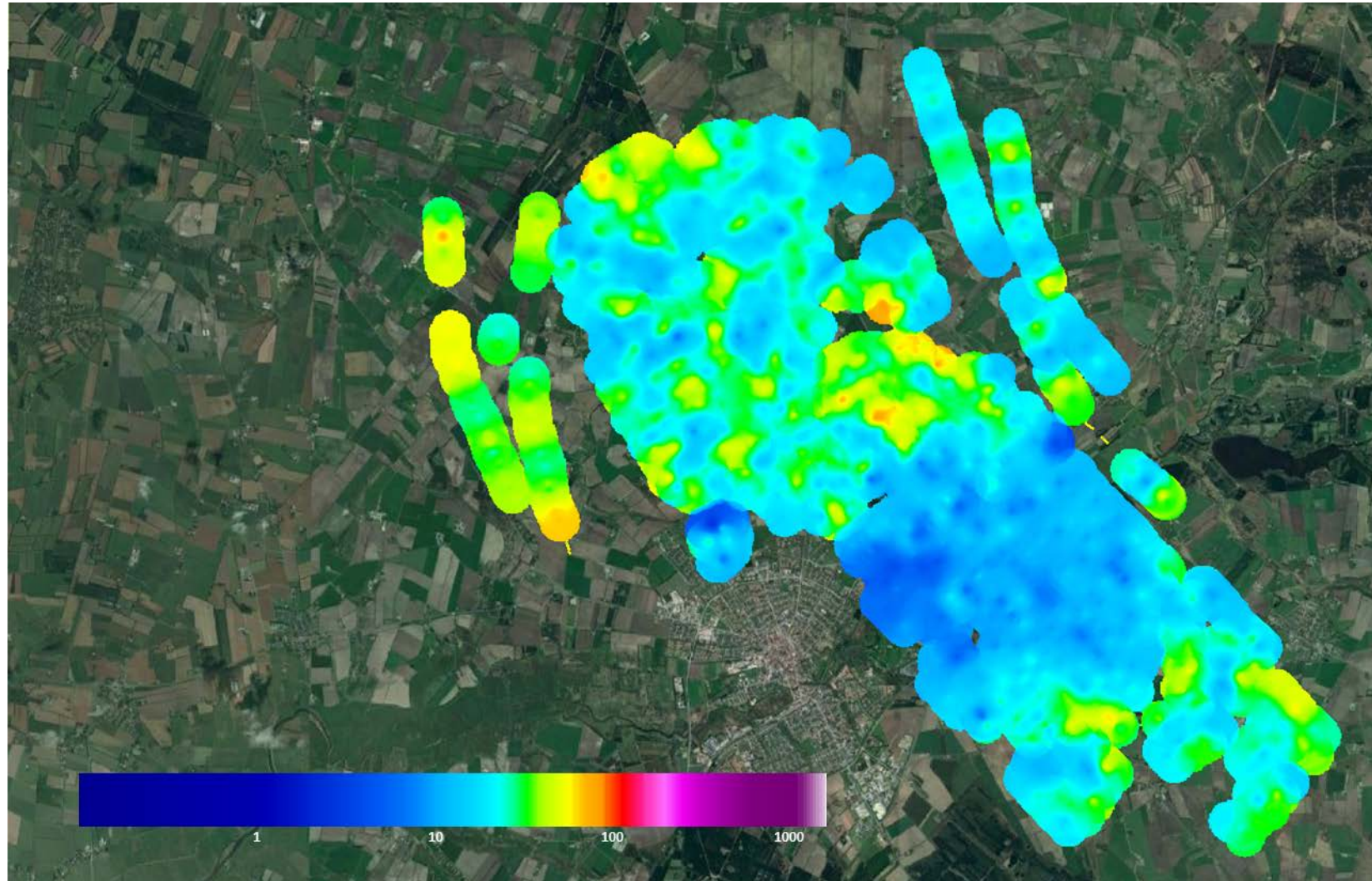
**Mean Resistivity  
Map [Ohmm].**

Elevation:  
-135m to -130m



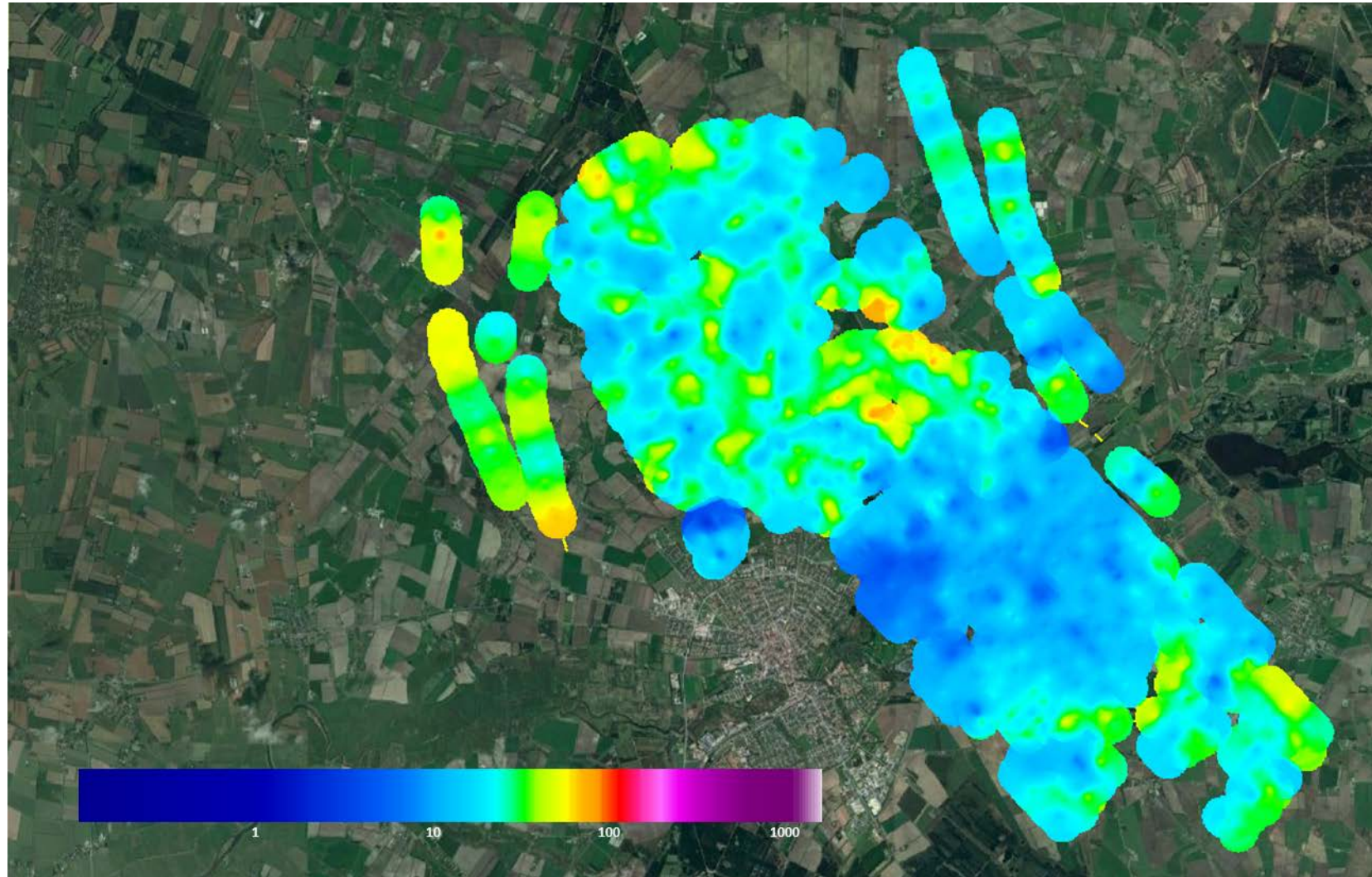
**Mean Resistivity Map [Ohmm].**

Elevation:  
-140m to -135m



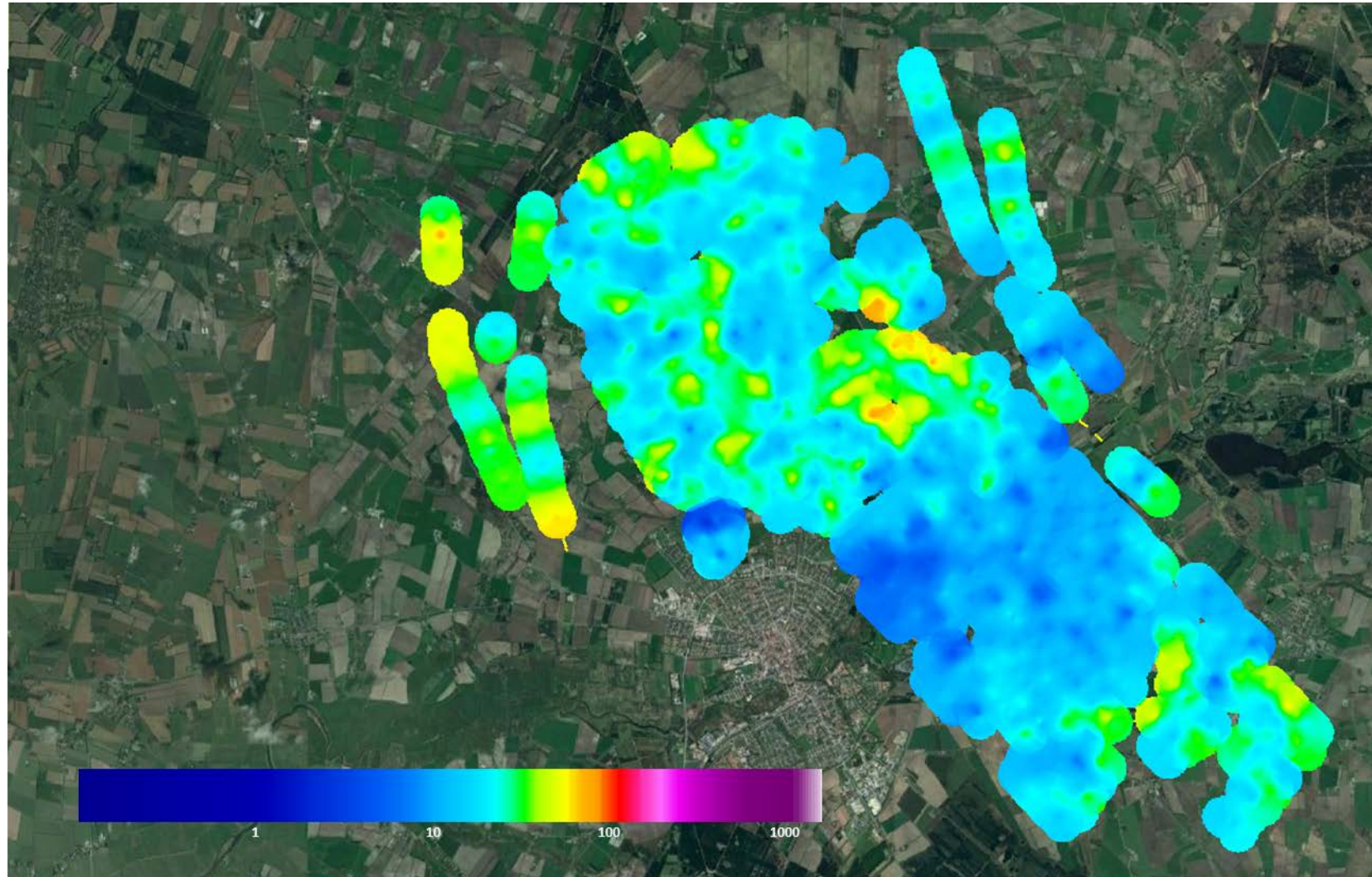
**Mean Resistivity Map [Ohmm].**

Elevation:  
-145m to -140m



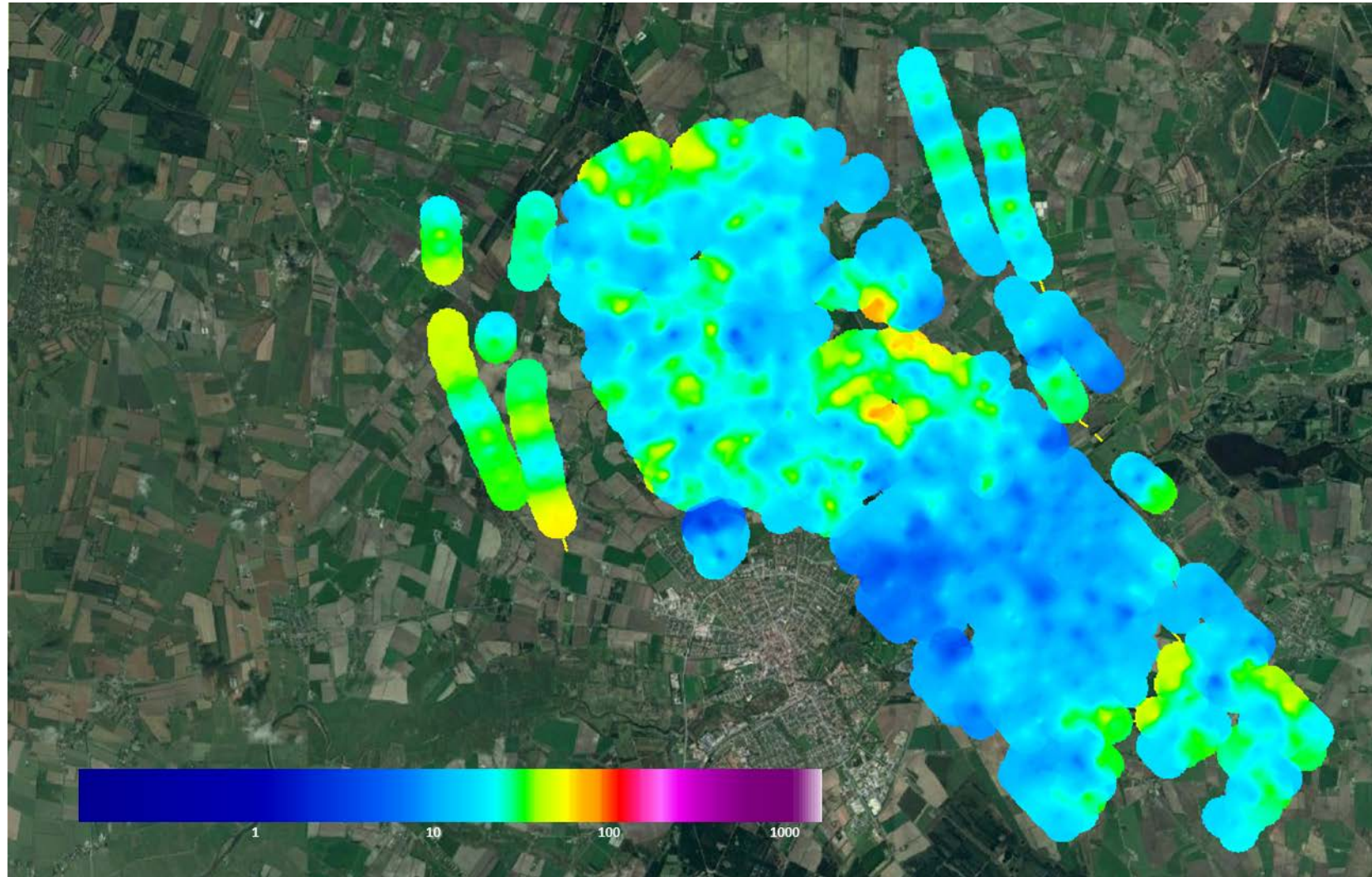
**Mean Resistivity Map [Ohmm].**

Elevation:  
-150m to -145m



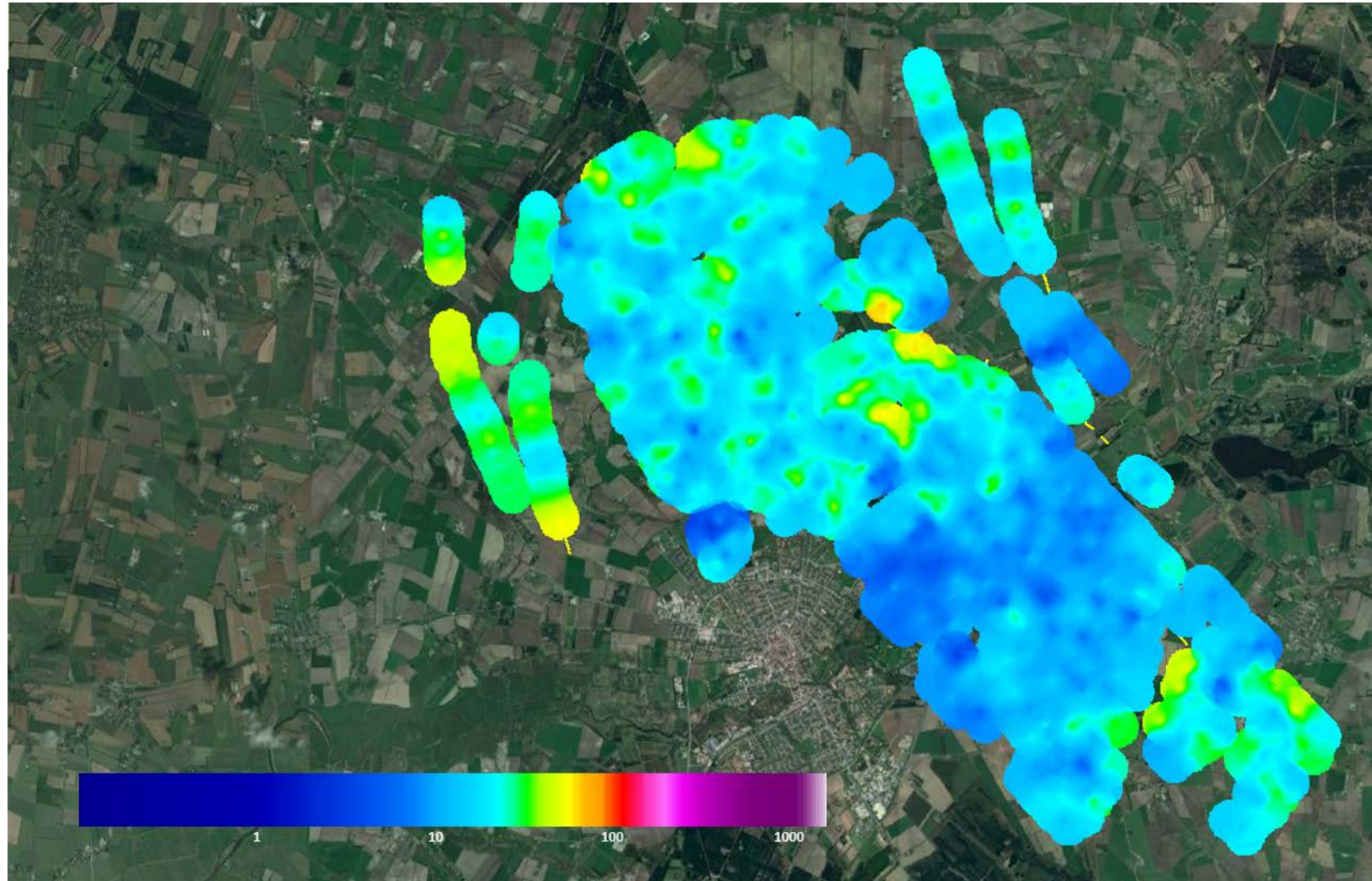
**Mean Resistivity Map [Ohmm].**

Elevation:  
-155m to 150m



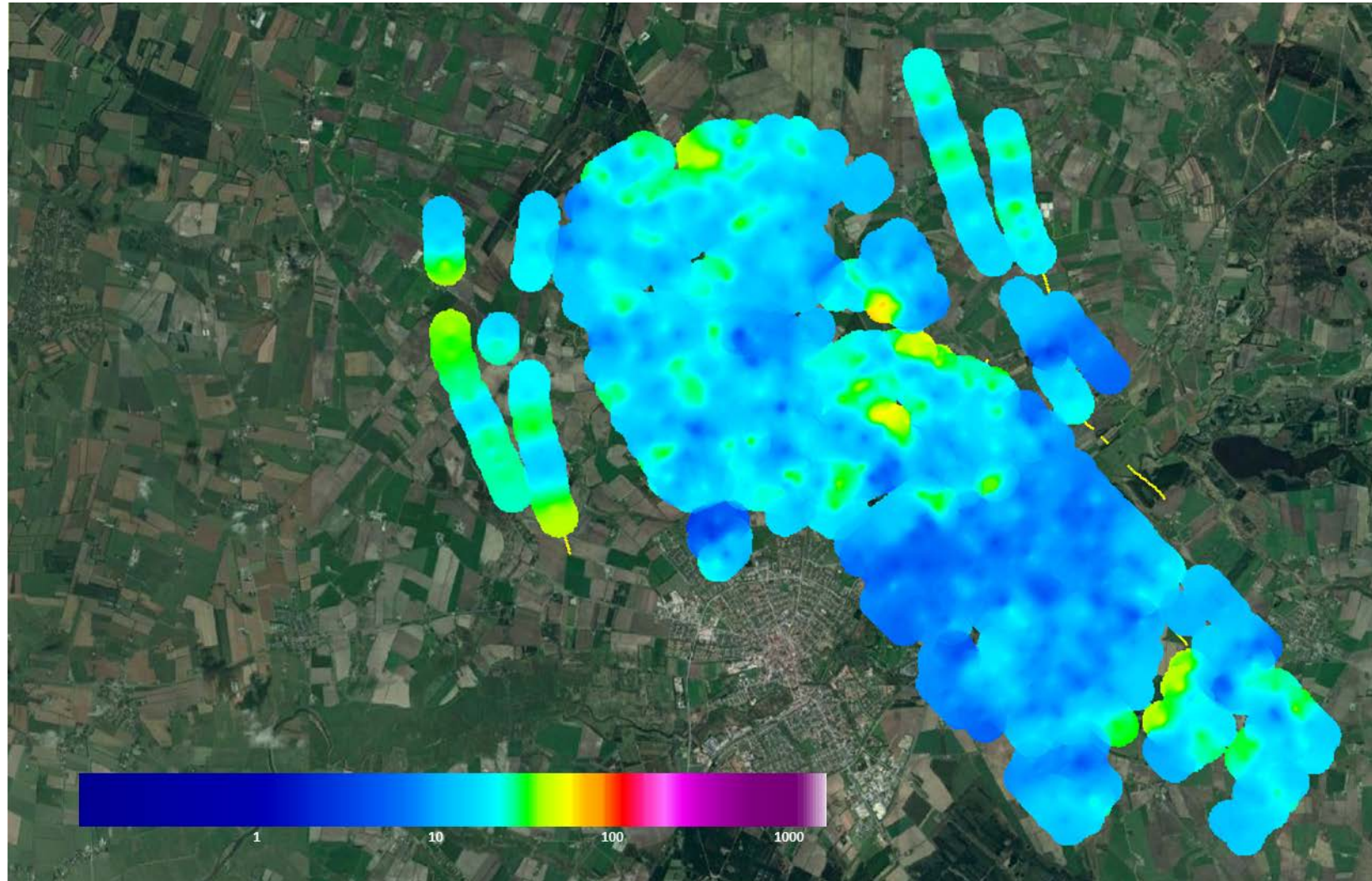
**Mean Resistivity  
Map [Ohmm].**

Elevation:  
-160m to 155m



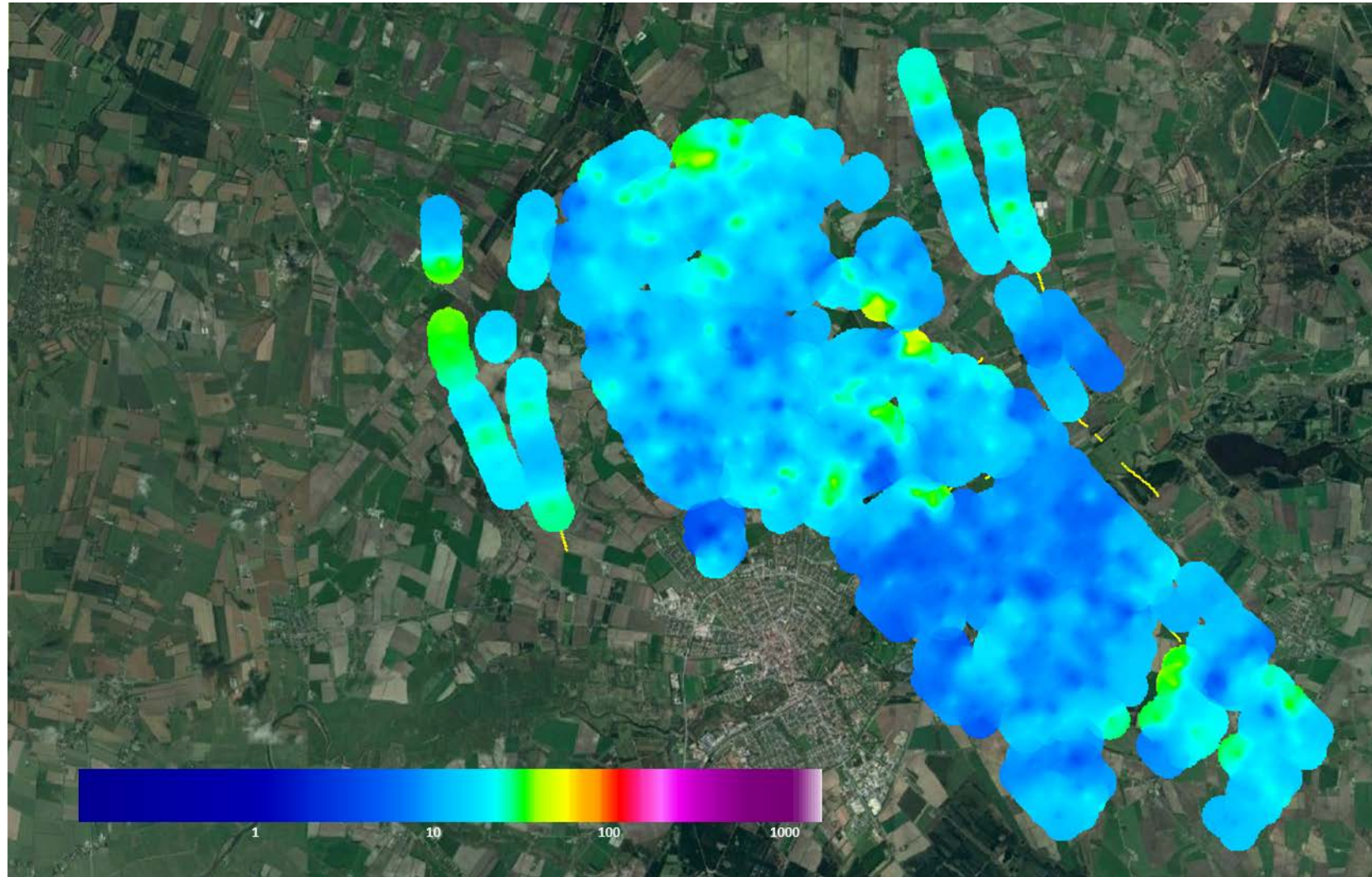
**Mean Resistivity Map [Ohmm].**

Elevation:  
-170m to 160m



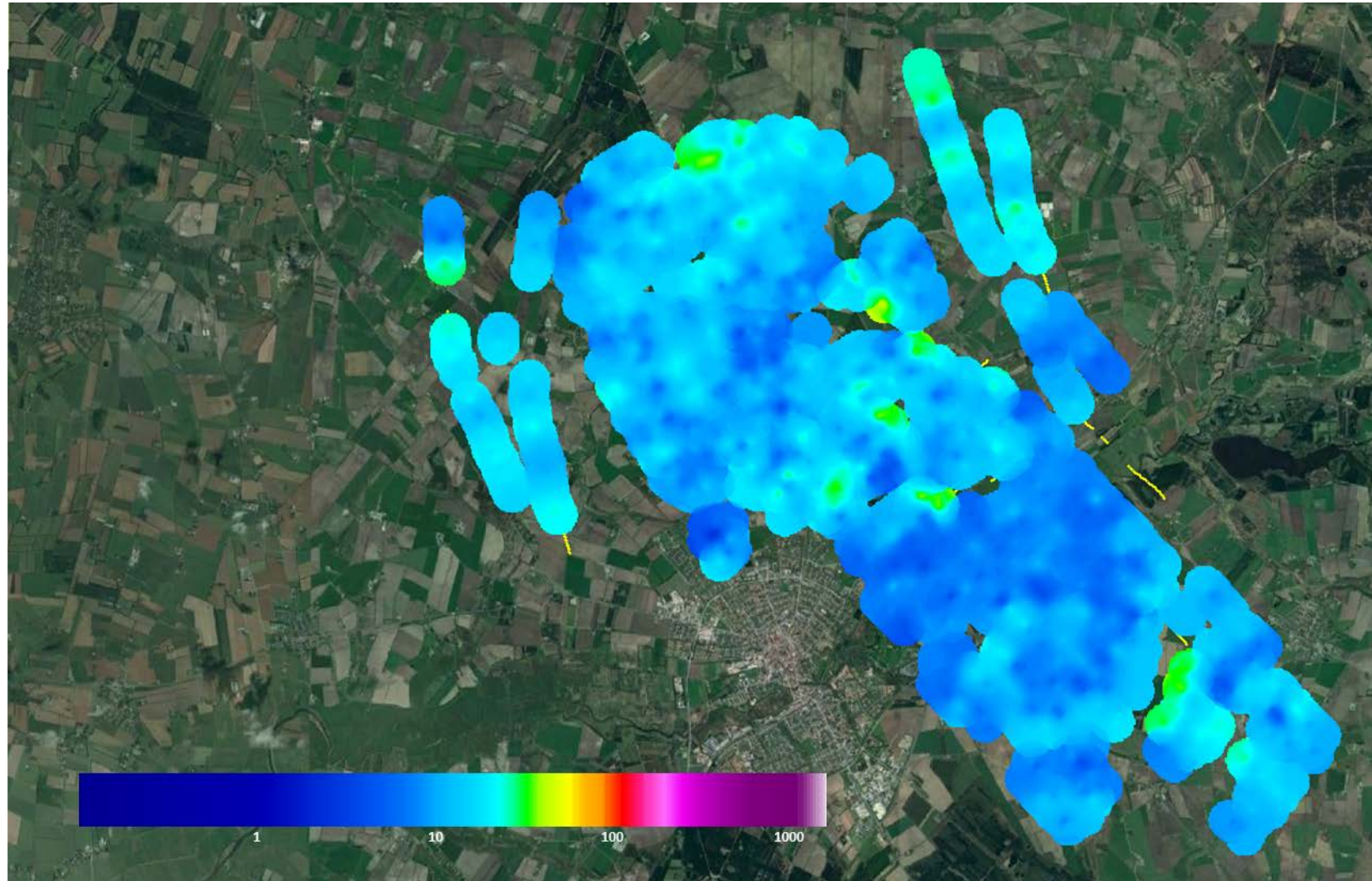
**Mean Resistivity  
Map [Ohmm].**

Elevation:  
-180m to -160m



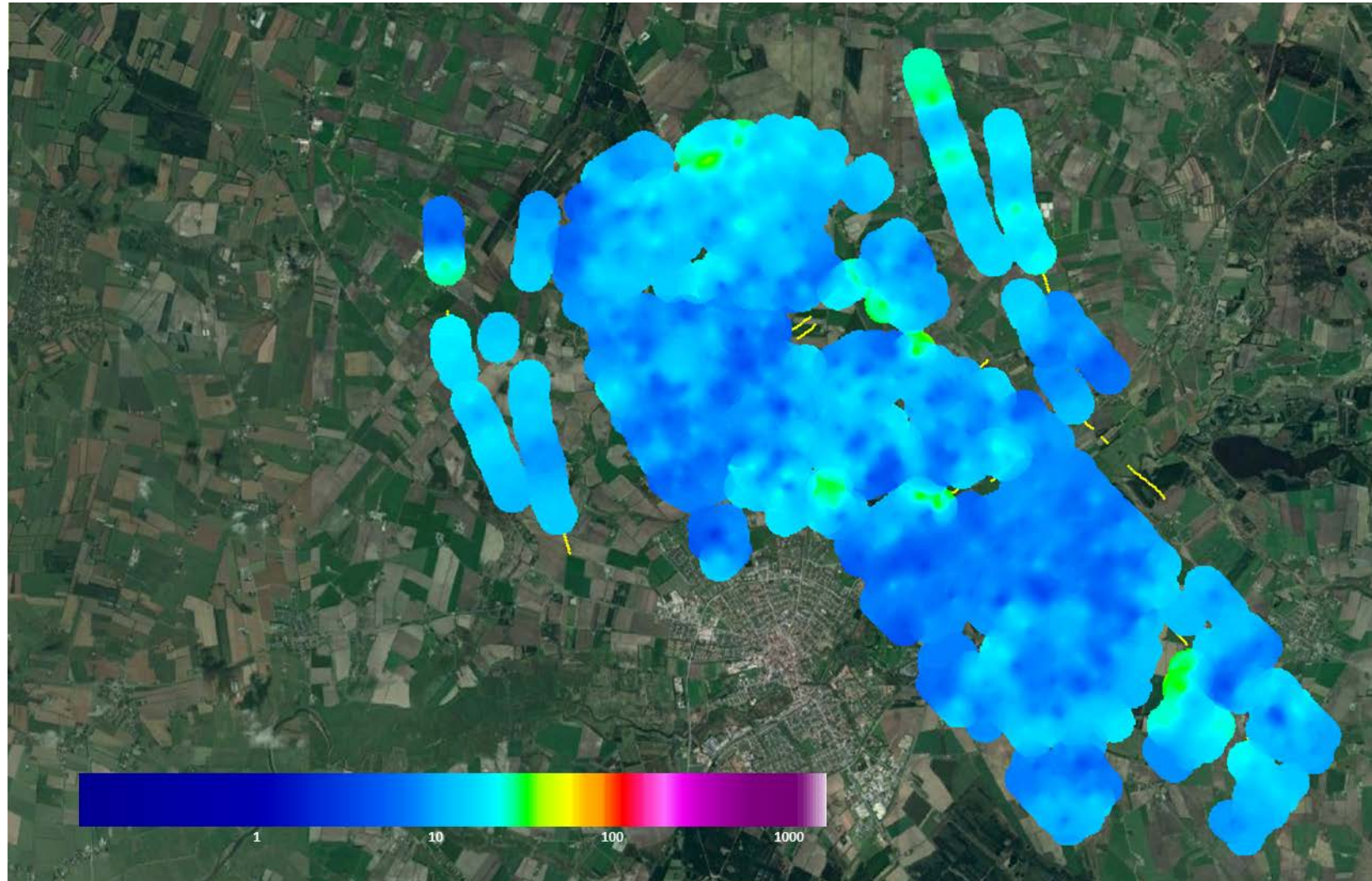
**Mean Resistivity Map [Ohmm].**

Elevation:  
-190m to -180m



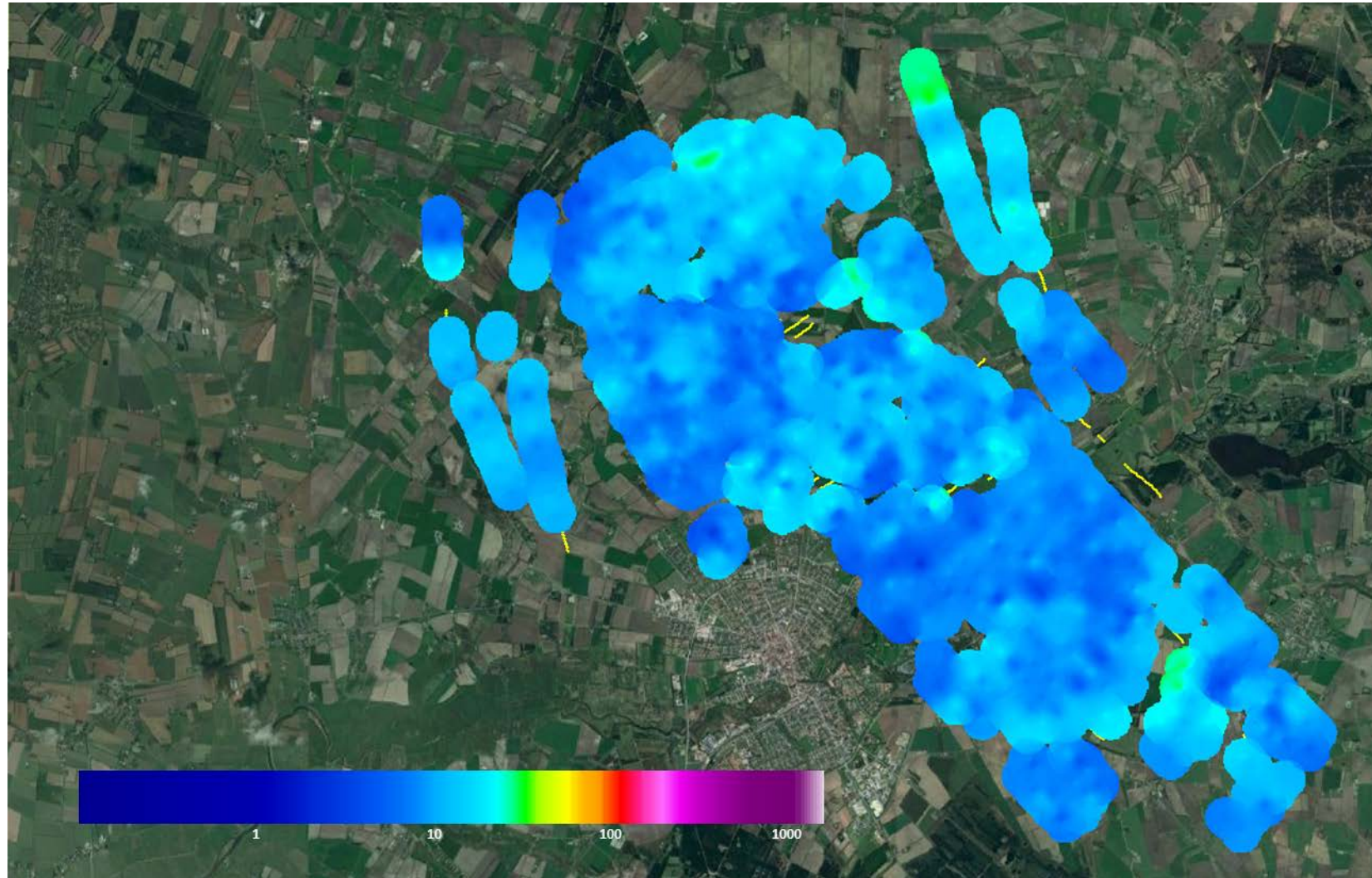
**Mean Resistivity Map [Ohmm].**

Elevation:  
-200m to -190m



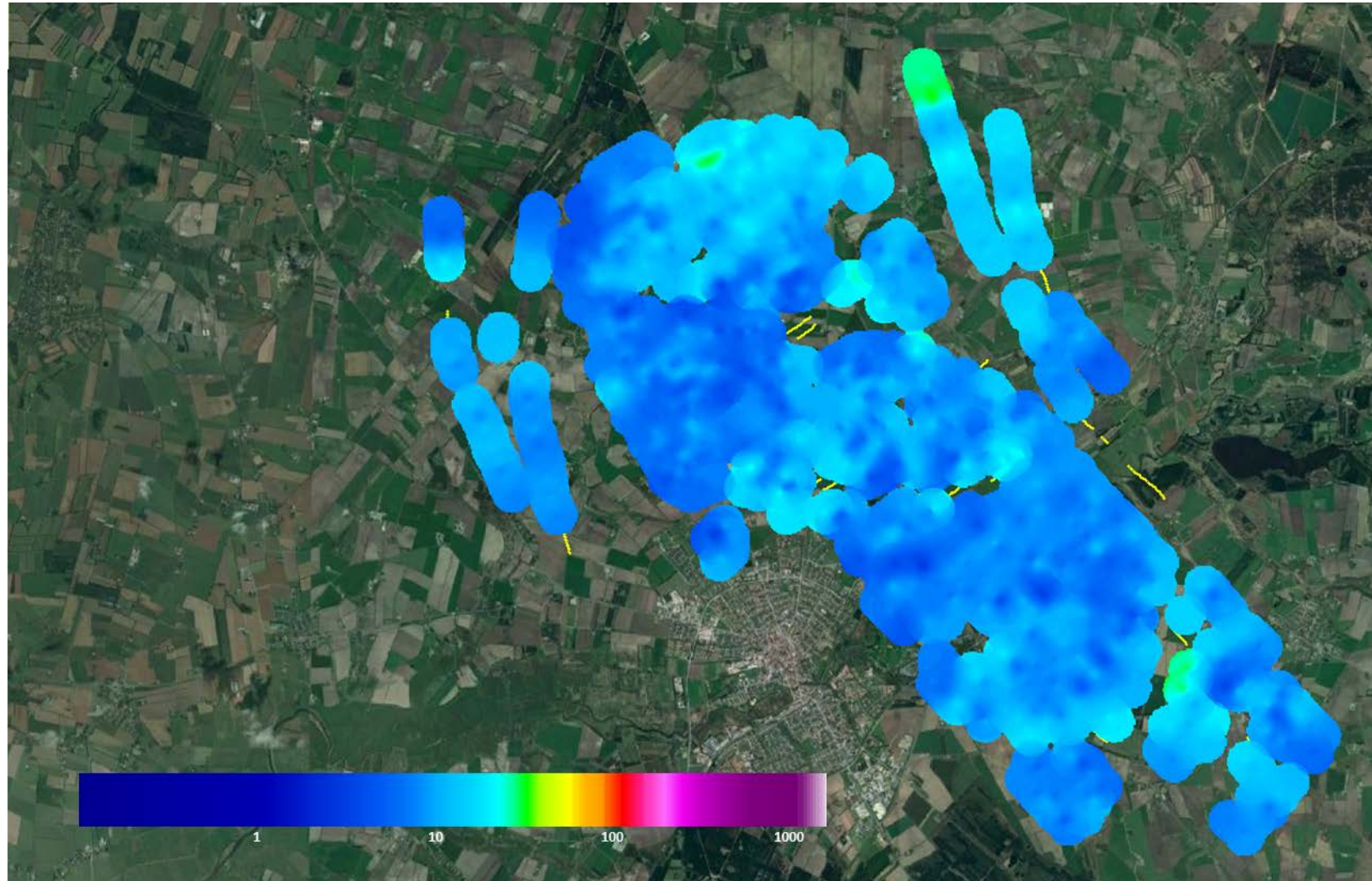
**Mean Resistivity Map [Ohmm].**

Elevation:  
-210m to -200m



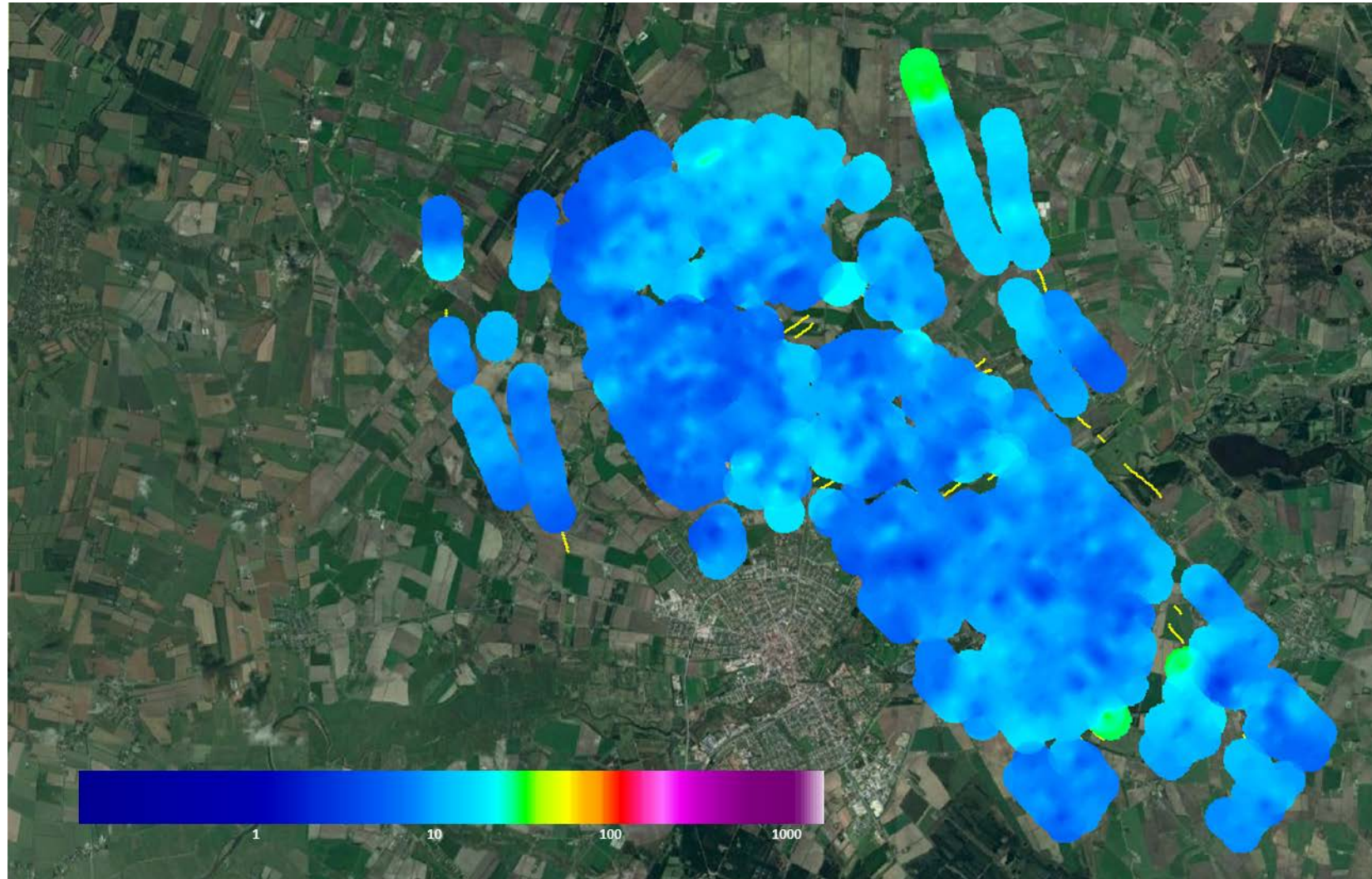
**Mean Resistivity Map [Ohmm].**

Elevation:  
-220m to -210m



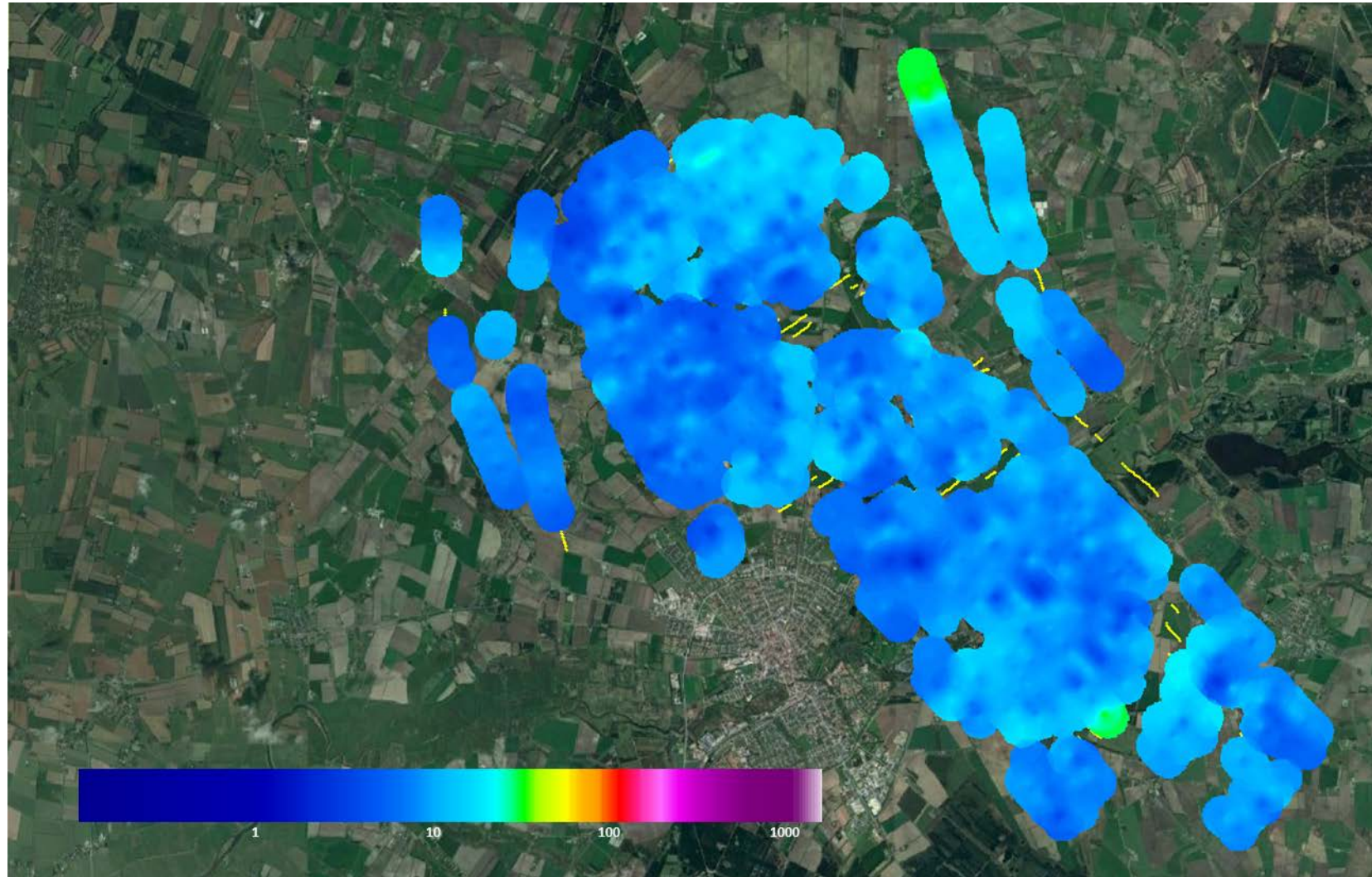
**Mean Resistivity Map [Ohmm].**

Elevation:  
-230m to -220m



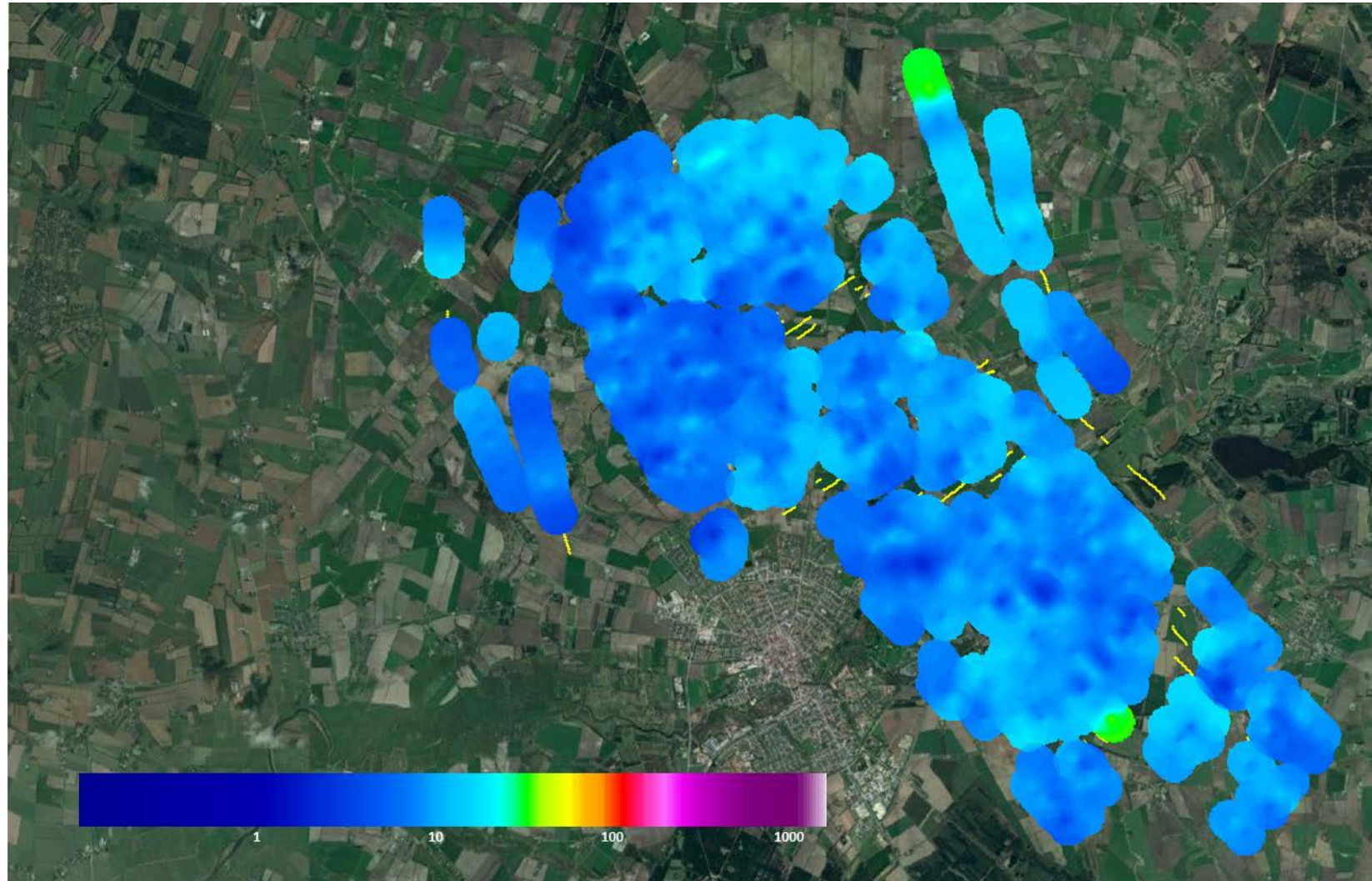
**Mean Resistivity  
Map [Ohm].**

Elevation:  
-240m to -230m



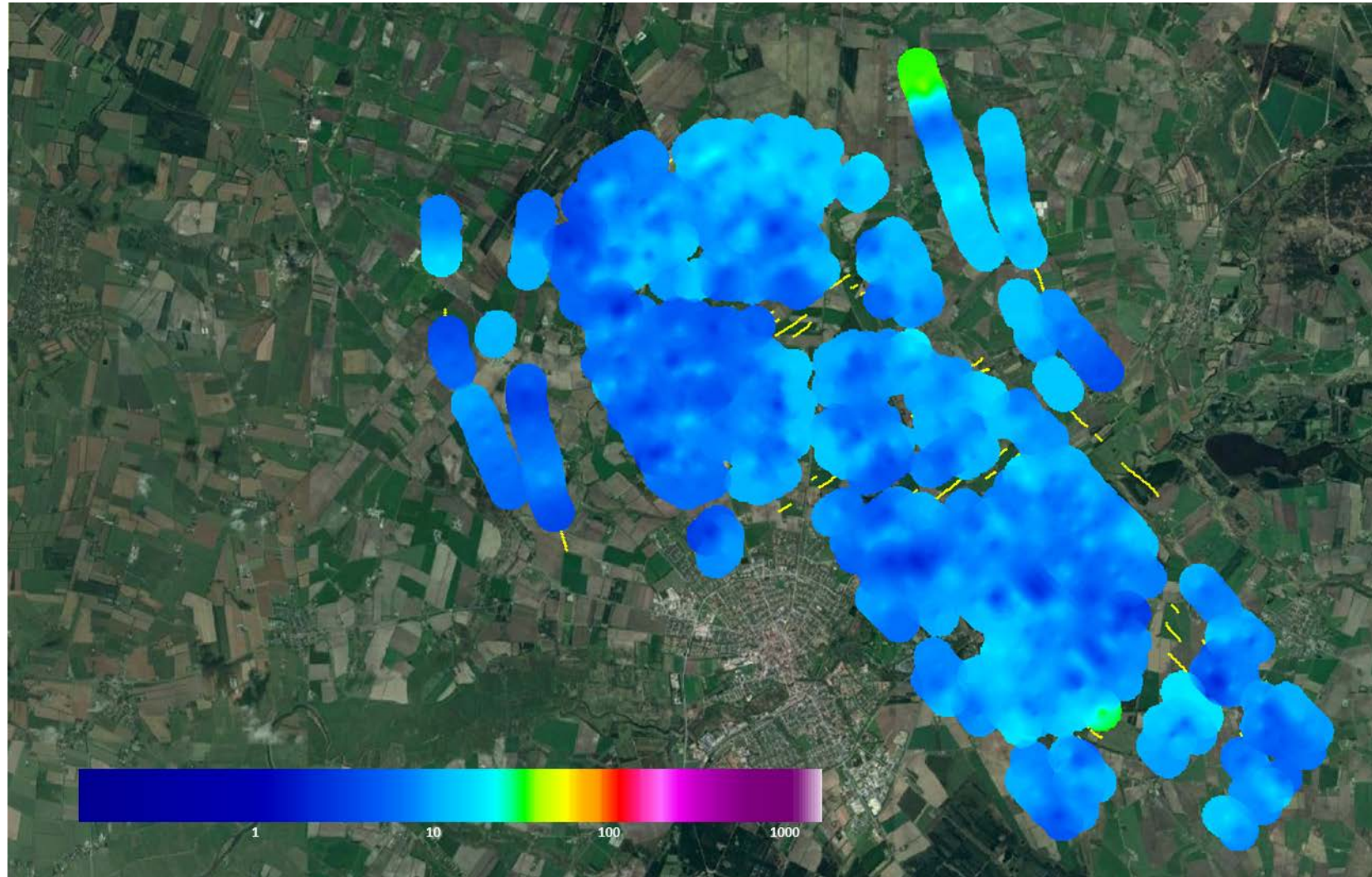
**Mean Resistivity  
Map [Ohmm].**

Elevation:  
-250m to -240m



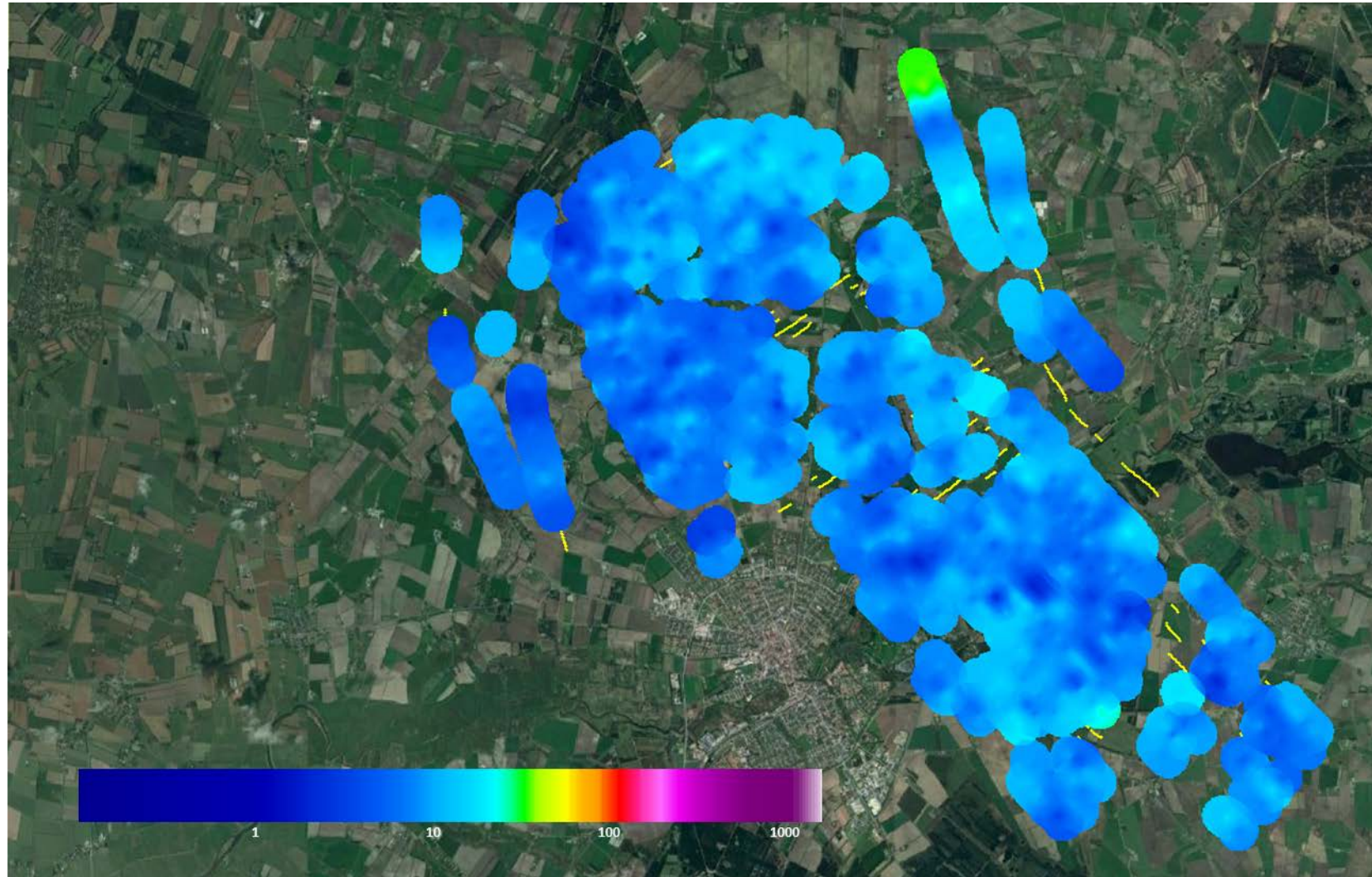
**Mean Resistivity  
Map [Ohmm].**

Elevation:  
-260m to -250m



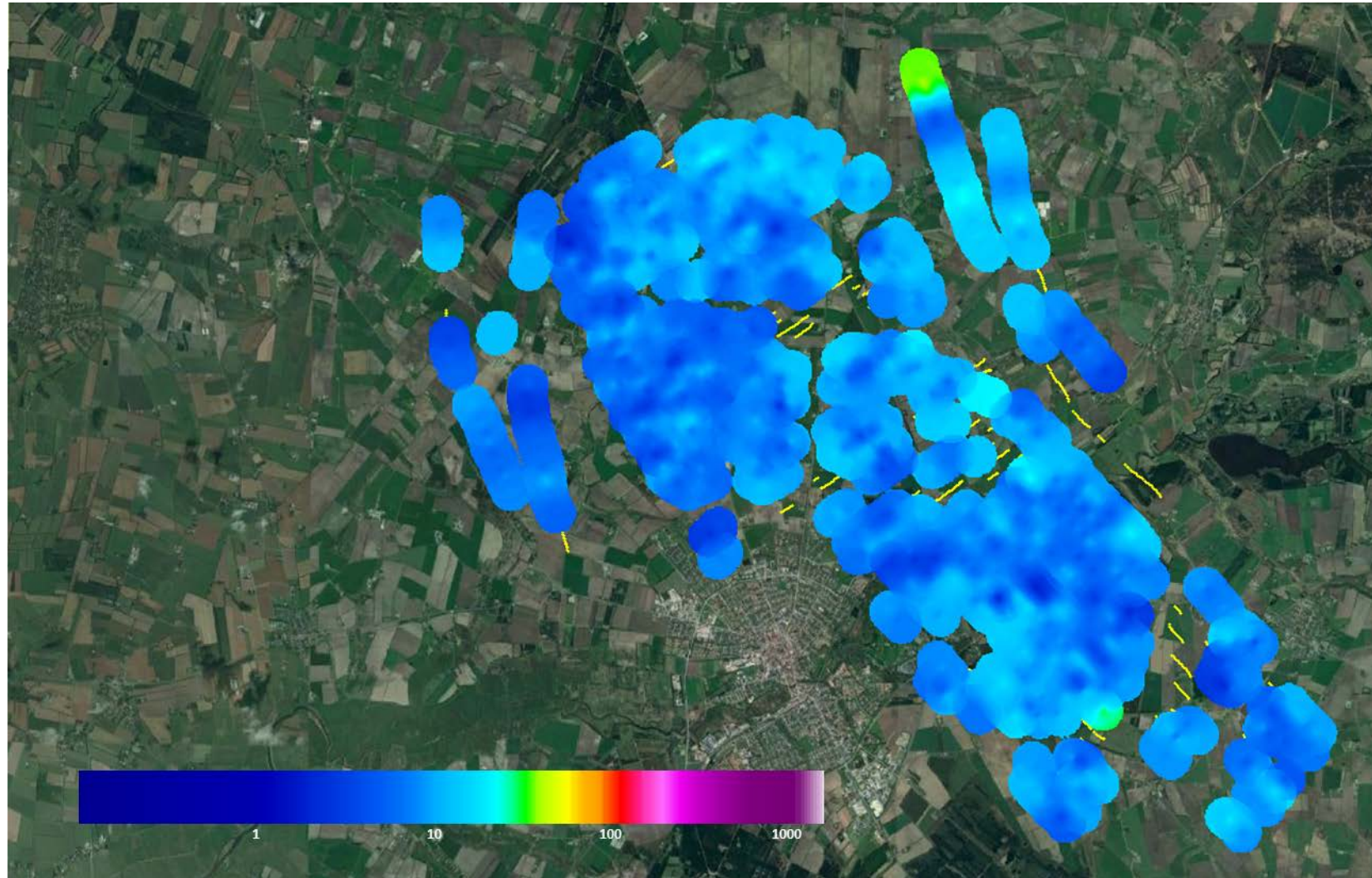
**Mean Resistivity  
Map [Ohmm].**

Elevation:  
-270m to -260m



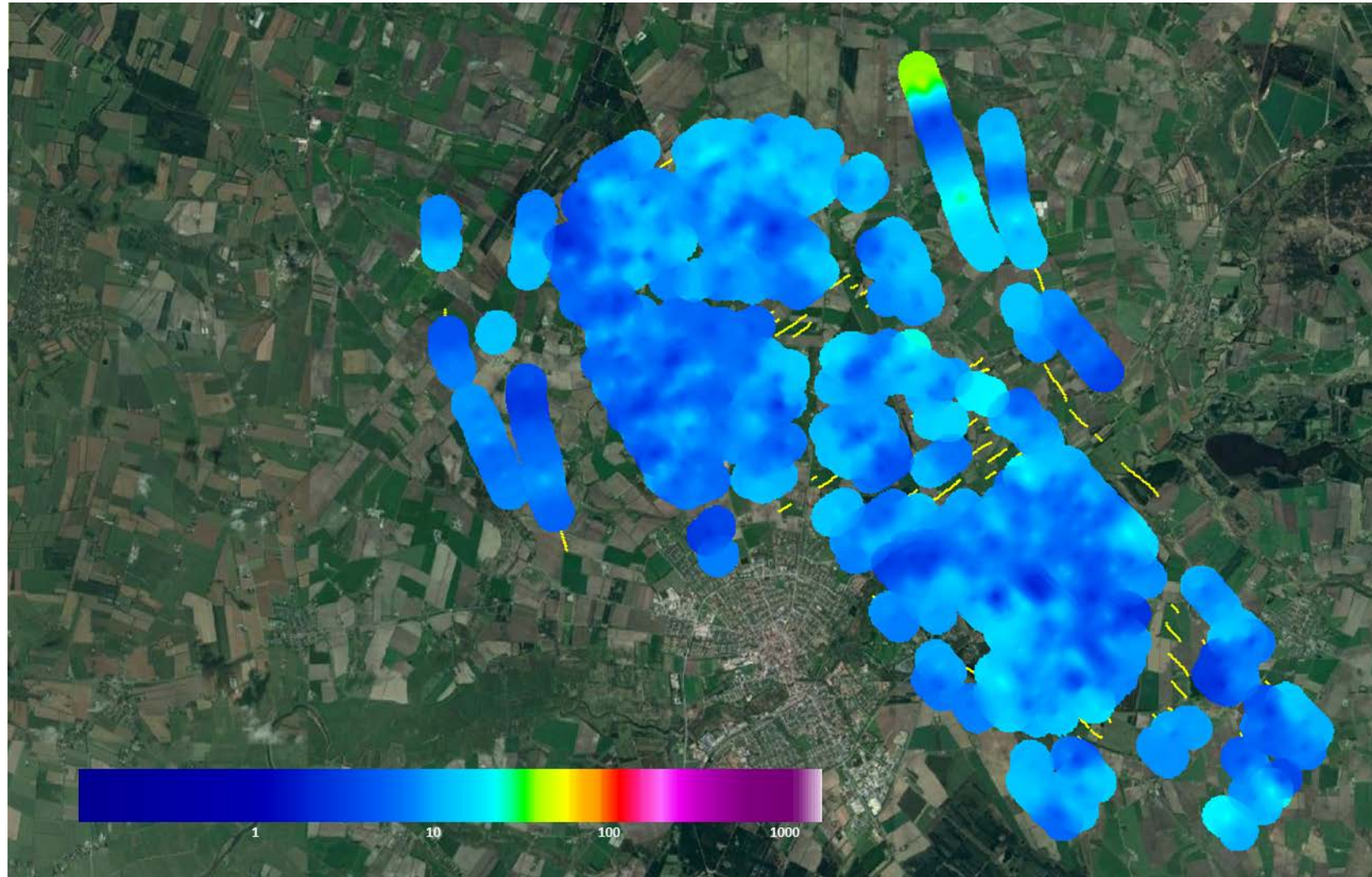
**Mean Resistivity Map [Ohmm].**

Elevation:  
-280m to -270m



**Mean Resistivity Map [Ohmm].**

Elevation:  
-290m to -280m



**Mean Resistivity Map [Ohmm].**

Elevation:  
-300m to -290m

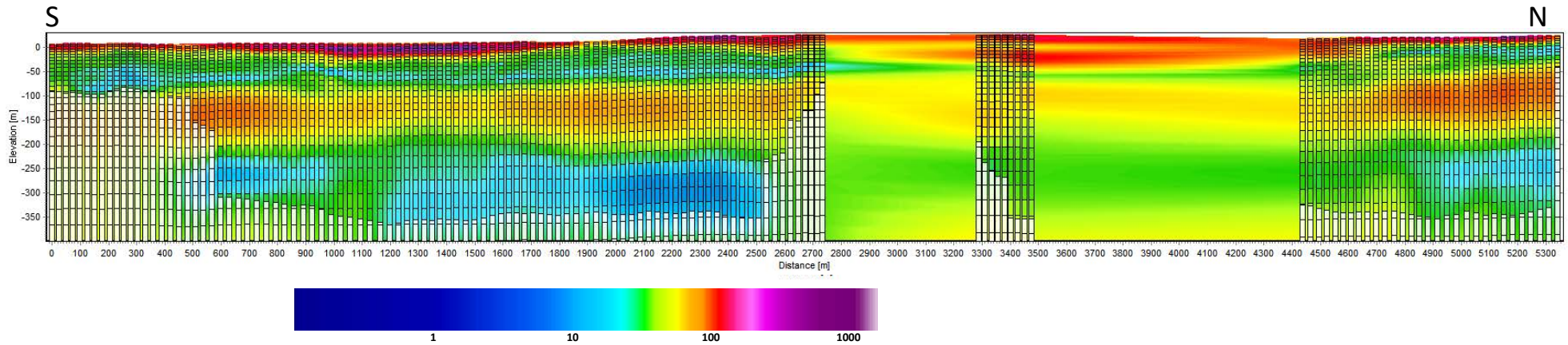
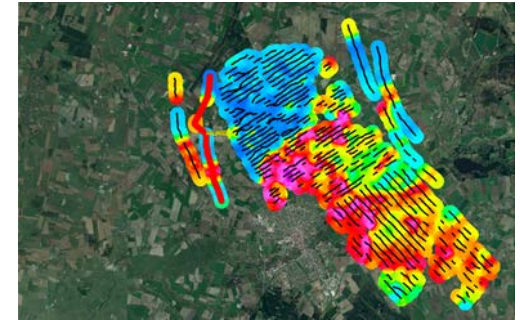
## Appendix III: Cross Sections

This appendix shows the cross sections through an interpolated resistivity grid. The interpolated cross sections are presented together with the original 1D inversion results. The 1D models have been faded towards white at depths below the DOI lower.

### Cross Section [Ohmm].

The inversion result models are plotted on top of the interpolated section. The white blinding represents the area below the DOI lower.

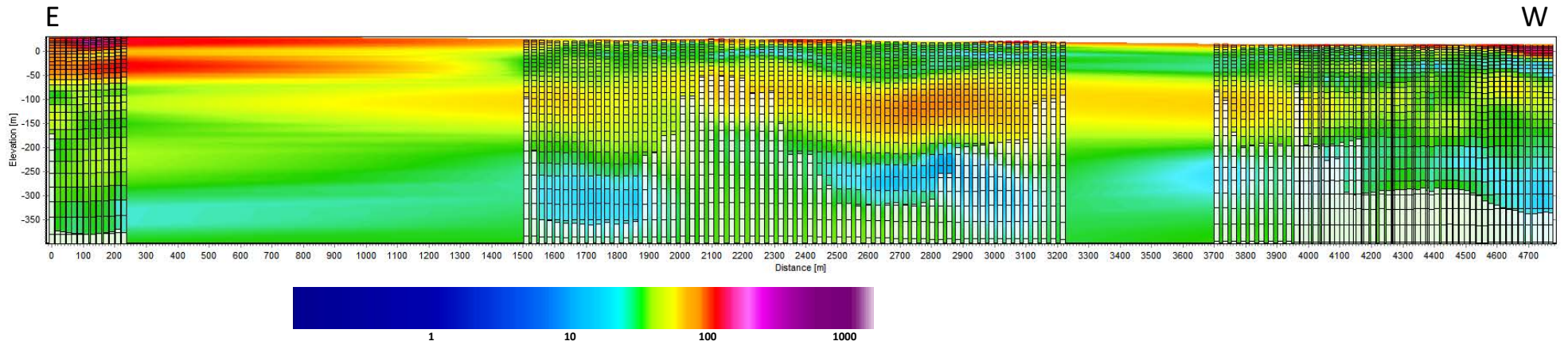
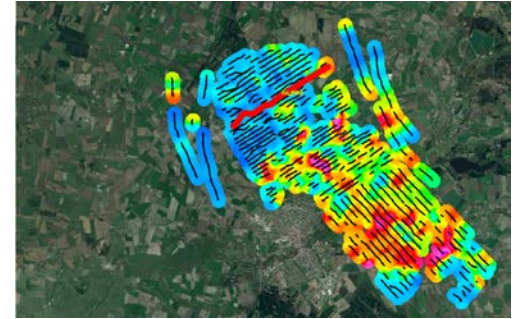
Location of the Cross Section



## Cross Section [Ohmm].

The inversion result models are plotted on top of the interpolated section. The white blinding represents the area below the DOI lower.

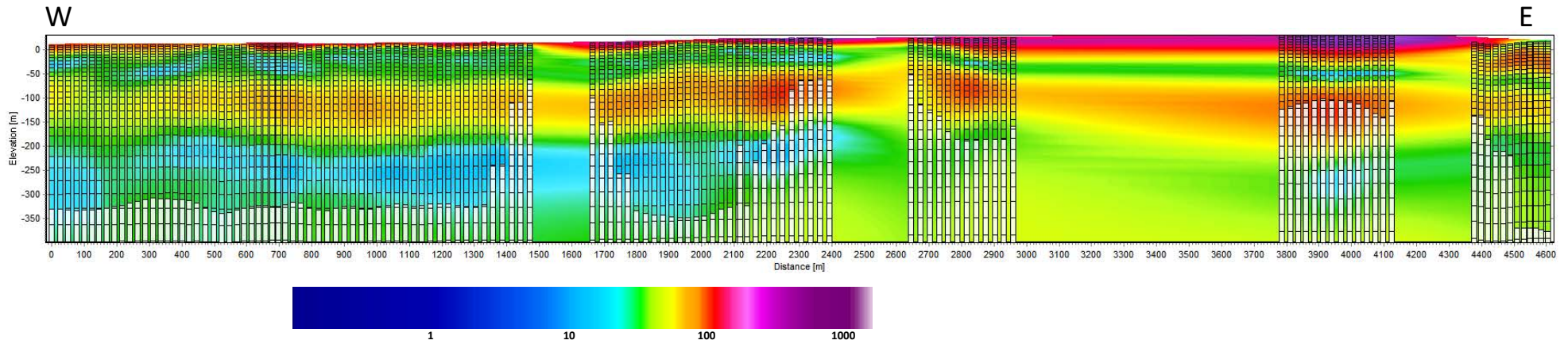
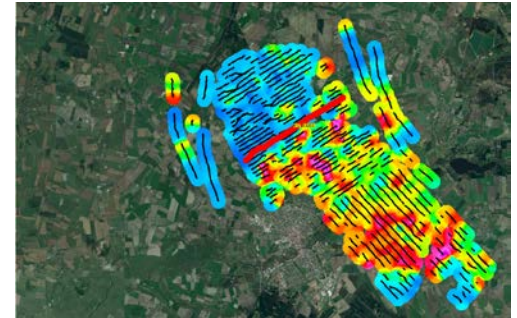
Location of the Cross Section



### Cross Section [Ohmm].

The inversion result models are plotted on top of the interpolated section. The white blinding represents the area below the DOI lower.

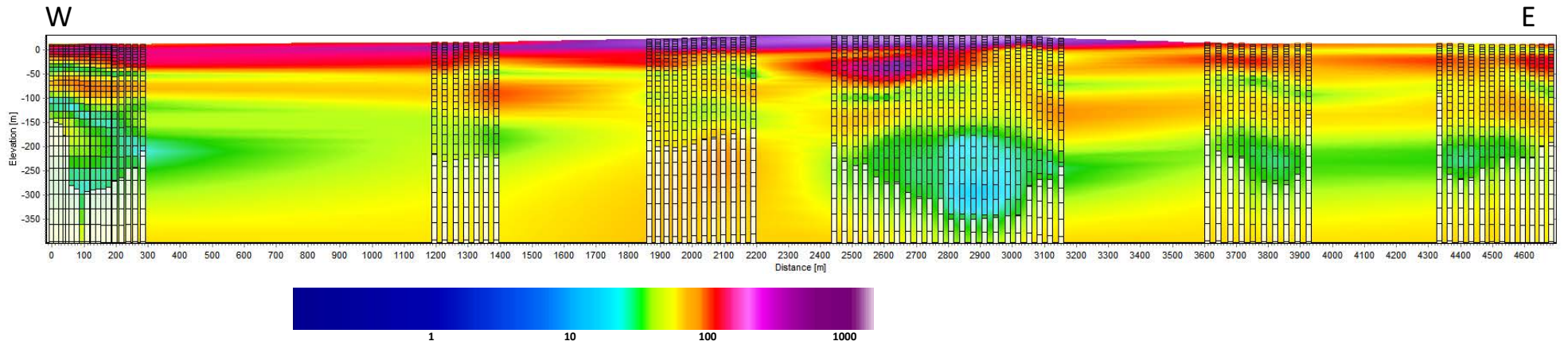
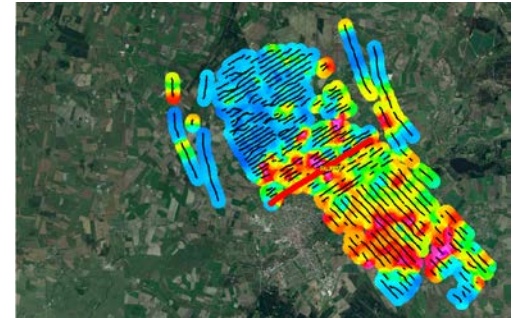
Location of the Cross Section



### Cross Section [Ohmm].

The inversion result models are plotted on top of the interpolated section. The white blinding represents the area below the DOI lower.

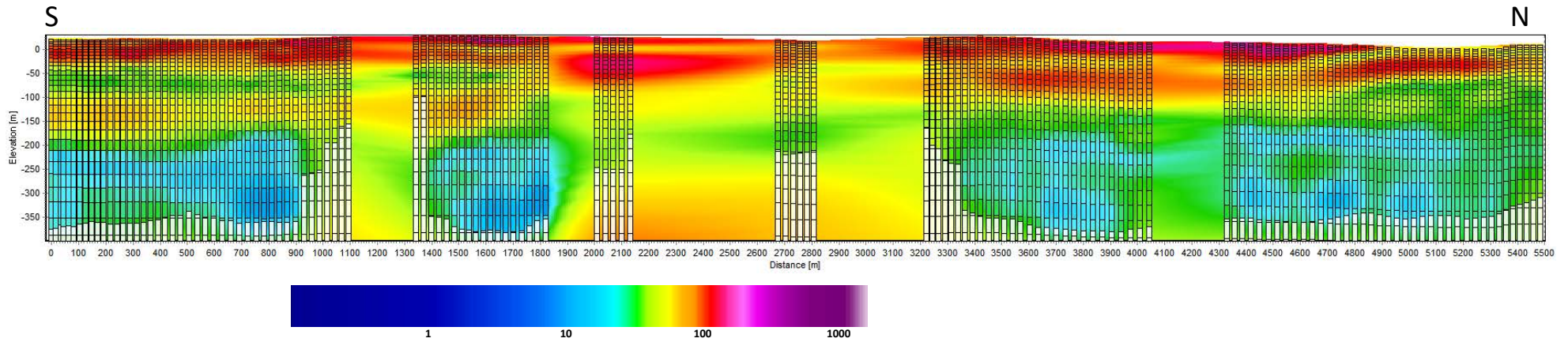
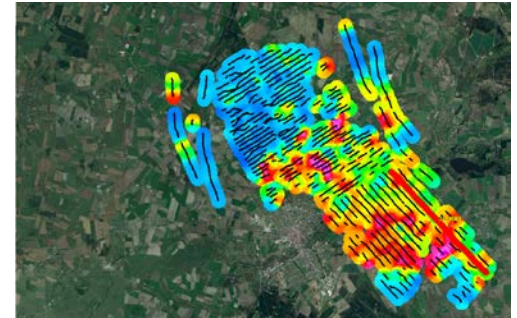
Location of the Cross Section



## Cross Section [Ohmm].

The inversion result models are plotted on top of the interpolated section. The white blinding represents the area below the DOI lower.

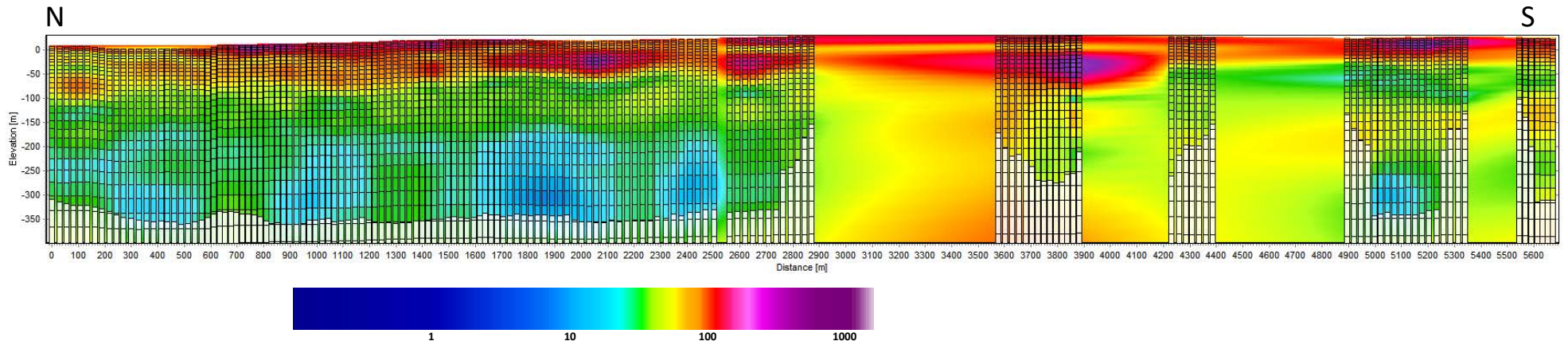
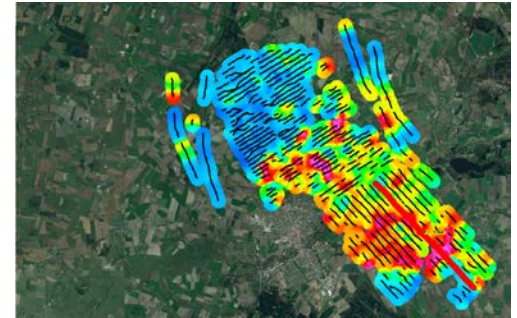
Location of the Cross Section



### Cross Section [Ohmm].

The inversion result models are plotted on top of the interpolated section. The white blinding represents the area below the DOI lower.

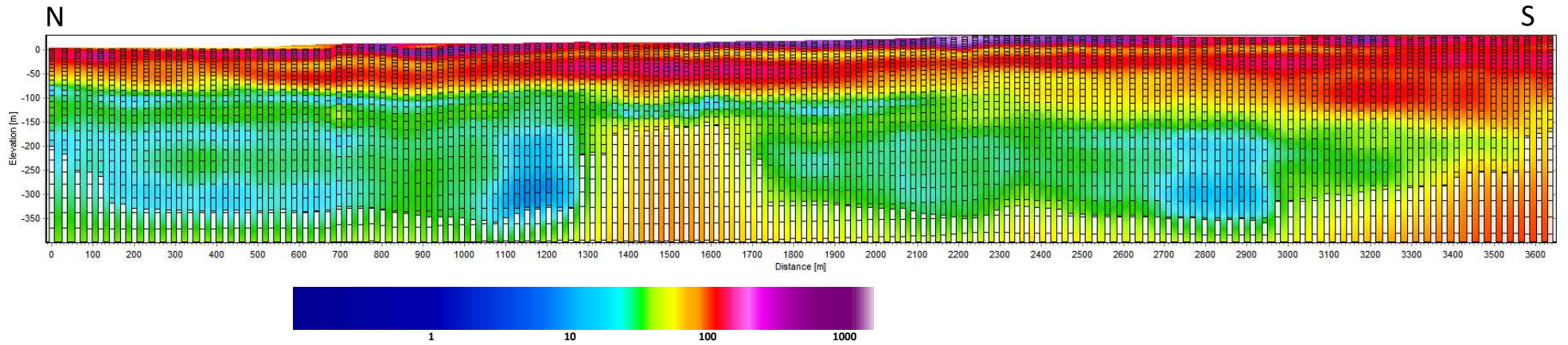
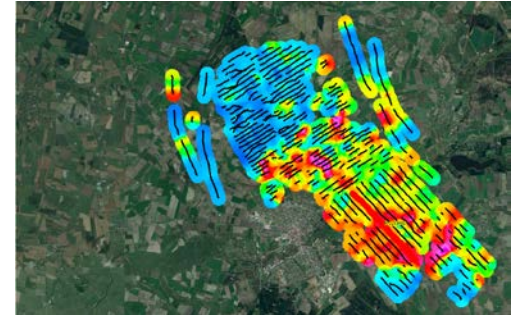
Location of the Cross Section



## Cross Section [Ohmm].

The inversion result models are plotted on top of the interpolated section. The white blinding represents the area below the DOI lower.

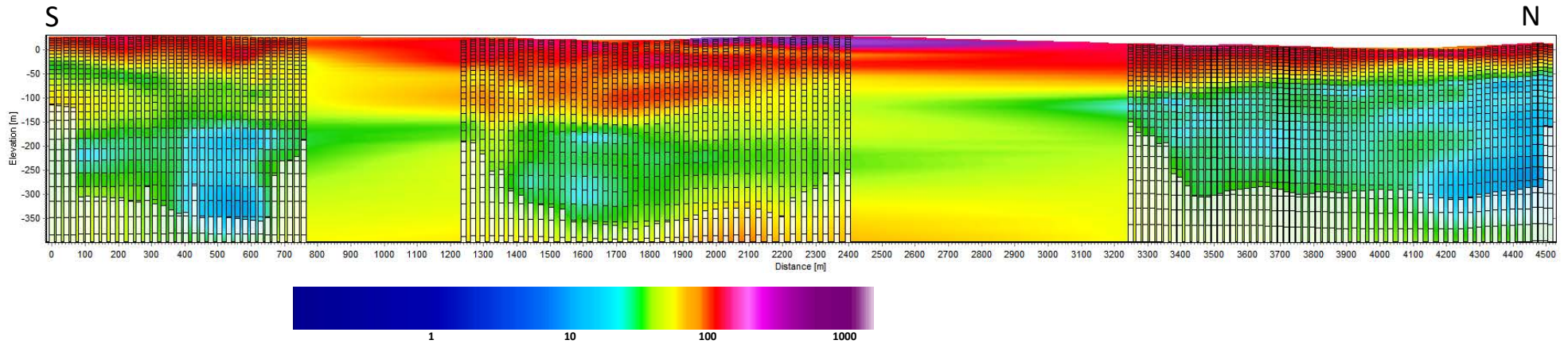
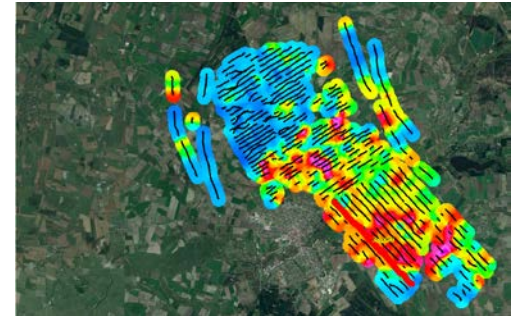
Location of the Cross Section



### Cross Section [Ohmm].

The inversion result models are plotted on top of the interpolated section. The white blinding represents the area below the DOI lower.

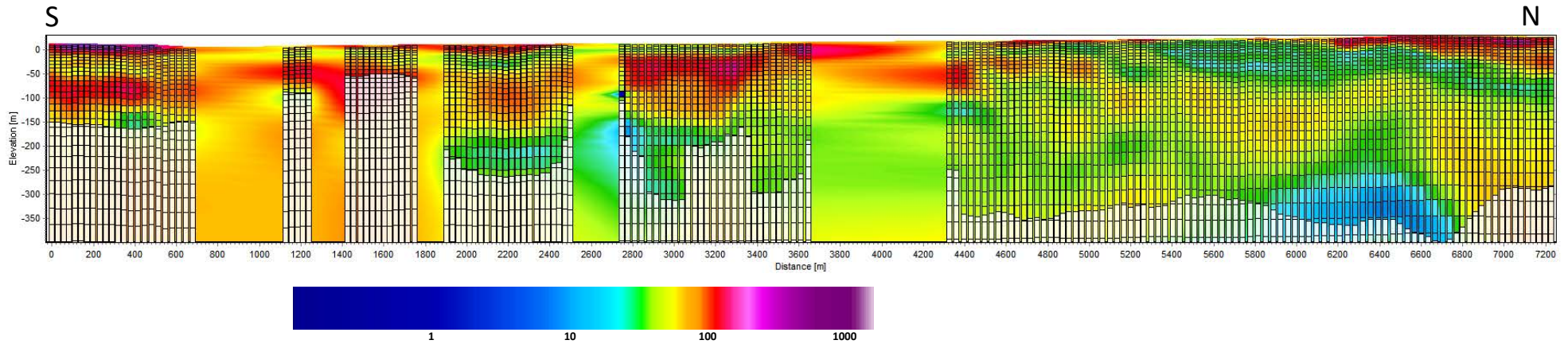
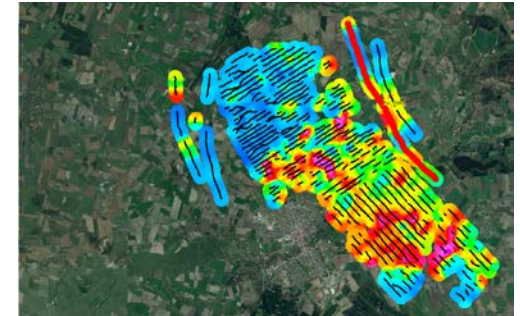
Location of the Cross Section



## Cross Section [Ohmm].

The inversion result models are plotted on top of the interpolated section. The white blinding represents the area below the DOI lower.

Location of the Cross Section



# Appendix IV: Digital deliveries

## Directories of the digital deliveries

### \Workspace

Aarhus Workbench's workspace containing SkyTEM data, inversion results, and maps.

### \Databases

The database .gdb file with the resistivity models and the grid .xyz files containing the DOI information (in elevation and depth).

## Varde Workspace tree

